26 Mar 93

FERMILAB-Proposal-872

Taiji,

We would like to submit this Letter of Intent to do a beam dump experiment which can measure the production of tau leptons from tau neutrino interactions. As the letter will reflect, we are confident that this goal can be achieved in one fixed-target run with a considerable safety margin for the number of visible tau neutrino interactions. The Letter also makes it clear that this effort is not a stand-alone, narrowly focussed measurement. It is a compellingly logical and, in my view, necessary precursor to a sensitive and complete program to measure neutrino mass/mixing here at Fermilab. The effort outlined here will provide what L. Wolfenstein describes as a true measure of the "discovery potential" of the ambitious proposal 803. We will measure, directly, the backgrounds and signals relevant to P803. From an experimentalists' point of view "appearance" experiments are the most sensitive while theoretical prejudices favor a signal from tau neutrinos given realistic constraints in sensitivity. The optimal solution with today's technology is still an emulsion target.

We do not view the problem of muon shielding as intractable due in part to the compact size of the target, but it is a problem that will require careful modeling AND measurement in order to assure adequate attenuation. The proposal that will follow can address these concerns in much greater detail.

I find neutrino physics a challenging frontier just waiting to be explored here at Fermilab. I also know that it will require a commitment soon in order to be a vigorous program. I think this experiment, important by itself, is an ideal way to commence a larger, but similar experiment to measure neutrino mixing at Fermilab.

Sincerely,

Byron Lundberg

Byron Lundberg

AA C0448

# Letter of Intent

# Measurement of $\tau$ Lepton Production from the Process $\nu_\tau + N \rightarrow \tau$

B. Lundberg, R. Rameika
Fermilab

K. Niwa
Nagoya University

N. W. Reay, N. Stanton
Ohio State University

V. Paolone
University of California at Davis

March, 1993

Abstract

We propose an experiment to measure the production of $\tau$ leptons produced in the charged current interaction of $\tau$ neutrinos. Using the Fermilab 800 GeV proton beam to produce $D_S$ mesons in a beam dump, a large flux of $\nu_\tau$ can be created. The interaction of the neutrinos in an emulsion target and the subsequent detection of the decay of the $\tau$ lepton using a hybrid emulsion spectrometer will provide the first direct evidence for the existence of the $\tau$ neutrino.

Scientific Spokesperson : B. Lundberg
Fermilab M. S. 221
708-840-2408

## Introduction

For well over a decade, the remarkable success of the unified theory of electroweak interactions has perhaps been the most compelling force in setting the course of high energy physics. The Standard Model framework arranges the quarks and leptons into pairs and generations, and explains their interactions via the photon and the intermediate vector bosons. The elegance and simplicity with which the model can explain the physical world has inspired experimental programs ranging from lepton scattering to the search for the top quark at the world's most powerful hadron collider. Yet despite its success, most physicists agree that the model is at best incomplete, in particular in its inability to easily motivate or predict the masses of the quarks and the leptons. As we have explored each of the generations, a hierarchy of masses and extremely short lifetimes has lead to many experimental challenges. Though most of these continue to be regularly met, it has admittedly required much effort in both time and money. The decisions to invest in the machines and experiments which enabled us to create heavy quarks, heavy leptons and W's and Z's has lead to some of the most beautiful science of the twentieth century. Though the top quark has yet to be found, few doubt its existence. Yet the compulsion to produce it and measure its properties is essential to our maintaining confidence in the basic framework of the Standard Model.

In the minimal Standard Model the introduction of spontaneous symmetry breaking provides for the observed masses of the charged leptons, but their neutral partners, the neutrinos are required to massless and restricted to appearing only in left-handed states. Being both massless, chargeless and weakly interacting has made the neutrinos perhaps the most elusive of the known elementary particles. From measurements of the neutron beta decay spectrum to the neutrino production of muons, the experiments which were done to prove the existence of both the electron and muon neutrinos are classic. Though these experiments preceded the theory which would lay down a pattern for further lepton generations, they established conservation laws which would isolate the leptons from each other and make them even more mysterious. The discoveries of the charm quark and tau lepton in the mid-70's lead to the model of paired particles and higher generations. The existence of a neutrino partner for the tau was assumed and indirectly confirmed by the tau decay spectrum.

However, unlike the definitive identification of both the electron and the muon neutrinos, which is accomplished by observing only flavor conserving charged current

interactions of a neutrino to its lepton partner, this has not been possible for the tau pair. Like with the top quark, few doubt that the tau lepton does have its own neutrino, however, direct observation of the $\nu_\tau$ -> $\tau$ charged current interaction would confirm its existence. Proposals have been made to do this experiment.[1,2] Unfortunately it is not easy. Like many other of the more tantalizing elementary particles, the $\tau$ lepton is not easily produced, is very short lived, and has difficult to reconstruct decay modes, hence making its neutrino partner much more elusive than either the $\nu_e$ or $\nu_\mu$. To do this experiment will require effort. However, for the reasons which we will outline below we feel that the time has come to make that investment.

**Motivation**

One of the most intriguing questions facing physicists today is whether or not the neutrinos are really massless particles. Though the minimal Standard Model requires that they be massless and existing experimental limits give no significant indication to the contrary, there is mounting evidence from several sources that all is not right with the massless assumption. The observed deficit of solar neutrinos reaching the earth, which for the longest time was attributed to not understanding the solar models well enough to predict the flux, is now postulated to result from the oscillation of electron neutrinos into neutrinos of a different flavor. Likewise there is an observed deficit of muon neutrinos from the decay of atmospheric cosmic ray muons, again possibly resulting from the oscillation of the neutrino.

Neutrino oscillations can occur if the neutrinos are massive and the observed flavor states are actually linear combinations of mass eigenstates. Since massive neutrinos could rather easily be accommodated into a *modified* Standard Model, as well as provide a possible explanation for at least some of the missing dark matter of the universe, the motivation to conduct experimental searches using accelerator produced neutrinos to observe such oscillations is quite intense. In spite of the current growing interest, this is not a new idea, though to date no evidence for oscillations has been uncovered by such experiments. The problem that arises in such searches is that a null result is expected and hence accepted.

There are two types of experiments which are performed to search for neutrino oscillations. Most, including the solar and atmospheric measurements, are called disappearance experiments. This means that a source of neutrinos of a single flavor is

created and the flux is measured at two different places separated by a distance. Differences in the flux at the two locations will indicate that the neutrinos have oscillated into a different flavor. Alternatively, in an appearance experiment, a source of neutrinos of a single flavor will travel a distance to a target where they can interact. Observation of a lepton of flavor different than the original beam will indicate that the neutrinos have oscillated. While more difficult to perform, appearance experiments are a necessary complimentary method for observing neutrino oscillations.

Though certainly motivated by theoretical prejudices, many advocates of neutrino oscillations believe that the most likely channel in which accelerator based oscillation searches will observe a signal is in the mode $\nu_\mu \rightarrow \nu_\tau$. To do this will require that the experiment observe the charged current interaction $\nu_\tau + N \rightarrow \tau$, the process which has yet to be observed from direct production of $\nu_\tau$'s. The Fermilab proposal P803 is a neutrino oscillation experiment designed to be sensitive to the appearance of the $\tau$ lepton.[3] The experiment uses a hybrid emulsion spectrometer similar to one used in E653 to detect the decay of charm and b mesons.

We propose here to carry out an experiment using the P803 production and detection technique to observe the decay of $\tau$ leptons produced by $\nu_\tau + N \rightarrow \tau$. We believe that this is an important first step in establishing the credibility of an oscillation signal which could be observable in P803. Where ever possible we will attempt to construct detector elements which are prototypes or actual elements which could become part of the P803 spectrometer. We believe that because of the uncertainty and likely delay of the Main Injector construction schedule, completion of this project is not only feasible, but is also an efficient use of our time and resources during the next several years and beyond.

In the remainder of this document we will describe the key issues which we have addressed to determine the feasibility of performing this experiment. We realize that there are a number of technically challenging as well as logistical problems which will need to be addressed in more detail than we have presently done. We are currently working on a complete proposal, including cost estimates for major components. We will submit this to the laboratory as soon as possible.

**Tau neutrino production**

Tau neutrinos can be produced from the semi-leptonic decay of the $D_S$ meson in the decay sequence $D_S$ - > $\tau + \nu_\tau$, $\tau$ -> $\nu_\tau$ . We will transport 800 GeV primary protons to a beam dump where both the $D_S$ and the $\tau$ will be produced and decay. Below we summarize the parameters required to estimate the number of $\nu_\tau$ per incident proton which will emerge from a tungsten beam dump. We have used a Monte Carlo calculation to generate the $D_S$ and $\tau$ decays in the dump. The energy spectrum of the $\nu_\tau$'s from the $D_S$ - $\tau$ decays is shown in Figure 1.

$N(\nu_\tau) = [\sigma_{Ds}/\sigma_{tot}] * BR(D_S \rightarrow \tau)*(A^1/A^{0.7}) * 2$

$\sigma_{Ds}$ = $D_S$ cross section : 21 $\mu$ barns [4]

$\sigma_{tot}$ = total pp cross section : 40 m barns

$BR(D_S \rightarrow \tau + \nu_\tau)$ = branching ratio : 0.037[5]

A = atomic number of target : 184 for tungsten

2 = factor from two $\nu_\tau$'s produced per $D_S$ decay

$\Rightarrow N(\nu_\tau)$/ proton = $1.86 * 10^{-4}$

**Tau neutrino interactions**

Approximately twenty -five meters downstream of the end of the beam dump we will place an emulsion target. Below we summarize the parameters required to determine the number of $\nu_\tau$ charged current interactions which will occur per centimeter of emulsion. The neutrinos from each of the decays have very different cross sections. The direct one ($D_S$) has a weighted (energy and kinematics) average of $0.11*10^{-37}$ cm$^2$ and the neutrino from the $\tau$ decay is $0.74*10^{-37}$ cm$^2$. We have assumed a symmetric $(1-x)^n$ form for $D_S$ production with n=6.9.[4] However, the $\nu_\tau$ cross section is not very sensitive to n. Increasing n to 9 gives a 16% reduction, decreasing n to 5 gives an increase of 25%.

$N(\tau_{cc}) = N(\nu_\tau) * \sigma_\tau * N_{Av} * d$

$\sigma_\tau$ = weighted average cross section for $\nu_\tau$ : $0.42 *10^{-37}$ cm$^2$

$N_{Av}$ = Avogadro's number : $6.02 *10^{23}$

d = density of emulsion : 3.72 g/cm$^3$

=> N ($\tau_{cc}$) / cm emulsion / proton = $18 * 10^{-18}$

[Note this number is consistent with the background estimate from direct $\nu_\tau$ production described in the P803 proposal.]

**Tau detection efficiency and backgrounds**

From the neutrino angular distribution we find that 80% of the interactions are contained within ±20mr (see Figure 2). This along with the combined efficiency for finding the interaction vertex with known fiducial cuts to be 0.8 [6] gives an overall efficiency of 0.64.

It is expected that nearly all interactions will be scanned, as there is no need to reduce the data sample with kinematic cuts. The interactions from $\nu_e$ and $\nu_\mu$ constitute the major background and is calculated to be approximately $8*10^{-16}$ interactions/cm of emulsion / proton.

An important aspect of this experiment will be ensuring that background arising from upstream decays of $\pi$'s and K's are minimized. This will require extremely clean transport of the primary proton beam.

**Tau Yields**

Given N ($\tau_{cc}$) / cm emulsion/proton = $18 * 10^{-18}$ a reasonable **goal** for this experiment is to use **10 cm** of emulsion and **$2*10^{18}$ integrated protons.** This will yield (on paper) :

$$N_\tau = 18 *10^{-18} * 0.64 * 10 * 2*10^{18} = \mathbf{230}$$

The corresponding number of background interactions will then be $1.6*10^4$. Based on experience from E653, this number of interactions can be fully reconstructed and scanned on the time scale of one year.

Note : These numbers are based on conservative estimates or on measured cross sections and branching ratios. We present them here to establish feasibility, however, as we continue to develop a full proposal we expect to refine calculations of background and actual reconstruction efficiencies.

An integrated proton flux of $2*10^{18}$ can be achieved if the experiment can take **$1*10^{13}$ protons per pulse.** Thirty six weeks of running at 60% efficiency will be required. Recent fixed target runs have been reaching efficiencies of 70% or better.

**Muon Flux**

A technical challenge in doing this experiment is reducing the intense flux of muons which will emerge from the beam dump directed toward the emulsion and the spectrometer. The experience of E653 has shown that track densities in emulsion can exceed $3*10^5$ per $cm^2$ without degrading the efficiency for finding the events. This translates into an allowable muon flux of a few times $10^4$ per cycle over the area of the emulsion ($\leq$ 1 square meter).

At the present time we do not see this as an insurmountable problem since the area which needs to be protected (e.g. the emulsion) is relatively small . We are using existing data and models to study the momentum distributions of the muons emerging from a beam dump. [7] A possible solution is a large powerful dump magnet followed by approximately 15 meters of magnetized shielding. We believe it is necessary to perform beam tests and make flux measurements prior settling on a final design. A proposal for how this can be accomplished is discussed in the **E S & H** and **Schedule** sections.

**E S and H issues**

Because of the high intensity required for this experiment and the resulting muon flux, careful consideration must be given to both groundwater activation and prompt radiation limits. Neither of these can really be addressed with out a determined location for the experiment. At the present time we are investigating the possibility of using the **P-West beamline** and the **PW8 experimental hall** To determine if this is feasible we will perform a shielding evaluation of the primary beam transport through PW7 and do a first order design of a beam dump to be located in PW8. We believe that physically there is enough room to do this. We need to address issues of groundwater and overburden.[8]

## Cost estimate

It will not be possible to make a detailed cost estimate without proceeding with a complete design for the experiment. However, we have attempted to outline major, up front costs. We have separated these into two categories, those uniquely associated with the beam dump experiment, and those which would be required for P803 as well. We believe that on the time scale of completing our full proposal, reasonable estimates for each of these items will be available.

- This experiment
  - Shielding modifications to the primary beamline (bulk shielding and labyrinth hardening)
  - Modifications to beam transport for cleanliness
  - Tungsten beam dump
  - Radiation/groundwater shielding around beam dump
  - Muon spoiling system (using existing magnets and steel)
  - 85 liters of emulsion

- Common with P803
  - Emulsion scanning facility
  - Detector R & D , prototyping and possible production modules for :
    - scintillating fiber tracker
    - drift chambers
    - electromagnetic and hadronic calorimeters
  - Data Acquisition

## Manpower

If approved, we believe most members of the P803 collaboration will participate, in particular those who will have major detector system responsibility.

**Schedule**

The ideal schedule for doing this experiment would be during a Fixed Target run which occurs after 1996 but prior to the commissioning of the Main Injector. However, we believe that we must demonstrate that we are able to reduce the muon flux to the level discussed above **prior** to building the spectrometer and exposing the emulsion. We believe that this can be done given a test run of two to three months during the 1995 fixed target period. This would require rigging to configure magnets and shielding and to construct an adequately shielded beam dump. At that time we would run at moderate intensity (≤1E12 protons/pulse) and measure the muon fluxes in the hall.

Serious R & D and prototyping for all major spectrometer elements must begin as soon as possible following the experiment's approval.

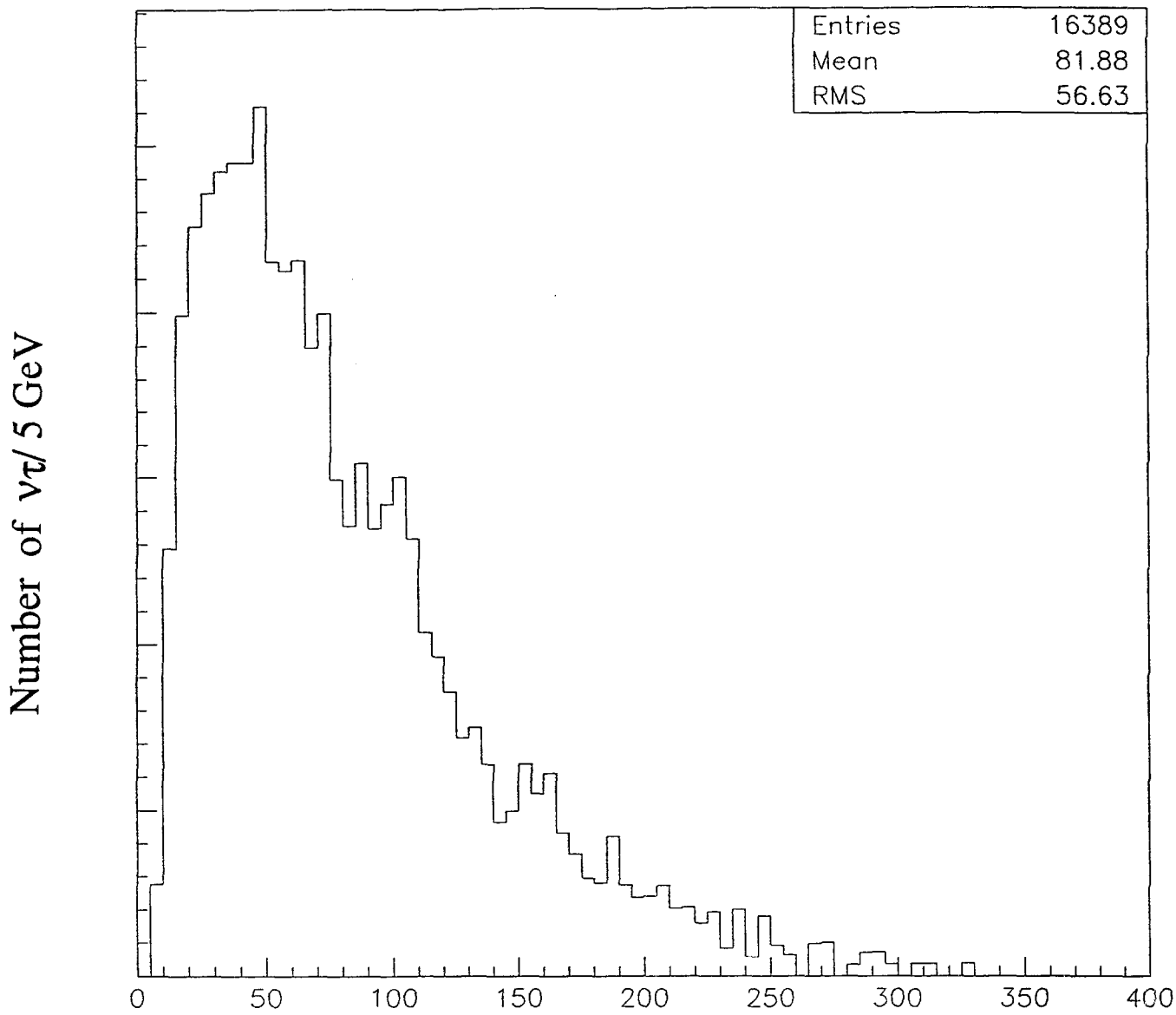


**Figure 1** Energy distribution of interacted $\nu_\tau$ from Monte Carlo with an acceptance cut of ±20 mr.

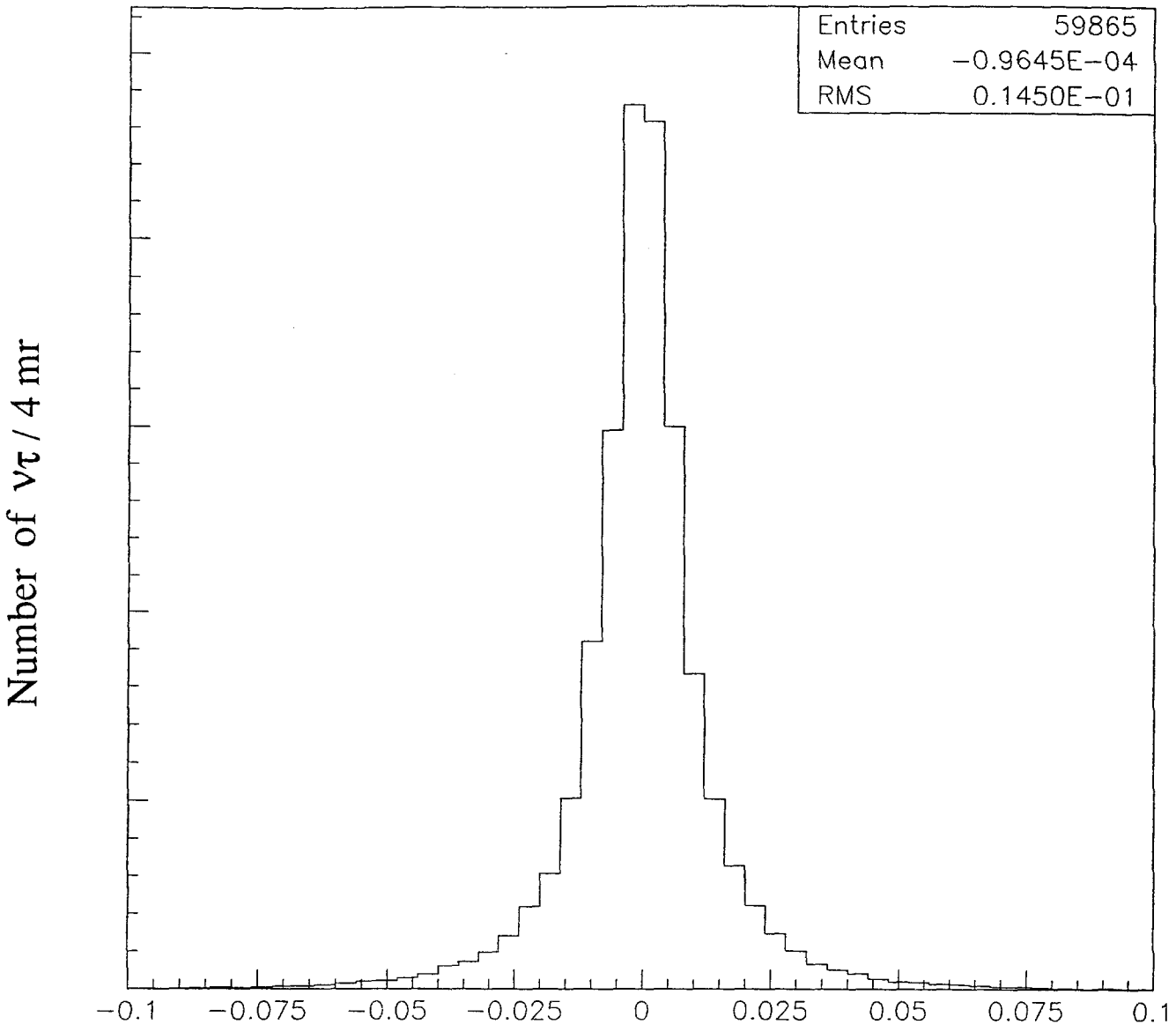


**Figure 2** Angular distribution of interacted $\nu_\tau$ from Monte Carlo.

**References**

[1] Proposal 636 - Neutrino Interaction Studies using a Beam Dump Technique to Produce the Neutrino Beam, 1980

[2] Proposal 646 - Search for the $\nu_\tau$ and Study of $\nu_e$ and $\nu_e$-bar Interactions, 1980

[3] Proposal 803 - Muon neutrino to tau neutrino oscillations, October 1990

[4] Charm meson production in 800 GeV/c proton-emulsion interactions, E653 collaboration, Physics Letters B, Vol. 263, no. 3,4 (1991); Inclusive charm cross sections in 800 GeV/c p-p interactions, LEBC-MPS collaboration, Physics Letters B, Vol. 183, no.1 (1987); Measurement of the branching ratio for $D^+ \rightarrow K^*\mu^+\nu$ ; E653 collaboration, Physics Letters B, Vol. 286 (1992) 187-194

[5] The first observation of the muonic decay $D_s \rightarrow \mu^\pm \nu_\mu$ , WA75 collaboration, CERN-PPE/92-157.

[6] The production mechanism and lifetimes of charmed particles, S. Frederiksen, PhD thesis, University of Ottawa, 1987.

[7] FN-434 - The Intensity and Spectra of Leptons Emerging from a High Intensity Beam Dump, J. Morfin, July 1986

[8] Research Division P-West Beamline Review, L. Spiegel (presentation notes), April 1992 ; Research Division Shielding Assessment, P-WEST Discussion and Action Items, A. Malensek and M. Gerardi, May 1991

# P872
# Measurement of $\tau$ Lepton Production from the Process $\nu_\tau + N \rightarrow \tau$

B. Lundberg *, R. Rameika
*Fermilab*

V. Paolone*
*University of California at Davis*

K. Niwa
*Nagoya University*

S. Aoki
*Kobe University*

D. Potter
*Carnegie Mellon University*

J.O. Wilcox
*Northeastern University*

G. Tzanakos
*University of Athens*

F. Avignone, C. Rosenfeld
*University of South Carolina*

R. Rusack
*University of Minnesota*

A. Napier, T. Kafka, W. Oliver, J. Schneps
*Tufts University*

January 1994

Abstract

We propose an experiment to measure the production of $\tau$ leptons produced in the charged current interaction of $\tau$ neutrinos. Using the Fermilab 800 GeV proton beam to produce $D_S$ mesons in a beam dump, a large flux of $\nu_\tau$ can be created. The interaction of the neutrinos in an emulsion target and the subsequent detection of the decay of the $\tau$ lepton using a hybrid emulsion spectrometer will be the first direct measurement to confirm the existence of the $\tau$ neutrino.

* Spokespersons

## 1. Introduction

Though there is a great deal of experimental evidence that the $\nu_\tau$ exists as a unique lepton and that its couplings are not anomalous at the present level of sensitivity, interactions from $\nu_\tau$'s have yet to be seen in the manner of the $\nu_e$ and $\nu_\mu$ discoveries. Since the discovery of the tau lepton in 1975, the desire to detect its neutrino partner has been strong, however the proposed experiments[1,2] were technically challenging and required significant resources. Two experiments, E636 and E646, approved to run with the Fermilab Tevatron, were designed but later canceled due to the cost. In retrospect, those experiments would have proved to be more than just difficult and expensive; it is likely that they would have failed. Many of the parameters which determine the yield and ability to detect the interactions had not been measured at the time the experiments were proposed. Knowledge gained over the past ten years about both the physical parameters and detector capabilities have remedied this situation, though the original requirements remain. In short, this experiment requires high proton intensities, high energy and extremely good detector resolution. A proposal has been made to do this experiment using the 3 TeV accelerator at UNK[3], and feasibility studies of doing the experiment at the LHC or SSC have been done[4]. We leave it to the reader to judge the likelihood of these proposals coming to fruition. Meanwhile, we believe that using the Fermilab Tevatron in conjunction with a high resolution detector meets the requirements for doing this experiment. In P872 we propose to produce tau neutrinos in a beam dump and directly measure $\nu_\tau$ charged current interactions by seeing $\tau$ decays in an emulsion target.

Aside from the obvious satisfaction which would result from observing direct $\nu_\tau$'s, another motivation for making this measurement stems from one of the most intriguing questions facing physicists today: are neutrinos really massless particles?

Flavor changing neutrinos imply that the neutrinos are not massless, hence experiments which can detect neutrino oscillations provide an extremely sensitive way to probe neutrino masses far beyond direct, kinematical methods. Very general arguments, based on the appeal of a mass heierarchy as observed in both the quark and charged lepton sectors, imply that the tau neutrino would be the heaviest of the three neutrino species.[5] The possibility that a heavy $\nu_\tau$ (7 eV < m < 28 eV) could be a candidate for the cosmological dark matter has lead to much recent interest in accelerator based oscillation searches, in particular in the appearance channel, $\nu_\mu \rightarrow \nu_\tau$. To date, all terrestrial experiments have yielded negative results.

Over the next two years, two experiments at CERN, commonly referred to as CHORUS and NOMAD[6], will collect data to search for this process. If oscillations were

to occur just beyond the present limits, CHORUS would expect to observe ~60 $\nu_\tau$ interactions. If no interactions are observed by either experiment, the limit on the mixing angle will extend to ~ $10^{-4}$ for $\delta m^2 > 1$ $eV^2$. This limit can be significantly extended by Fermilab experiment E803[7], which was recently approved for running with the new Main Injector, now scheduled for completion in 1998.

We *will* see the interaction that the oscillation experiments *hope* to see, if the $\nu_\tau$ is "standard", but there is more. We will measure the interactions using the *same* techniques of emulsion analysis. P872 will be sensitive to, and measure the processes that give rise to backgrounds for these experiments. In doing so, one can be sure that no other process is at work, such as fast decay, preventing the observation of the oscillation signal.

In Sections 2-5 of this proposal we will discuss the key issues which we have addressed to determine the feasibility of performing this experiment and briefly describe the methods and apparatus we propose to use. We describe other physics which is totally unique to a $\nu_\tau$ beam (5% of the flux) that we can build. Finally in Section 6 we propose a beam test, which we believe is required to verify the feasibility we have demonstrated in simulation. We would like to perform this beam test during the next fixed target run.

## 2. Feasibility of the Experiment : Physics Issues

2.1 Tau neutrino production and interactions

Tau neutrinos are produced predominantly from the leptonic decay of the $D_S$ meson in the decay sequence $D_S \rightarrow \tau + \nu_\tau, \tau \rightarrow \nu_\tau$ . Tau neutrinos will also be produced from several other sources. In our final estimates we have included additional production from b meson decays, charged D decays, Drell-Yan and secondary production from charm.

In this experiment the $D_S$ will be produced by 800 GeV protons interacting in a tungsten beam dump. Both the $D_S$ and the daughter $\tau$ will decay in the dump, each decay producing one $\nu\tau$ . The number of $\nu_\tau$ per incident proton which will be produced in the beam dump is given by Equation 1. The parameters required to estimate this yield are listed in Table 1.

| | | |
|---|---|---|
| Atomic weight of tungsten | 184 | Refs. |
| $\sigma$ (pp) total cross section | 40 mb | |
| $\sigma$ (pp) A-dependence | $\alpha = 0.7$ | |
| $\sigma_{D^\pm}$ total cross section | 29±6 $\mu$ barns | [8,9] |
| $\sigma_{D_s} / \sigma_{D^\pm}$ | 0.54±0.10 | [10,11] |
| $\sigma_{D_s}$ for p + N -> $D_S$ | 15.4±4.4 $\mu$ barns | [12,13,14] |
| BR ($D_S$ -> $\tau\ \nu_\tau$ ) | 0.041±0.011 | [15] |
| A-dependence | $\alpha$ = 1.0±0.05 | |

Table 1. Factors in $\nu_\tau$ production from $D_S$ decays

$$N(\nu_\tau) / \text{proton} = [\sigma_{D_S} / \sigma_{tot}] \times BR(D_S \rightarrow \tau) \times (A^1 / A^{0.7}) \times 2 \qquad (1)$$

$$\Rightarrow N(\nu_\tau)/ \text{proton} = 1.51 \times 10^{-4}.$$

We have used a Monte Carlo to generate the $D_S$ and $\tau$ decays in the dump. The $D_S$ momentum spectrum is generated using a parameterization for the cross section $\sigma \sim e^{-bp_T^2}(1- |x_f|)^n$ with $n$ = 7.7 and b= 0.83± 0.08 [16].

The $\tau$ is decayed in accordance with its major branching fractions which are listed in Table 2. The $\tau$ decay is weighted to give the proper angular distribution from

| Decay mode | Branching fraction (%) |
|---|---|
| $\tau \rightarrow \mu\nu\nu$ | 17.8 |
| $\tau \rightarrow e\nu\nu$ | 17.7 |
| $\tau \rightarrow \rho\nu$ | 22.8 |
| $\tau \rightarrow \pi\nu$ | 11.0 |
| $\tau \rightarrow \pi\pi\pi\nu$ | 14.6 |
| Total (in Monte Carlo) | 83.9 |
| Table 2 :Tau decay modes and branching fractions | |

electroweak considerations (approximately for hadronic decays) but no polarization was included. The polarization does not appear to have a large effect and at the $\tau$ momenta typical of this experiment does not appreciably change the neutrino distributions. The electroweak weights are given below:

| | |
|---|---|
| Leptonic Decays | $(p_\tau \cdot p_\nu)\,(p_l \cdot p_{\nu\tau})$ |
| Hadronic Decays | $x\,(3 - 2x)$ ; $x = 2E_{\nu_\tau}/m_\tau$. |

The number of $\nu_\tau$ charged current interactions which will occur in the emulsion target is determined by the $\nu_\tau$ energy and interaction cross section, and the density and thickness of the emulsion. To estimate yields we have determined an effective interaction cross section. Because of the energy dependence of the $\nu_\tau$ cross section, the neutrinos from each of the decays ($D_S \rightarrow \tau + \nu_\tau$ and $\tau \rightarrow \nu_\tau$ ) have very different interaction probabilities. The shape of this spectrum is determined by the longitudinal $x_f$ dependence of the $D_S$ production cross section. The energy weighted and kinematic weighted (due to large $\tau$ mass) cross sections for each of the neutrinos, as well as a combined weighted average cross section, are given in Table 3.

| | |
|---|---|
| $\sigma_{\nu_\tau}$ (from $D_S$) | $0.086\times10^{-37}$ cm$^2$ |
| $\sigma_{\nu_\tau}$ (from $\tau$) | $0.75\times10^{-37}$ cm$^2$ |
| $\sigma_{\nu_\tau}$ (weighted) | $0.42\times10^{-37}$ cm$^2$ |
| Table 3 : $\nu_\tau$ interaction cross sections | |

The number of charged current interactions which will occur per centimeter of emulsion can be calculated from Equation 2, where $N_{Av}$ is Avogadro's number ( 6.02

$\times 10^{23}$) , $\rho$ is the density of the emulsion (3.72 g/cm$^3$) and $\beta$ is the weighted angular acceptance ($\beta$ = 0.46, corresponding to ±9 mr angular acceptance). In Section 3 will discuss the optimization of experimental parameters, such as the choice of solid angle.

$$N(\tau_{CC})/\text{proton} = N(\nu_\tau)/\text{proton} \times \sigma_{\nu_\tau} \times N_{Av} \times \rho \times \beta \qquad (2$$

$$\Rightarrow N(\tau_{CC}) = 6.5\times 10^{-18}\ /\text{cm emulsion / proton.}$$

The energy spectrum of the $\nu_\tau$'s which interact in the emulsion target from both the $D_S$ and $\tau$ decays is shown in Figure 2.1. The $\tau$ neutrinos emerging from the beam dump, which will interact in the emulsion, have an angular distribution which is shown in Figure 2.2.

All of the above calculations for the rates and event distributions assume that the source for all of the $\nu_\tau$'s is $D_S$ decay to $\tau\nu$. As mentioned earlier, there are other processes which give a $\nu_\tau$ in the final state :

1) charged charmed mesons, $D^\pm$, can also decay to $\tau\nu$ but with suppression due to allowed phase space and $|V_{cd}|^2$ which greatly offsets the larger production cross section. The rate compared to $D_S \rightarrow \tau\nu$ is 4.5%.;

2) semi-leptonic decays of B mesons contribute1.4% relative to the interacted flux from $D_S$ decays;

3) secondary interactions in the proton dump can be estimated in a similar manner to estimating the $\mu$ flux from non-prompt sources, i.e. $\pi$'s and K's from the hadron cascade in the dump using Monte Carlo. The result is that these secondary products increase the interaction rate by 8%;

In summary, sources other than $D_S$ decay contribute an extra 14% to the total number of $\nu_\tau$ interactions in the emulsion target. This gives

$$N(\tau_{CC}) = 7.4\times 10^{-18}\ /\text{cm emulsion / proton}$$

Given this interaction rate, we have set as a reasonable goal for this experiment to use 15 cm of emulsion and $2\times 10^{18}$ integrated protons. Before fiducial volume and efficiency cuts this will yield

$$N_\tau = 7.4\times 10^{-18} \times 15\text{cm} \times 2\times 10^{18} = 222 \text{ interactions}$$

## 2.2 Backgrounds to the $\nu_\tau$ Signal

In P872 all interactions which trigger the experiment will be scanned for in the emulsion, with the possible exception of events with two muons. The signal for a $\tau$ decay is one ( and only one) secondary vertex with no $\mu$ or $e$ matched to the primary vertex. Therefore the only backgrounds are those events which are indistinguishable from $\nu_\tau$ charged current (CC) interactions in the emulsion target. In 86% of these interactions the short track from the created $\tau$, typically 2mm, decays to only one charged particle thus leaving a "kink" in one of the tracks emerging from the primary interaction. Although there are in principle many processes that could mimic this signature, only charm production and the so-called "white-star kink" process are at a level high enough to merit further discussion here.

First we consider single charm production from charged current $\nu_e$ or $\nu_\mu$ interactions. For example, if the $D^+$ decays to just one charged particle, it will look like a $\tau$ decay and constitutes an unavoidable background *if and only if* the lepton from the neutrino interaction is lost or misidentified. The calculation is

$$\%\text{Bkg} = \frac{N_{CC} \rightarrow \tau\text{-like charm decays}}{N_{CC} \text{ from } \nu_\tau} = \frac{(\text{charm produced})}{(\nu_\tau \text{ interactions})} (\text{frac } D^{\pm}) (\text{frac "kinks"}) (1-\varepsilon)$$

where we take the number of charm produced as 7.7% of the total number of interactions[17],[18] and is equal to 310 events for each flavor. The fraction of charged D mesons is 0.4 and the fraction of kink decays is 0.4 [19] . The efficiency for detecting and properly identifying the lepton is given by $\varepsilon$. For muons, $\varepsilon_\mu$ is expected to be at least 95%. This gives a relative background in this channel of 0.6%. For $\nu_e$ interactions, $\varepsilon_e$ may be lower, but if the vertex is located in the emulsion we expect it to be at least 90%, giving an additional 1.2%. Therefore we expect the background due to charged current produced charm to be 1.8%.

One can also estimate the background of charm pairs from neutral current interactions. It is much smaller since the fraction of neutral current interactions with charm is less than 0.01 and one of the charm decays (presumably a $D^0$) has to be lost. This source of background is negligible.

Another type of background arising from elastic scattering of secondaries or what *appears* to be a kink in a secondary track is more problematic. In the emulsion, most secondary interactions are associated with highly ionizing "dark" tracks and "blobs" from nuclear break-up. However, there is an annoying class of events which do not have this tell-tale mark and are referred to as "white star" kinks (in contrast to the "black stars" of nuclear break-up). The white star kinks have a $p_T$ distribution that is very steep so that if one wanted to eliminate them, one could, in principle, make an appropriate cut. However, the steepness of the $p_T$ distribution is not known to a great deal of precision and must be extracted from emulsion exposures themselves.

To estimate the amount of background due to this source, we first estimate the total track length scanned in the emulsion for neutral current events ( no lepton at primary) and then compare to the measured mean free path between white star kinks. The number of charged tracks from a NC interaction averages 4.3. The total number of NC interactions is 2000 and on average we will scan each track 7.5mm, for a total of 6500cm of integrated emulsion tracking. For tracks with a kink $p_T$ of 0.2 GeV/c and above, the mean free path for white star kinks is 50±18 m and is 370±180 m [20] for $p_T >$ 0.3 GeV/c. Since 85% of $\tau$ decays have a kink $p_T > 0.2$ GeV/c the background is not severe and can be made vanishingly small for a cut of $p_T > 0.3$ GeV/c. For the full sample of $\nu_\tau$ interaction candidates without any cuts we expect a background of 4.3%.

### 2.3 $\nu_e$ and $\nu_\mu$ Interactions

Charged and neutral current interactions from $\nu_e$ and $\nu_\mu$ constitute the bulk of the data in this experiment. The rate of these interactions has been calculated to be $3\times10^{-15}$ interactions in the emulsion per proton for a total number of background interactions of $6\times10^3$.

Eliminating $\nu_\mu$ interactions from the $\tau$ sample will be relatively easy. The muons will be identified in the spectrometer and tracked back into the emulsion. Any event containing a muon from the primary interaction vertex will be eliminated. Electron interactions will be more difficult to identify because most of the electrons will convert and shower in the emulsion itself. We will rely on the spectrometer to find (at least) one charged track which is not an electron that can locate the primary interaction in the emulsion by tracing it backwards through the target. Once the primary is found, the other charged tracks are scanned forward. It is during this process that conversions from a bremmstrahlung photon are detected by scanning a sufficient distance along a track

To determine the number of tau interactions which we will actually be able to observe in P872, we need to determine the experimental acceptance and reconstruction efficiency. We have used the generated tau neutrino spectrum, described above, as the input to the Lund Monte Carlo program (LEPTO v6.1) for the simulation of interacting the tau neutrinos in the emulsion target. All default settings were used except the effects of QCD in the final states, which were switched off. The leading order parametrized parton distribution of Gluck, Reya, and Vogt (GRV LO) were used with $Q^2_{min}$ and $W^2_{min}$ set to 0.2 $GeV^2$ and 3.0 $GeV^2$ respectively which are appropriate for the kinematic range of P872. An atomic number value of 26.64 (Z=12.42) was used for the target material.

The momentum of the $\tau$'s produced from the interacted $\nu_\tau$ 's of Figure 2.1 is shown in Figure 2.3. Note, in this and subsequent figures of the tau decay parameters we show the distribution for 200 $\tau$ decays.

The $\tau$ lepton has a $c\tau$ of 0.091 cm. The decay distribution for $\tau$'s produced by the beam dump $\nu_\tau$'s is shown in Figure 2.4. These decay lengths will be easily visible in the emulsion. Only the small hatched region in the distribution will be beyond the achievable resolution. The challenge for this experiment will be in reconstructing the decay products of the $\tau$ as well as other tracks from the primary interaction in order to locate the interaction vertex in the emulsion.

The angular distribution of the $\tau$'s with respect to the incoming neutrino is shown in Figure 2.5.

The decay modes of the $\tau$ lepton are summarized in Table 2. Eighty five percent of all $\tau$ decays are single prong decays. The characteristics which are important in these decays are the kink angle between the tau and the charged decay track, and the momentum of the charged decay track. These are shown in Figures 2.6 and 2.7. In contrast with E803, where the challenge is to *reduce* the number of interactions which will require emulsion scanning, in P872 the *goal is to reconstruct and scan all interactions*. The trigger for the experiment is simply a signal of one or more minimum ionizing particles from the emulsion target ( i.e. not a muon from the dump) and should have little effect on the efficiency for detecting $\tau$'s.

Although we will deal primarily with kink events, the emulsion analysis (see sec. 4.1) does not exclude the 15% of the $\tau$ decays which have 3 or more charged tracks, and in fact such events are topologically much easier to recognize.

In Table 4 we summarize the factors which will determine the number of $\tau$ leptons which should be observed in this experiment. In order to understand how significant the

estimate of the number of $\nu_\tau$'s is, we have performed the following exercise. We select a value for each of the five main numbers (rows 3, 4, and 5 in Table 1, $n$ in the $x_f$ parameterization and $f_{D_s}$ (the form factor for $D_S \rightarrow \tau\nu$ which affects the branching ratio) from a distribution with the central value given by the weighted mean over all the measurements we could find. This distribution is a product of normal distributions representing each measurement of the same quantity. We then compute the cross section for $\nu_\tau$ weighted by the interaction probability for each set of numbers. The distribution of $10^5$ such trials is shown in Fig 2.8. From this distribution we see that the 90% confidence level is 120 events. After all acceptance and fiducial volume cuts are applied the signal is still 94 events, which we believe is a comfortable lower limit.

The number of interactions per centimeter of emulsion shown in Table 4 is taken from the mean of the distribution shown in Fig. 2.8.

| | |
|---|---|
| $\nu_\tau$ interactions per cm | 15 |
| cm of emulsion | 15 |
| prob. finding primary | 0.97 |
| fiducial volume cut | 0.90 |
| $\tau$ identification efficiency | 0.90 |
| final yield | 177 |

Table 4: Summary of $\tau$ lepton yield

(about three radiation lengths or 6cm). The efficiency for identifying electrons in this way is high, about 90% for the interactions occurring in target stacks 1 to 4 [see section 4.1.2]. For the interactions in stacks 5 and 6 we assume an identification efficiency of greater than 85% by supplementing emulsion tracking with information from the calorimeter.

## 3. Technical Feasibility of the Experiment

In principle, creating a prompt neutrino beam is simple. After interacting the primary protons in the dump, charged secondary particles are swept away or absorbed, and an unaffected neutrino beam emerges. In practice, eliminating a large muon flux produced in conjunction with the semi-leptonic decays which produce the prompt neutrinos, as well as muons from other sources, is quite challenging and in fact is the driving issue in determining the feasibility of doing this experiment. In the following sections we will discuss each of the major aspects of creating a clean prompt neutrino beam. These include a discussion of the muon flux and momentum spectrum, the level of attenuation required by the apparatus, and a description of the elements.

The design of the experiment is an optimization of the following variables subject to their constraints (the values chosen for this proposal in brackets) :

1) The volume (mass) of the emulsion [60 liters or 230kg]
2) The area transverse to the beamline protected from dump muons at the level of less than $3\times10^5$ muons per $cm^2$ [$60\times60$ $cm^2$].
3) The thickness of the emulsion target [15cm].
4) The distance of the emulsion from the dump [35m for our model beamline, PW, the absolute maximum is 40m].
5) The amount of active (magnetic) and passive sheilding [7m @3T supplemented by 5m @ 2T ; 13m steel].
6) The $\nu_\tau$ angular acceptance weighted by interaction probability [see Fig. 3.1].
7) Total number of protons on target [$2\times10^{18}$].
8) The size of the spectrometer elements downstream of the emulsion [calorimeter 2m×1].

Naturally, the major constraint in this multi-dimensional optimization is the total cost which, although easy to quantify for items like 1), is generally a complex function of the variables. A rigorous minimization of cost per event is very difficult to carry out and

even harder to verify. We have attempted to understand the interplay between them and have arrived at a compromise which we believe will result in a successful experiment. A list of items for for a preliminary cost estimate has been made appears in Section 6 below.

### 3.1 Primary Beam and Dump

This experiment requires an 800 GeV (or higher) primary proton beam. The model we have chosen, for the purpose of this proposal, is to use the PWest beamline which presently is capable of transporting an 800 GeV proton beam into PW8. In our model we consider an intensity of $1\times10^{13}$ protons per spill. Thus to reach a total integrated proton intensity of $2\times10^{18}$, will require twenty perfect weeks of running time. A preliminary shielding analysis of the PWest beamline running at this energy and intensity has been performed. The results show that at this time we see no major problems in upgrading the shielding to handle the requirements of this experiment.

One of the major requirements on the primary beam for this experiment is to limit the production of upstream muons and neutrinos from the interaction of the beam halo with the transport elements. We have studied the present layout of the transport elements (major bends and focusing) in PW6 and PW7. As presently configured, the beam can be focused to a small spot size in PW8. The preference for P872 would be to rearrange the elements to move the major bend strings upstream as far as possible, maintaining the beam size as small as possible through the required bends, and then allowing the beam to diverge as it approaches the target. We would like to have only a large diameter vacuum pipe between the last required bend and the beam dump. At the present time we have not completed such a design, but do not see any major "show stoppers" that would prohibit our ability to construct a beam with the required cleanliness.

The dump for the protons consists of a water cooled copper box 30cm on a side and a meter long. A set of tungsten inserts, 10cm in diameter and 60cm long, is intended to interact all of the 800 GeV protons plus the second generation hadrons. Most of the data will be taken with a solid insert, but a substantial fraction of data will be taken with a 1/3 density target to determine the non-dump neutrino background. It is advantageous to put this dump as close as possible to the beginning of the large muon sweeping magnet, SELMA, described below.

### 3.2 Muon Shield

#### 3.2.1. Introduction

In creating a sufficient flux of $\nu_\tau$ at the emulsion target we need to have the distance between the proton dump and the target be small enough so that the angle

subtended by the emulsion is adequate. For our purposes adequate means a majority of the interacted $\nu_\tau$ flux is contained by the target. We have set $\pm 9$ mr as the smallest desired angle (see Fig 2.2) which corresponds to a distance of 35m from the proton dump. The protons and their hadronic products are mostly contained in the dump and the dump magnet. Some low energy neutrons escape and are absorbed downstream of the magnet. The $\mu$s created from the products must be dealt with by a suitable combination of shielding by range and active, magnetic sweeping. As we will see, the relatively small target offers advantages in shielding at close range and it is much less sensitive to a residual $\mu$ flux. Recall that P872 will use *slow* spill 800 GeV protons and not a pulsed ( few milliseconds) beam.

3.2.2. Simulation

There are two main ingredients to the simulation of the $\mu$ flux at the emulsion. First, the absolute flux as a function of transverse and longitudinal momentum must be known. And second, the $\mu$ flight path must be computed individually, taking into account energy loss in material as well as deflections due to magnetic fields. We have already indicated above (variable "2") that the maximum permissible density of stray tracks in the emulsion is $3\times10^5$ cm$^{-2}$ and that we used a value for its area of 3600cm$^2$. So for the entire run, "only" $10^9$ muons are permitted through the target, and since $\approx 10^{16}$ muons are produced the net reduction is enormous. Clearly when such a reduction is required one cannot be too careful and one must use all reliable sources when determining the parameters of distributions. However, one is forced to extrapolate data and functional forms beyond their proven value, as one examines and attempts to attenuate rarer and rarer processes and trajectories. For example, how well known is the $p_T$ distribution of $\eta$ mesons? Or their production rate at $x_F > 0.6$? With this disclaimer in mind we proceed to describe the Monte Carlo.

Unlike neutrinos, where there are few distinct sources with very different mometum spectra, $\mu$s can originate from many more sources. There are, of course, the same sources which give rise to $\nu$'s: $\pi$ and K decay (low momentum component) and charm decays. In addition there are other sources which could be problematic at high momentum, like vector meson decays and so-called "soft annihilation" di-muon production. A compendium of sources of $\mu$'s and useful tables can be found in Ref. [21]. The evolution of the differential cross sections is an important issue as the relative amount of flux at high momenta ( $p > 300$ GeV/c ) is sensitive to the $x_f$ dependence. Figure 3.1 shows our estimate for the momentum spectra of all major sources of prompt

$\mu$'s and the resultant sum. Unlike the $\nu$ spectrum, the muon spectrum is not dominated at the highest momentum by charm decays, if the extrapolations to 800 GeV proton production are correct. The distributions are normalized to $D_S$ production, so the integral over all momenta yields 1.0 for muons from $D_S$, and the sum yields ($\Sigma$ on plot) 1.3. Using the numbers from Sec. 2.1 we compute the total yield for prompt sources of muons to be $9.5\times10^{-4}$.

The soft $\mu$ component ( $p < 20$ GeV/c ) is dominated by $\pi$ and K decays in the dump. The absolute spectrum was calculated using the hadronic Monte Carlo FRITIOF. The $\pi$ and K's from primary and all other subsequent interactions were weighted according to their decay probability and summed for a large number of events. The result is strongly peaked at the lowest momenta. When added to the prompt component the net flux is shown in Fig. 3.2. For the total yield of muons from all sources we get $8.9\times10^{-3}$. In the simulation software, muons are generated from the distribution of Fig. 5.3, individual decays are not generated since it would be prohibitive in terms of CPU time and in terms of longitudinal momentum, makes no difference. For the actual $p_T$ spectrum, individual sources *are* distinct. For example, $\mu^+\mu^-$ from $\eta$ decays follow a much softer $p_T$ dependence than high-mass Drell-Yan pairs. For the P872 simulation the $p_T$ dependence assumed for *all* generated muons is the one measured from charm meson decays [22] i.e. $e^{-0.84p_T^2}$. This is conservative, since other sources such as vector mesons and $\pi$ decays have much smaller coefficients, i.e. the dependence is $e^{-0.35p_T^2}$.

The simulation uses discrete steps along the muon flight path calculating the energy loss and scattering angle for each interval. If the energy loss per step (approximately 10cm in steel) exceeds 0.3 GeV and a probability threshold is exceeded then a $\mu$ pair is generated along the direction of the initial muon and all three muons propagated. For these direct $\mu$ pairs ("trident") the probability is $3\times10^{-5}$ at 1 GeV energy loss to $1\times10^{-2}$ at 100 GeV loss for a 200 GeV parent muon. The corresponding probabilties for losing 1 GeV or more and 100 GeV or more are 0.6% and $10^{-4}$ respectively. Therefore direct $\mu$ pair production is most damaging for the highest momentum muons passing through material while aimed at the target.

The individual $\mu$'s are propagated through the shield by means of a software package TRAMU [23]. Its virtue is that the energy loss of muons through dense matter is treated rigorously and agrees well with available data. The shield geometry and magnetic fields are relatively easy to incorporate but it is not particularly fast. On a SGI 4000 machine one is limited to a run of about $10^7$ generated $\mu$'s per day. Recall that this is about eight orders of magnitude less than the actual number which is created in a run of $2\times10^{18}$ 800 GeV protons. One might wonder whether *any* piece of simulation in particle

physics is reliable to such a degree, but it is invaluable for the indentification of discrete sources and paths that are not intuitive. It is also necessary (maybe not sufficient) to simulate proposed solutions to measure their effectiveness.

The muon shielding philosophy is simple. Since one cannot range out the high momentum μ's in material they must be cast aside by magnetic sweeping in powerful, suitably placed magnets. The lowest momentum μ's, for $p_\mu < 12$ GeV/c, are by far the most numerous, and are eliminated by their energy loss in steel. This leaves the intermediate energy μ's, between 20 and 100 GeV which must be carefully simulated to study the paths they can take to the emulsion target. It is clear that the design can only be as good as the model and simulation software, not a very comfortable situation. Nevertheless one must demonstrate with a reasonably conservative approach that a design is robust enough to meet the following two criteria:

1)The highest momentum μs are not the limiting factor and

2)The scattered or deflected component which is more or less uniformly distributed across the emulsion does not exceed the critical track density of $3\times10^5$ non-interacting tracks per $cm^2$.

3.2.3. SELMA Magnet

In the design we propose, the proton dump is followed by a 7m long magnet which was originally built for E615 as an analysis magnet for dimuon pairs and still sits in PW8. With proper modification of pole pieces it is an excellent magnet for sweeping high momentum μ's away and ranging the low momentum component, those less than 10 GeV/c. The magnet is capable of fields of over 3 tesla, for the central region of the (to be built) pole pieces. Although the maximum field is accomplished with a solid iron pole piece (3.34T), the optimum design for our shielding requirement, demands an air gap of at least 2cm for the length of the magnet. Hard coulomb scattering events and muonic trident production put too many tracks through the target (per incident proton) if the highest momentum μ's are allowed to traverse material while they are still aimed at the emulsion. A design with a 2cm pole gap, 20cm wide, puts the central ray of 300 GeV at 80cm from the beamline at 35m from the dump. The central field used is 2.98T.

This magnet plays a critical role in the shield design. There are two other magnets at Fermilab which would also be appropriate: the hyperon magnet in P Center and the SM12 dump magnet in M East.

3.2.4. Other Active and Passive Shield Components

Simplicity is a virtue in the shield design. As an example, one might be concerned that the return flux in steel of the SELMA magnet would provide a path for a muon, swept away from the central field, to be turned back into the emulsion. Also, charm and vector mesons created with unusually large transverse momenta could be focused directly to the emulsion, for a certain range of longitudinal momenta. These muons have enough transverse momentum to leave the high field pole region of the SELMA magnet and enter the low field region near the coils where they receive a $p_T$ kick as low as 2.4 GeV/c (compared to 6.3 GeV/c in the pole gap). Thus a muon with an initial $p_T$ of 2.4 GeV/c can be *focused into the emulsion*. Simulation indicates that if 15GeV of range material is put in front of the emulsion, the muons which are *focused* into the emulsion all lie within 40cm of the central (infinite momentum) ray and have total momenta less than 80 GeV/c (higher momenta muons cannot escape the pole piece unless they have exceptionally high $p_T$). This indicates that if an additional amount of magnetic sweeping were added at some distance from the emulsion, it would act like a "field lens" deflecting the troublesome muons just far enough from the area that must be protected.

We propose to add a square-frame toroid magnet without a gap and with the coil around a pole piece 40 cm wide centered on the beamline and 5m long. A sketch of this magnet is shown Fig 3.3. The saturated steel provides material for range as well as sweeping. The other sides of the "frame" must be far enough away so other paths for lower momenta $\mu$'s are not introduced. An important design feature is to make sure that the field in the return steel is smaller in magnitude than the piece used for sweeping on-axis $\mu$s. Therefore the "frame" is constrained on one side by the size of the emulsion target, and thickened by 50% on the other sides, thereby reducing the field strength.

In addition to the active shielding, we require the space downstream of the toroid filled with steel as a passive range material which shadows the emulsion and protects against the muons directed by the toroid return field into the critical area. Including the steel of the toroid there is at least 23m of steel-equivalent material between the dump and the emulsion which is about 38 GeV of range for 40 GeV muons.

Another type of protection must also be provided by the beamline/shield system which is just as crucial. If the power is interrupted to the shield magnets during a full intensity run, the flux of muons will increase by a factor of about $10^5$ during the spill, which implies a track density close to the maximum allowable. To prevent this, a fail-safe system, similar to a beam safety chassis, must be in place and connected to critical

elements, such as dipole strings, which can shut the beam off from far upstream within 50 milliseconds of detecting a failed shield magnet.

### 3.2.5. Results

The shield system results presented here are a simulation of the configuration shown in Fig. 3.4. The high energy muons are swept clear of the emulsion target as shown in the transverse distribution at 35m from the dump in Fig 3.5. Each dot in Fig. 3.5 represents an estimated $2\times10^7$ $\mu$'s integrated over the run and corresponds to a track density in the emulsion of $0.4\text{x}10^5$ $cm^{-2}$ if they are uniformly distributed. Recall that for background tracks which have a broad angular spread the maximum allowed density is about $3\text{x}10^5$ $cm^{-2}$.

One other process that is potentially troublesome is muons interacting with the large coulomb field of the nuclei and producing hadron showers in the steel, the so-called photo-nuclear interactions. For a 300 GeV muon this process has a cross section of 300$\mu$b for an energy loss of $\geq$3 GeV. This process is not incorporated into the simulation explicitly. To estimate its effect we use the calculated muon flux, momentum spectrum and energy loss in the last 2m of steel and the 1m of concrete to get the number of interactions. Each interaction is then weighted by the probability of penetrating the remaining shield, i.e. punching-through, and summed. We do not account for the direction of the shower even though they must populate the region to either side of the emulsion, where the high energy muons populate the distribution in Fig. 3.5. We do, however, not count interactions to those within 1m of the emulsion. The result is that we expect $1\times10^{-4}$ showers per muon to escape the material which, assuming three minimum ionizing tracks per shower, will add an additional $3\times10^7$ tracks in the emulsion or $3\times10^{-2}$ of the maximum allowed density.

In the early proposals to do this experiment, eliminating this flux was also a major technical challenge. The 15 foot bubble chamber detector, which was operated in the fast spill neutrino beam, was limited to < 100 muons per $10^{13}$ protons over the fiducial area. The bubble chamber was located 190 meters downstream of the dump. The proposed solution for this problem included strong magnetic fields for sweeping high energy muons followed by range absorber (dirt) to eliminate the low energy muons.

It is the compactness, the rate capability (!) and the ultra-high resolution which makes emulsion the only contender for successfully doing P872 in the present decade.

# 4. Experiment

## 4.1. Apparatus

In each of the following sections we briefly discuss each of the detector elements. Since the philosophy behind doing P872, is to use the same technique and spectrometer design as E803, we have not yet put a lot of independent review into the design, but rather rely on the earlier work done for the E803 proposal. However, in the interest of economics and schedules we are beginning to try and match the experiment requirements to possible existing equipment.

### 4.1.1. Charged particle veto

This will be a conventional scintillator, photo tube hodoscope. It must be large enough to be an effective "shield" against the muon flux from the dump and hence must cover about $3\pi$ sterad relative to the emulsion. We have located large ($20\times30\times300$ cm$^3$) scintillation counters ideal for a "wall" veto just upstream of the target. This would be supplemented with more conventional counters on the sides and above the target. It is desirable to keep the trigger rate low, and hence scan load small, by rejecting straight through muon triggers. Since the ratio of muons from the dump to the actual interaction rate is $\approx3\times10^5$ the amount of "protection" afforded by the veto should be at least $10^4$ and should be designed for $10^5$. This is possible in a carefully designed system with three independent layers of counters covering the front of the target ($60\times60$ cm$^2$).

### 4.1.2. Emulsion target

The area of the emulsion will be approximately $60\times60$ cm$^2$. If the problem of identifying electromagnetic showers in the emulsion can be solved, we will use six, 2.5 cm thick modules, for a total target thickness of 15 cm (of active emulsion). This constitutes a volume of 60 liters. Each module consists of 25 sheets of emulsion coated polystyrene (0.5mm on each side of the 0.10mm plastic backing) with another sheet 1 cm downstream, termed a "changeable sheet", since it will be replaced about once a month. Its purpose is to provide very reliable linking between the fiber tracker and the emulsion, with its track density low to reduce random associations. The proposed emulsion target and fiber tracker configuration are shown in Figure 4.1.

4.1.3. Scintillating fiber tracker

Interleaved between each of the emulsion modules are a set of x and y scintillating fiber tracking modules. At the present time we anticipate that the design of this system will be very similar to the system being installed in the CERN CHORUS experiment.

4.1.4. Drift chambers

We hope to be able to find previously used chambers which meet the requirements of this experiment.

4.1.5. Analysis magnet

The existing PW8 analysis magnet (ROSIE) has an aperture of 202 cm (horizontal) by 94 cm (vertical). The length is 230 cm. The current will be set to provide a $p_T$ kick of 0.3 GeV/c.

4.1.6. Muon identifier

We intend to modify existing steel plate stacks into a suitable muon identifier using range only, no pulse height information. It must be greater in total depth than one suitable for E803 since the muon energies are on average about 2.5 times greater .

4.1.7. Calorimeter

We have yet to fully specify what kind of performance we need with the calorimeter and must study it with Monte Carlo work. Its dimensions must be about 1.5m×2.5m for full acceptance of the products of interactions. We will look for existing equipment to meet our needs, or perhaps use a design from E803 scaled to P872.

4.2. Trigger and Data Acquisition

We anticipate that the trigger and data acquisition needs of this experiment will be easily met by use of existing/"off the shelf" components.

## 5. Analysis

### 5.1. Emulsion scanning

After exposure, the emulsion is first developed at Fermilab, then shipped to Japan for more processing before being scanned. The target sheets are cut up into a 9×9 array and then "remapped" by placing a piece from each successive target sheet on a new plate so that for most tracks, scanning to or from the primary interaction does not involve changing plates on the scanning table, providing a big savings in time. Each plate must be calibrated relative to fiducial marks and distortions in the emulsion understood. Processing 60 liters this way will take about six months. We hope to keep the actual number of events to scan for physics down to about $10^4$ by having a good trigger / veto system and excellent muon tracking. It should take an additional six months to reduce the data to a couple of hundred $\tau$ candidates.

Given one track which has been matched to the emulsion target module (by linking successively hits in the spectrometer, fiber tracker and changeable emulsion sheet) the primary interaction is found by scanning back (upstream) and seeing the vertex. If there is a muon reconstructed in the spectrometer it is scanned back and if it is linked to the primary vertex the event is dropped at this point, eliminating half of the scan load. If not, all tracks are followed down (downstream) until a cut-off distance is reached, probably about 7.5mm, which accepts 97% of the $\tau$ decays. If any track shows a discernible kink, it is kept as a candidate event.

#### 5.1.1. Spectrometer reconstruction

The role of the spectrometer in the $\nu_\tau$ analysis is two-fold: 1) to reconstruct at least one track from the interaction and 2) and to provide additional information after candidates are found in the emulsion, such as the $p_T$ of the daughter of a kink decay. Each emulsion module is 7% of an interaction length and we calculate from the charged particle multiplicity that only 3% of all events will be rejected for having all tracks reinteract in the remaining target.

For other analyses such as determining the $E_\nu$ spectrum, where the emulsion is not required, the spectrometer information on the whole event is necessary. It will be necessary to compute the total electromagnetic energy as well, which is not just simply summing the energy deposited in the calorimeter, but will involve estimating the energy

## 5. Analysis

### 5.1. Emulsion scanning

After exposure, the emulsion is first developed at Fermilab, then shipped to Japan for more processing before being scanned. The target sheets are cut up into a 9×9 array and then "remapped" by placing a piece from each successive target sheet on a new plate so that for most tracks, scanning to or from the primary interaction does not involve changing plates on the scanning table, providing a big savings in time. Each plate must be calibrated relative to fiducial marks and distortions in the emulsion understood. Processing 60 liters this way will take about six months. We hope to keep the actual number of events to scan for physics down to about $10^4$ by having a good trigger / veto system and excellent muon tracking. It should take an additional six months to reduce the data to a couple of hundred $\tau$ candidates.

Given one track which has been matched to the emulsion target module (by linking successively hits in the spectrometer, fiber tracker and changeable emulsion sheet) the primary interaction is found by scanning back (upstream) and seeing the vertex. If there is a muon reconstructed in the spectrometer it is scanned back and if it is linked to the primary vertex the event is dropped at this point, eliminating half of the scan load. If not, all tracks are followed down (downstream) until a cut-off distance is reached, probably about 7.5mm, which accepts 97% of the $\tau$ decays. If any track shows a discernible kink, it is kept as a candidate event.

#### 5.1.1. Spectrometer reconstruction

The role of the spectrometer in the $\nu_\tau$ analysis is two-fold: 1) to reconstruct at least one track from the interaction and 2) and to provide additional information after candidates are found in the emulsion, such as the $p_T$ of the daughter of a kink decay. Each emulsion module is 7% of an interaction length and we calculate from the charged particle multiplicity that only 3% of all events will be rejected for having all tracks reinteract in the remaining target.

For other analyses such as determining the $E_\nu$ spectrum, where the emulsion is not required, the spectrometer information on the whole event is necessary. It will be necessary to compute the total electromagnetic energy as well, which is not just simply summing the energy deposited in the calorimeter, but will involve estimating the energy

of electrons which are soft ( < 500 MeV) and whose tracks may not be seen downstream of the magnet. Studies with an E803 simulation show that recovering energy resolution is possible but probably only for electrons which originate downstream of the third (of the six) modules for the P872 target.

## 5.2. Physics results

### 5.2.1. $\nu_\tau$ Interactions

The expected yield of $\nu_\tau$ and the backgrounds were computed above in Sec. 2. Here we will briefly discuss some comparisons of the data to what is expected of the Standard Model $\nu_\tau$ interactions. The expectations are not based on detailed Monte Carlo work and are not intended to be rigorous at this point.

To a good approximation there are equal numbers of neutrinos and anti-neutrinos in the beam. Thus about one third of the interactions come from anti-neutrinos and at least 70% can be tagged unambiguously by observing the sign of the $\tau$. Then from Sec.3 we see that the total number of tagged $\nu_\tau$ interactions is about 40. So the anti-neutrino cross section can be computed to about 20% accuracy and the reconstructed $y$ distribution should show the characteristic shape, $N \approx (1-y)^2$. The analysis will also yield the first measurement of $F_2(\nu N)$ for the tau neutrino.

### 5.2.2. Extraction of $\nu$ spectrum

The major source of neutrinos above 50 GeV in energy is charm semi-leptonic decay. The other main component of $\nu$ flux is decays of $\pi$ or K, however in a beam dump configuration this component dominates only at $\nu$ momenta less than 20 GeV. Hence if one can measure $E_\nu$ one can extract the $x_f$ dependence of the source. Information from the emulsion is not necessary, as $E_\nu$ is determined from charged particle tracking and calorimetry. All charged current interactions ( above 50 GeV) can be used in the analysis, since electronic and muonic (as well as anti-neutrinos) are produced equally in charm decay as a first approximation. Critical for the $x_f$ dependence are high energy interactions, those in excess of 200 GeV. For P872 we predict that we can determine the large $x_f$ behavior for proton interactions to an accuracy of $\pm 0.4$ on the exponent, $n$ , for the differential cross section parameterization $\propto (1 - |x_f|)^n$ .

The absolute number of high energy CC interactions and their dependence on $E_\nu$ provide a degree of normalization for the number of $\nu_\tau$ expected in P872 by effectively reducing the uncertainty on two of the numbers crucial to calculating the $D_S$ yield (and hence $\nu_\tau$ yield). The error on the exponent $n$, determined from experiment, as well as the

$D^{\pm}$ cross section are reduced. Thus we will know how many $\nu_\tau$ interactions are expected to better precision after analyzing the majority of the interactions due to $\nu_e$ and $\nu_\mu$.

5.2.3. Lifetime of $\nu_\tau$

There are no laboratory limits for the $\nu_\tau$ lifetime, but a considerable number of astrophysical processes and events constrain the lifetime, especially for the radiative mode of $\nu_\tau \rightarrow \nu\ \gamma$ [24]. However, P872 can probe into a region not excluded astrophysically, from 10 MeV and 100 seconds in lifetime to very short values ($< 10^{-10}$ s) by looking for electron positron pairs created in air (for $m_\nu > 1$ MeV) or photons converting in a radiator sheet placed outside the emulsion. The sensitivity is predicated on the expected $\nu_\tau$ flux given above [Sec 2]. Majorana neutrinos can presumably also decay $\nu_M \rightarrow \nu\ g$ where $g$ is a Goldstone boson left over from the symmetry breaking which gave rise to $m_\nu$. Here we can only state a upper limit for very short lifetimes by observing a lower than expected number of $\nu_\tau$ interactions.

Lifetimes in the range of 10 seconds or less are not constrained by cosmological arguments such as nucleosynthesis and masses on the scale of MeV are not ruled out experimentally. Therefore a "direct" measure of the $\nu_\tau$ lifetime is worthy of the small amount of extra effort needed and does not compromise the number of $\nu_\tau$ interactions in the emulsion target.

5.2.4 Search for the Magnetic Moment of $\nu_\tau$

The present upper limit on the magnetic moment of $\nu_e$ and $\nu_\mu$ is $10^{-9}\ \mu_B$. For the tau neutrino the limit has been placed at $5.4\text{x}10^{-7}\ \mu_B$ by WA66 [25] which did not directly observe $\nu_\tau$ charged current interactions. A stable $\nu_\tau$ with a mass in the range of 1 to 30 MeV could be a component of Cold Dark Matter if it had an anomalous large magnetic moment of order $10^{-6}\ \mu_B$.

The proposed run for P872 would yield about $3\text{x}10^{15}\ (\mu_\nu/\mu_B)^2$ events due to the pseudo-elastic scattering events from the e-m coupling to electrons and the ratio of these magnetic moment induced scattering events to the Standard Model elastic scattering events is about $10^{14}\ (\mu_\nu/\mu_B)^2$. The signature for such events consists of a single electron track without evidence of nuclear breakup in the emulsion and with a $y$ distribution that peaks strongly toward $y = 0$. In addition, events which scatter from neutrinos with an observable $\mu_\nu$ does not peak at $\theta_{\nu e} = 0$ like elastically scattered events but is broader by an amount that should be visible in emulsion ( peak around 5 milliradians). Conservatively, we expect to place an upper limit of $5\text{x}10^{-8}\ \mu_B$ in P872.

## 6. Beam Test

### 6.1 Test beam requirements

We recognize that we have proposed a solution to the serious technical problem of attenuating muons based on simulations. For this reason, we feel that further pursuit of this experiment depends on successfully demonstrating that we have indeed achieved the required attenuation. It was stressed above that it might be presumptuous to assume that a design which is adequate against simulated muons will completely foil the real ones, since the attenuation must exceed $10^6$. Although we believe the simulation to be conservative with respect to the momentum spectrum and the shield components we propose to use, we need to be sure that the system meets the easily measured and known limits imposed by the emulsion target. This value, $3\times10^5$ tracks per $cm^2$, can be restated as approximately $5\times10^3$ muons through the emulsion per spill [assume 20 weeks at $10^4$ cycles per week] .

We propose to build the muon shield including the beam dump to test the design before exposing the emulsion, as soon as possible. We would require a flux of 800 GeV protons to be at least $10^{12}$ per spill, 10% of the intended beam for the emulsion run, in order to measure attenuation to a sufficient level in a short amount of time. We would require at least 3 months of time after installation of the steel and magnets but do not anticipate needing protons on a continuous basis for this test. We are considering ways of staging this test in order to minimize the financial impact. A list of pieces required for the test is given below.

- A beam dump with tungsten insert capable of handling $1\times10^{13}$ 800 GeV protons per 20 second spill, and its associated RAW system.

- Adequate shielding around the dump and magnet.

- New pole pieces installed in the SELMA magnet (7m long)

- A new magnet built as shown in Fig 3.3 (essentially saturated steel along beam centerline with return steel 3.5m from beamline).

• Approximately 1800 tons of steel for passive shielding, installed without any cracks or voids.

• Installed power to run SELMA, ROSIE and the spoiler at desired currents.

• A scintillation counter system, with data acquisition, to measure the muon flux as a function of position at the intended target position, 35m from the dump.

• A concrete block cave at 33m from the dump and detectors to measure the neutron flux within.

6. 2 Cost Estimates

We will persue detailed cost estimates for the beam test if we receive encouragement to perform P872.

---

[1] E636; "Neutrino Interaction Studies at Tevatron Energies using a Beam Dump Technique to Produce the Neutrino Beam" (1980) (proposal).

[2] E646; "Search for the $\nu_\tau$ and Study of $\nu_\varepsilon$ and $\nu_\varepsilon$ Interactions" (1980) (proposal) .

[3] A.E. Asrahyan *et. al.* Preprint ITEP-133 (1984)

[4] A. de Rujula *et. al.* Preprint CERN TH6452, IFAE-92/001

[5] H. Harari, Phys. Lett. B227 (1989) 489.

[6] CHORUS "A New Search for $\nu_\mu - \nu_\tau$ Oscillation" CERN-PPE/93-131.

[7] P803 proposals and updates

[8] E653, "Charm Meson Production in 800 GeV/c Proton-emulsion Interactions", Phys. Lett. B263 (91) 573.

[9] E743, "D-meson Production in 800 GeV/c pp Interactions", Phys. Rev. Lett. 61 (1988) 2185.

[10] E653, "Measurement of the Branching Ratio $D^+ \rightarrow K^*(892)\mu\nu$", Phys. Lett. B, 286 (1992) 187.

[11] E653, "A Study of the Semimuonic Decays of the $D_S$", Phys. Lett. B, 309 (1993) 483.

[12] WA75, "Observation of the Muonic Decay $D_S \rightarrow \mu\nu$", Progress of Theoretical Physics 89 (1993) 131.

[13] E653 Preliminary results (to be published)

[14] CLEO, "First Measurement of $\Gamma(D_S \rightarrow \mu\nu)/\Gamma(D_S \rightarrow \phi\pi)$", CLNS 93/1238.

[15] E769; G. Alves Proceedings DPF 92: The Fermilab Meeting (1992) 718, World Scientific Publishers, Singapore.

[17] C. Foudas *et.al.* Phys. Rev. Lett. 64 (1990) 1207

[18] E531, N. Ushida *et. al.* Phys. Lett. B206 (1988) 375.

[19] reference 1

[20] S. Hasegawa *et. al.* Prog. Theor. Phys. Suppl. 47 (1971) 126.

[21] A. VanGinneken, "MUSIM-Program to Simulate Production and Transport of Muon in Bulk Matter", FERMILAB-FN-594 (1993).

[22] *op. cit.* 9,10

[23] *op. cit.* 22

[24] E. Kolb and M. Turner, "Limits to the Radiative Decays of Neutrinos and Axions from $\gamma$-ray Observations of SN1987A", Phys. Rev. Lett. 62 (1989) 509.

[25] WA66, "Bound on the tau neutrino magnetic moment from the BEBC beam dump experiment", Phys. Lett. B280 (1992) 153.

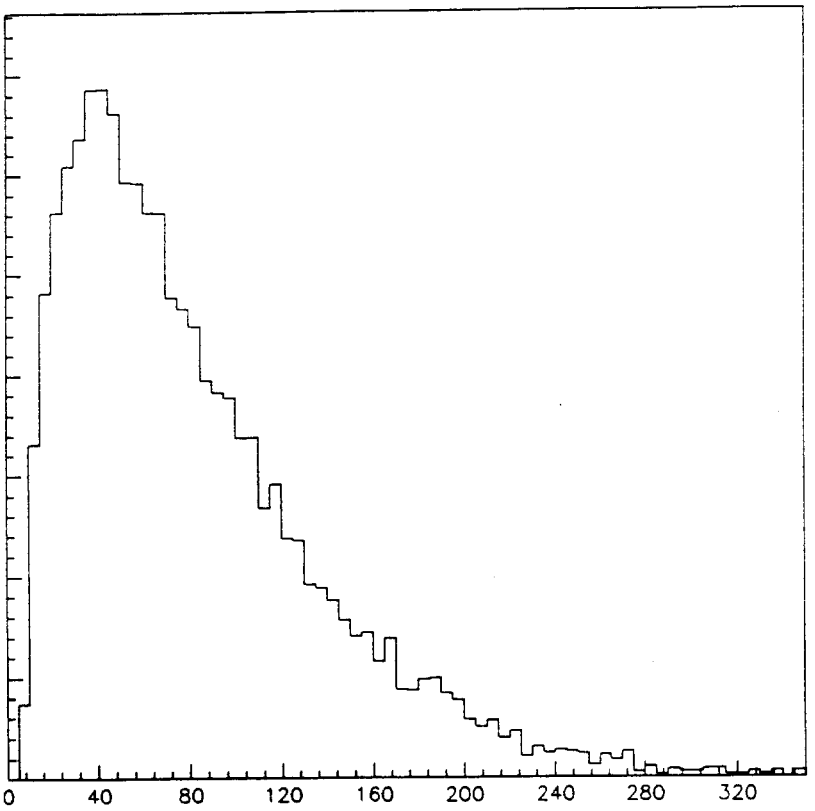


**Figure 2.1** The energy spectrum for the $\nu_\tau$ flux generated in the dump and passing through the emulsion target. Each entry is weighted by the interaction probability.

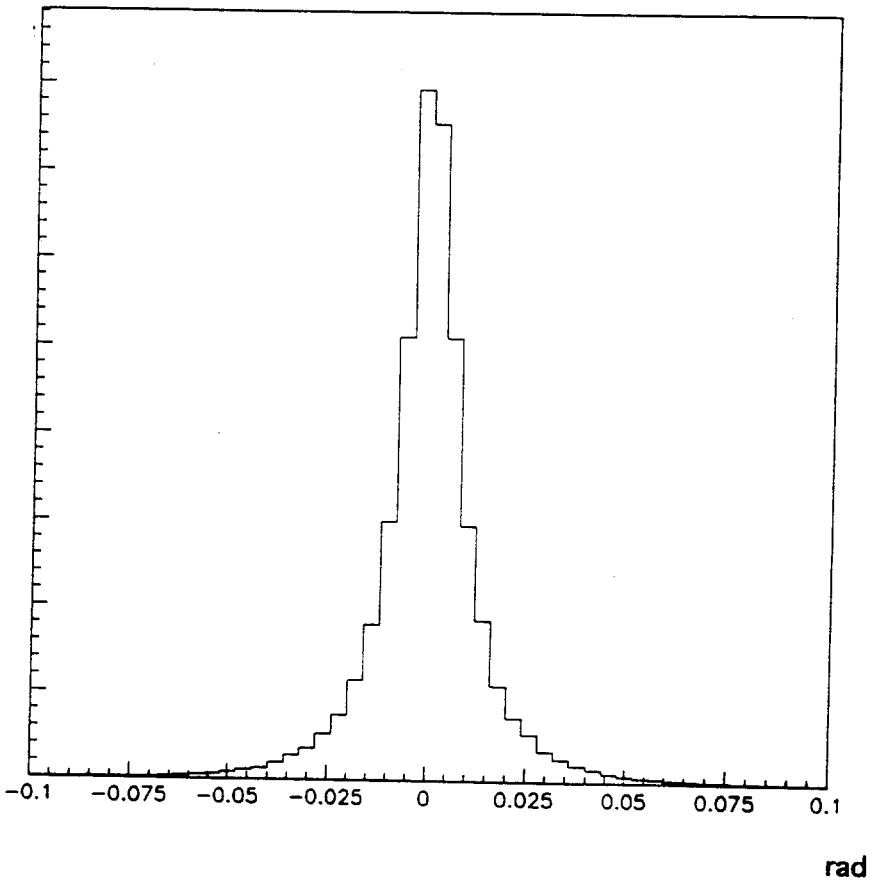


**Figure 2.2** The angular distribution of the $\nu_\tau$ flux weighted by the interaction probability.

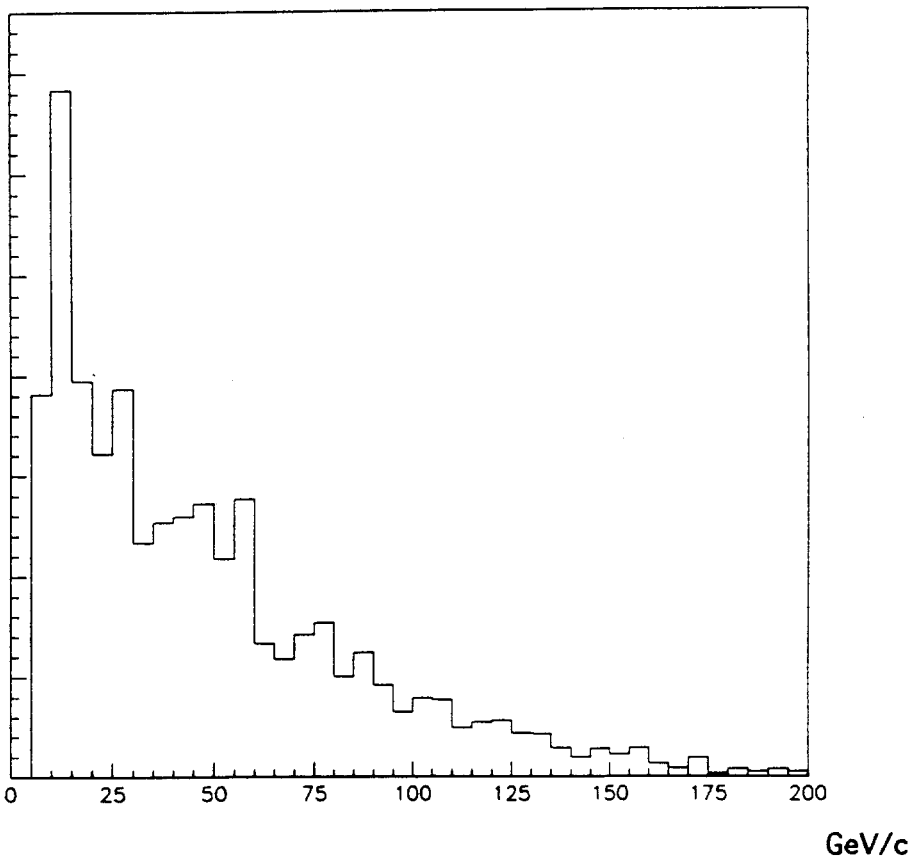


**Figure 2.3** The distribution of $\tau$ momenta from simulated emulsion CC interactions.

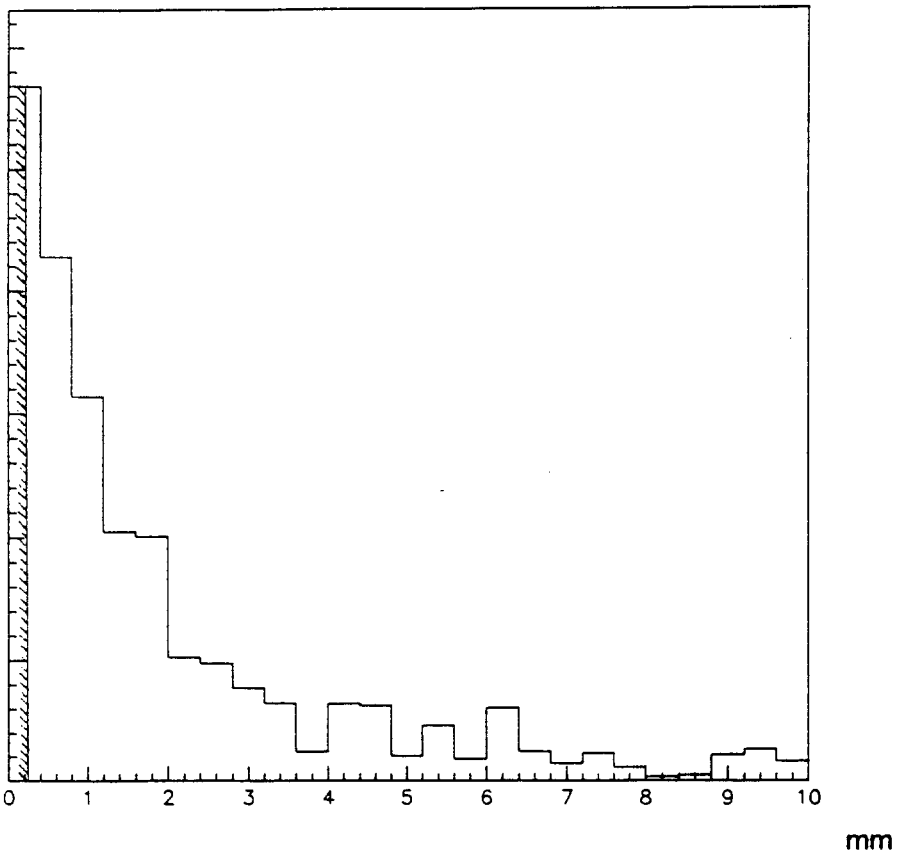


**Figure 2.4** The $\tau$ decay length distribution. The emulsion track cut-off for scanning is 7.5 mm.

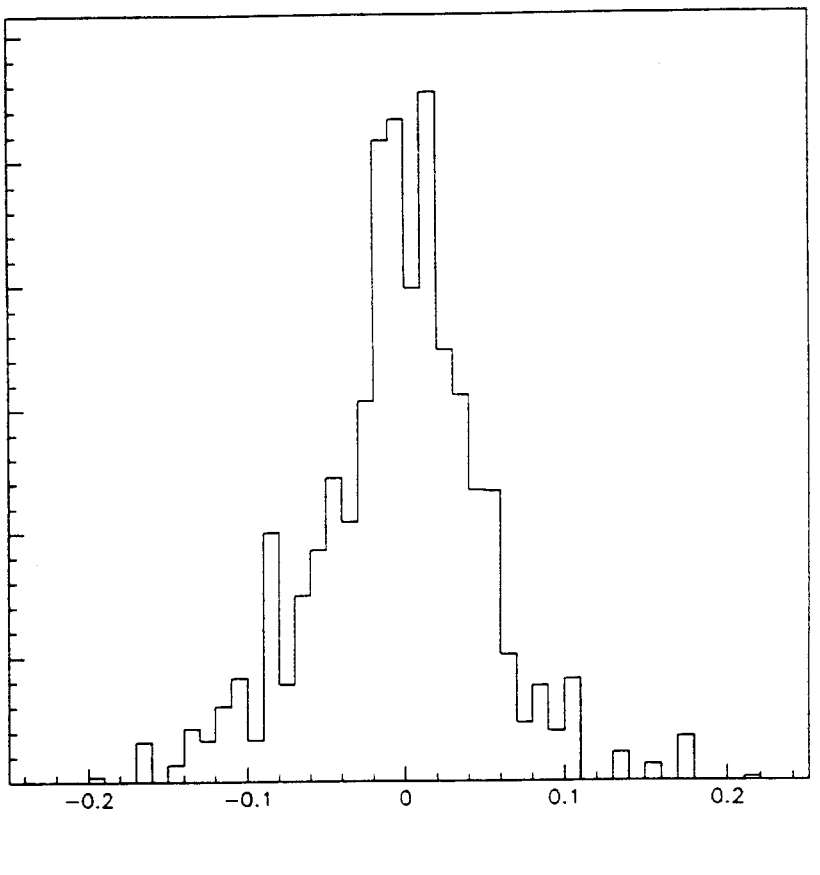


**Figure 2.5** The angular distribution of the $\tau$ with respect to the $\nu_\tau$.

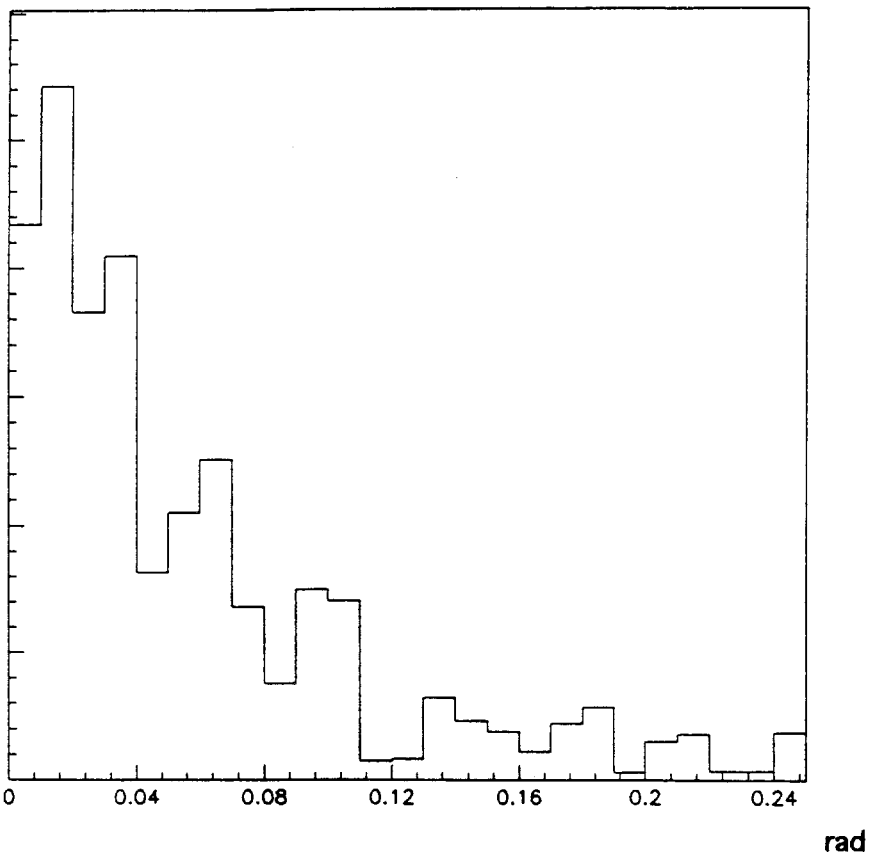


**Figure 2.6** The "kink" angle between the $\tau$ and its charged daughter. This decay topology has a probability of 85%. The efficiency for seeing kinks in the emulsion is >90% for angles >0.004.

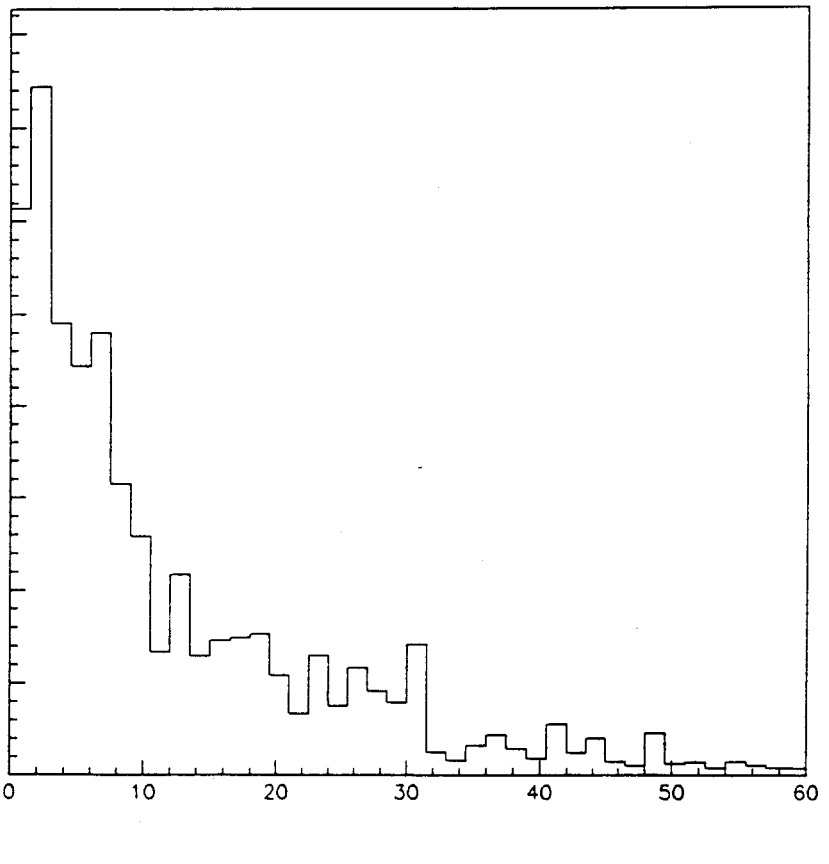


**Figure 2.7** The momentum of the daughters of $\tau$ decays for all modes.

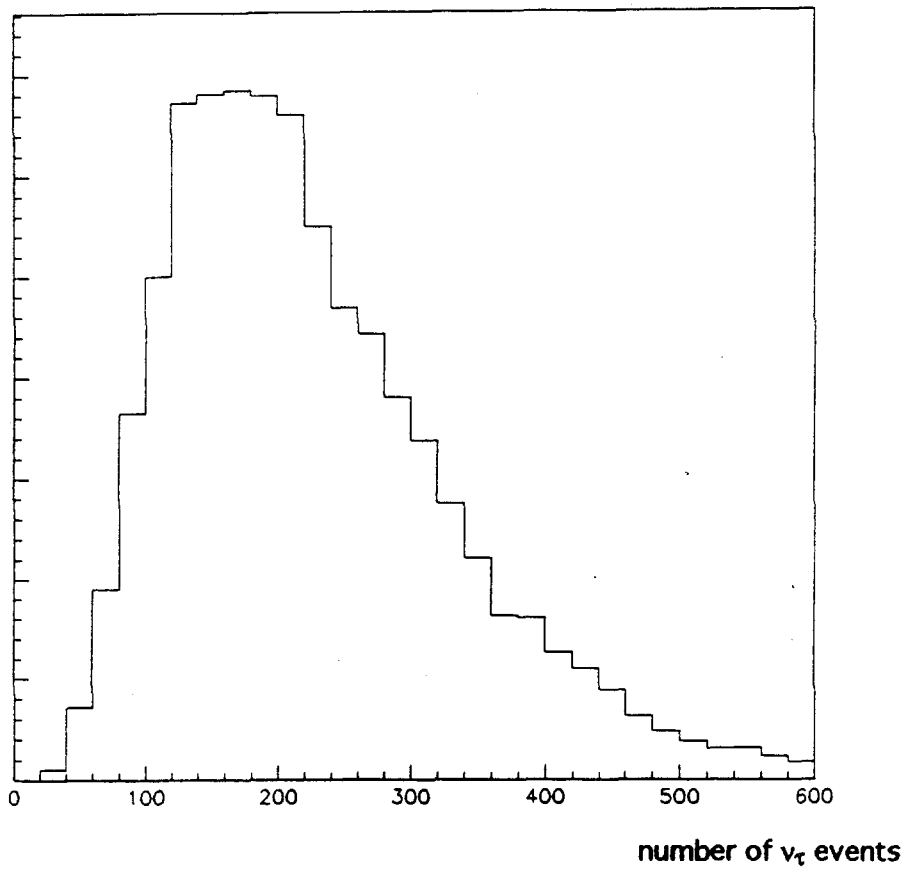


**Figure 2.8** The number of found $\nu_\tau$ interactions from an ensemble of $10^5$ "experiments" where the five measured quantities needed for predicting the of $\nu_\tau$ interactions are chosen from distributions derived from the data and its uncertainties. From this set there is a 90% chance that there will be at least 120 interactions in the final sample. This distribution should improve, i.e. become narrower after the $\nu_e$ and $\nu_\mu$ CC interactions are analyzed.

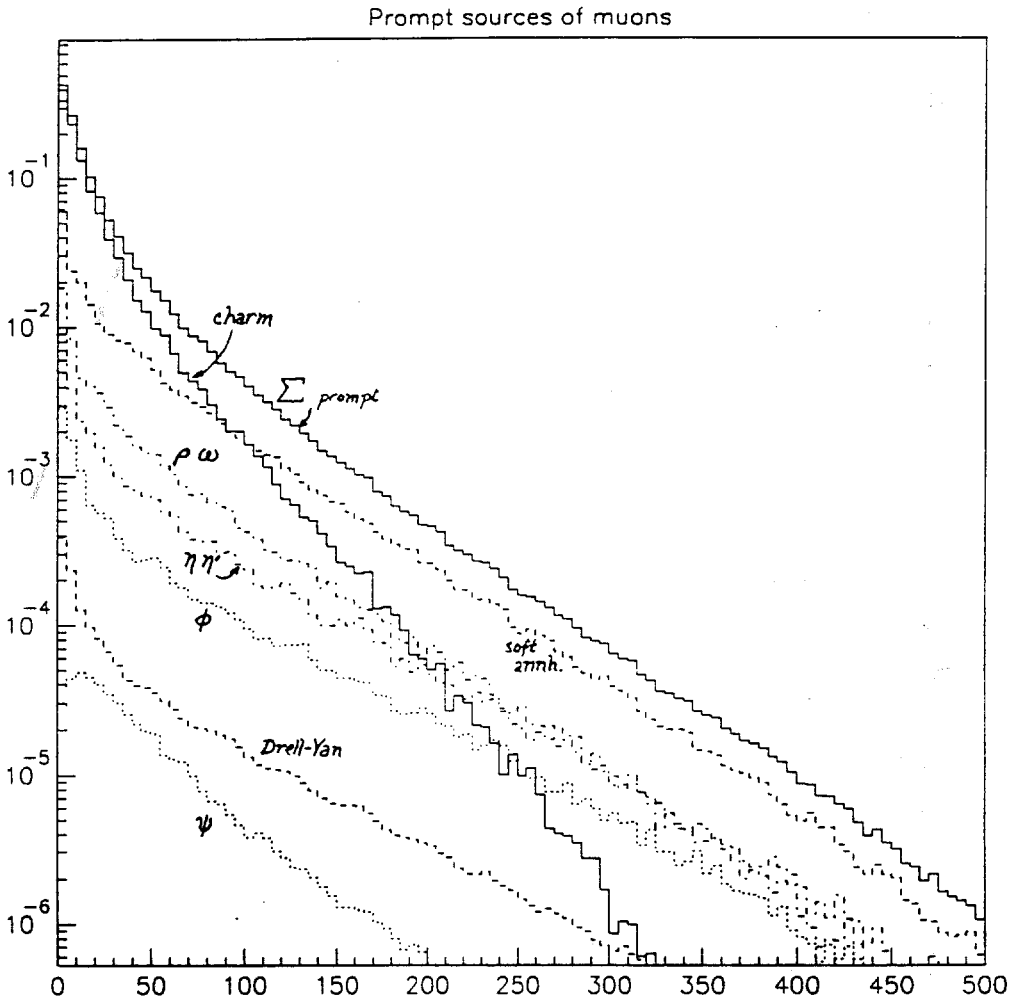


**Figure 3.1** The calculated muon spectrum from prompt sources including charm meson decay. It is normalized but the total integrated flux from these sources is computed to be $9\times10^{-4}$ muons per incident 800 GeV proton.

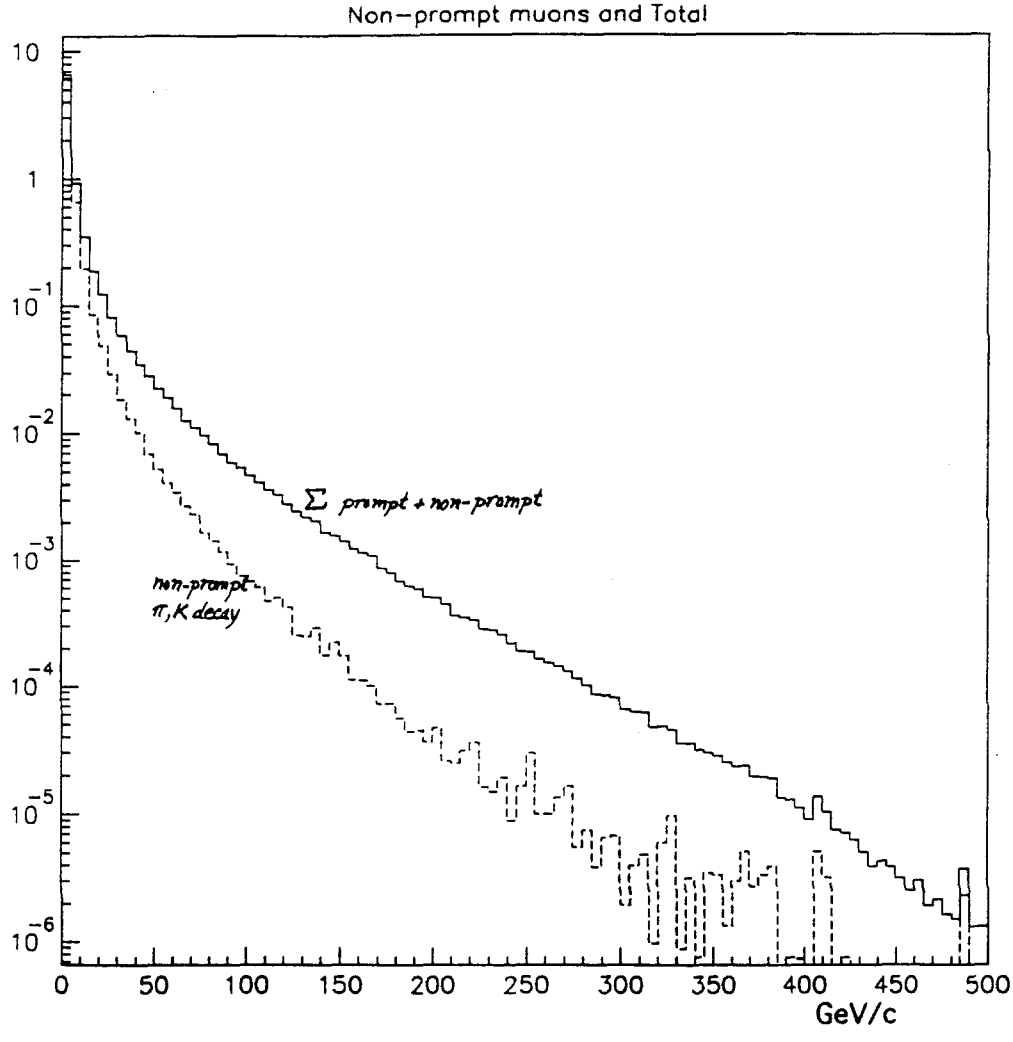


**Figure 3.2** The estimated muon spectrum used in the Monte Carlo which transports them through the elements shown in Fig. 4.2. The great number of low momentum muons (from $\pi$ and K decay) are not a concern as the emulsion is completely shielded against $p_\mu < 20$ GeV/c.

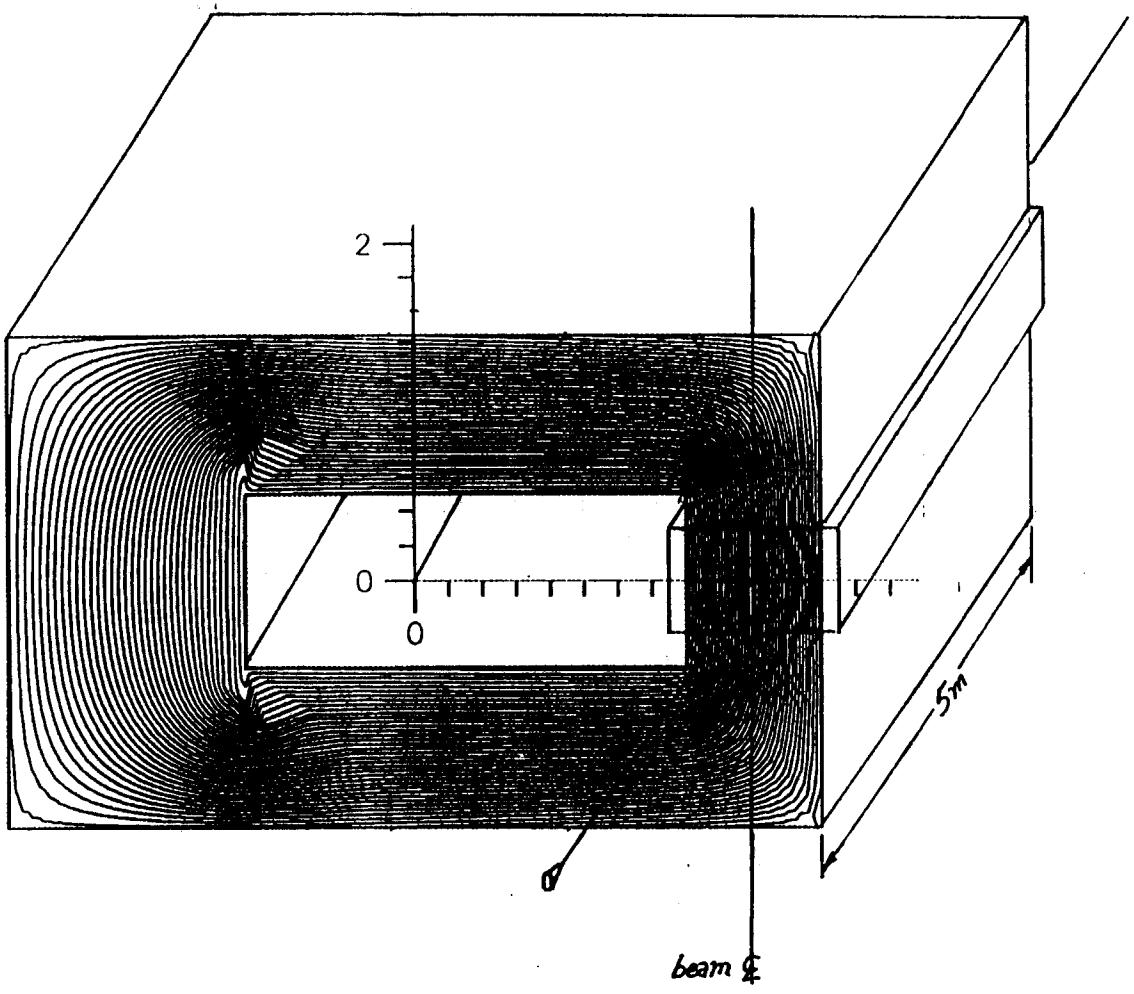


**Figure 3.3** A sketch of the toroid spoiler magnet used in the simulation. A coil with 50 K amp-turns yields a central field of 2.05T.

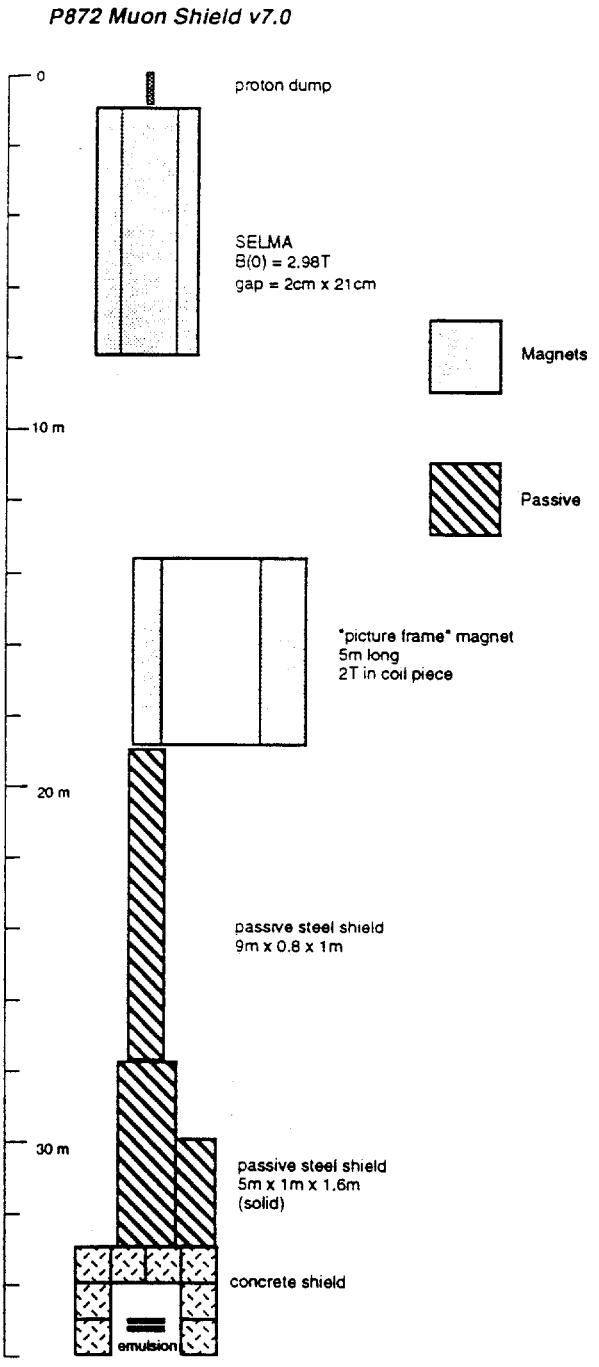


**Figure 3.4** The muon shield configuration (plan view) showing the size and relative position of the components. The two magnets are shaded gray, the passive shield is cross-hatched.

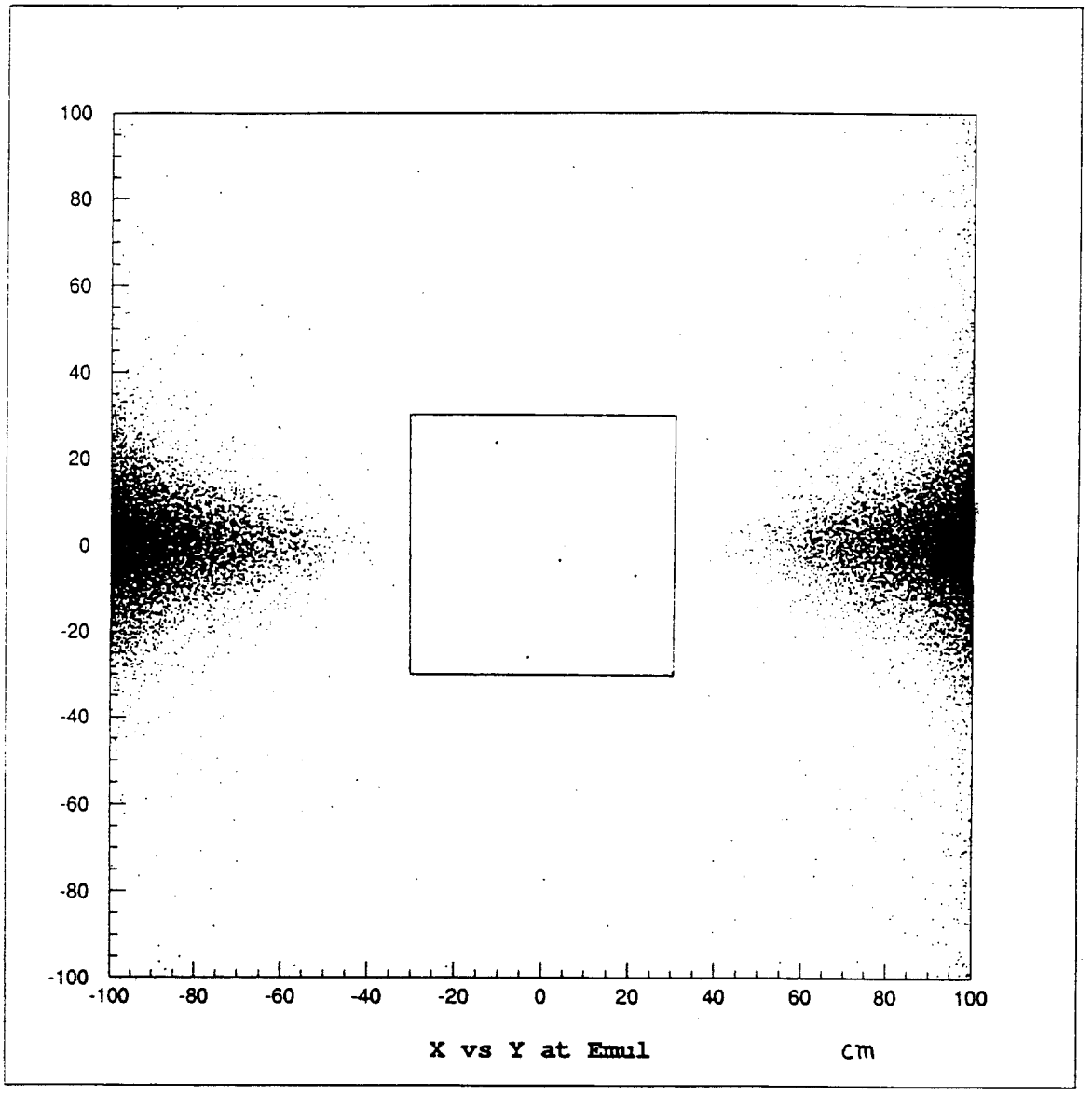


**Figure 3.5** The distribution of muons at the emulsion, 35m from the dump, as simulated by the Monte Carlo software. Each dot on the plot represents $6\times10^{7}$ muons for a run with $2\times10^{18}$ protons. The maximum allowable density of tracks in the emulsion is $1\times10^{9}$.

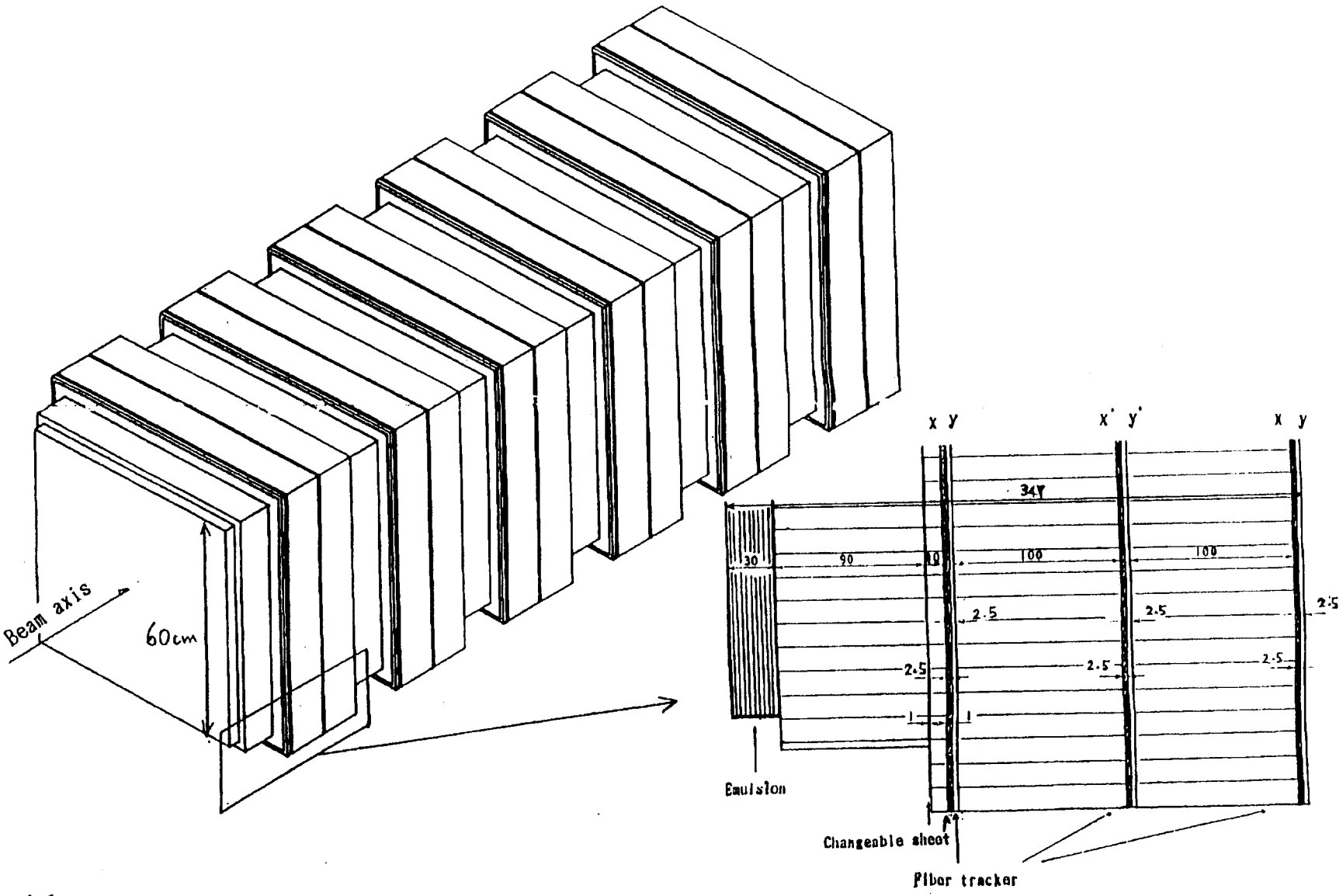


**Figure 4.1** The emulsion target configuration presently favored. It consists of six identical modules, each made of : emulsion target sheets, emulsion changable sheet, and three pairs of scintillating fiber planes, with spacers as shown. The true emulsion depth is 15 cm.

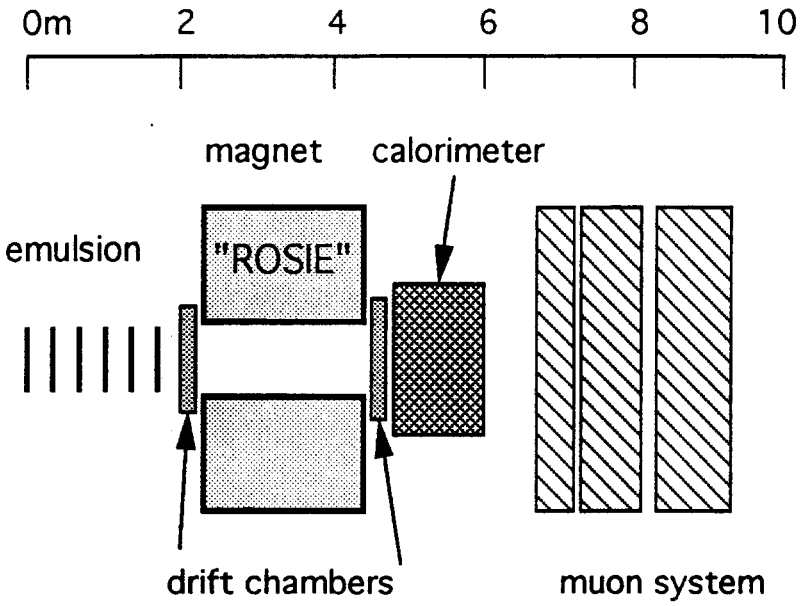


**Figure 4.2** Plan view of the spectrometer elements that are needed for P872. In the PW model, the spectrometer magnet and iron for muon identification exist.

A Proposal for Continuing

# E872

in the next

Fixed Target Run

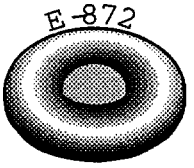


September 1997

# Abstract

Experiment E872 has completed a successful first run during the 1996-1997 fixed target period. During that time we demonstrated that a short prompt neutrino beam could be constructed and operated with a low enough background to use an emulsion target 36 meters from a primary beam dump. Our prompt neutrino beam was used to produce neutrino interactions in two different types of emulsion target modules. We commissioned all of the elements in our spectrometer and have determined that we efficiently triggered on neutrino interactions in the emulsion target. We estimate that the present emulsion contains 84±30 tau neutrino charged-current interactions. Of these events 27±10 were produced in the pure bulk type emulsion. After applying spectrometer and live time efficiency estimates, we anticipate being able to identify approximately two-thirds of these interactions.

While we are confident that we will make the first direct observation of the charged-current interaction of the tau neutrino, the results from our first run will fall short of the goals of our original proposal by about a factor of five. The opportunity for a second run is therefore quite appealing to our collaboration. In such a run we believe that we can significantly increase and improve the final data sample, with lower background, an improved spectrometer, and with improved experiment live-time. With more than 100 events we will be able to make measurements of the tau lifetime and branching ratios.

In the document which follows we present a review of the design and first run performance of the E872 beam and detector. We then present a description of the modifications that would be made for a follow on run and a preliminary estimate of the resources which would be required.

# The E872 Run 2 Collaboration

K.Kodama, N.Ushida
*Aichi Univ. of Education*

S.Aoki, T.Hara
*Kobe Univ.*

K.Hoshino, K. Ito, M.Kobayashi, M.Miyanishi, M.Nakamura, K. Nakajima, T. Nakano, K.Niwa
*Nagoya Univ.*

H.Okabe
*Science Education Insitute of Osaka Prefecture*

M.Adachi, M.Kazuno, Y.Kobayashi, E.Niu, S.Ono, H.Shibuya, Y.Umezawa
*Toho Univ.*

Y.Sato, I Tezuka
*Utsunomiya Univ.*

P. Yager
*University of California at Davis*

B. Baller, D. Boehnlein, B. Lundberg, J. Morfin, R.Rameika
*Fermilab*

P. Berghaus, M.Kubanstev, D. Naples, N.W.Reay, R.Sidwell, N.Stanton, S.Yoshida
*Kansas State University*

K. Heller, R. Rusack, R. Schwienhorst
*University of Minnesota*

T. Akdogan, V. Paolone (spokesperson)
*University of Pittsburgh*

F. T. Avignone, A. Kulik, C. Rosenfeld
*University of South Carolina*

T. Kafka, A. Napier, W. Oliver, J. Schneps
*Tufts University*

C. Andreopoulos, N. Saoulidou, G. Tzanakos
*University of Athens*

A. de Bellefon, T. Patzak
*College de France*

J.S. Song, I.G. Park, S.H. Chung, C.S. Yoon, H.I. Jang, M.S. Park, I.W. Lee
*Gyeongsang National Univ.*

C.H. Hahn
*Changwon National Univ.*

J.T. Rhee
*Kon-Kuk Univ.*

S.N. Kim
*Korean National Univ. of Education*

# TABLE OF CONTENTS

# LIST OF TABLES

# LIST OF FIGURES

# 1. Introduction

Over the past 25 years of particle physics the Standard Model has emerged as an elegant theory explaining the forces and interactions governing nature's most basic structure. So far, the model has survived all tests, from the assault of high-luminosity collider interactions to delicate probing by and of nature's most elusive particles, the neutrinos. The Standard Model contains three generations of quarks and leptons, implying the existence of three light neutrinos, $\nu_e$, $\nu_\mu$, and $\nu_\tau$. Still, nearly fifty years after the first direct observation of electron neutrino interactions, very little is truly known about neutrinos in their own right. In particular, we do not even know whether or not neutrinos have mass, and to date physicists have directly observed the interactions of only $\nu_e$ and $\nu_\mu$.

With the completion of the 1996-97 Fixed Target run, Fermilab experiment E872 (a.k.a. DONUT for Direct Observation of Nu Tau), expects to make the first direct observation of $\tau$ neutrino interactions. The continuing success of the Standard Model leaves small room for doubt that the $\tau$ neutrino will interact as predicted and dozens of $\tau$ neutrino interactions now reside in the E872 data sample waiting to be "discovered." Directly observing the decay of $\tau$ leptons produced in the charged current interaction $\nu_\tau + N \rightarrow \tau$ will not only yield the definitive discovery of the third neutrino but will allow us to begin the study of this elusive lepton.

From its conception in 1993, the proponents of E872 have believed that the experiment would provide important experience in the observation of $\tau$ neutrino interactions that will leave them poised to move from confirming to confronting the Standard Model. Despite the success of the Standard Model over the past quarter century, there has arisen a growing suspicion that the neutrino might not be as simple a particle as postulated. Massive neutrinos, manifesting their mass via neutrino oscillations, could possibly explain the persistent deficit of solar neutrinos, as well as the anomaly in the observed flux of atmospheric neutrinos. A massive $\tau$ neutrino could provide an elegant contribution to the yet-to-be-identified dark matter in the universe.

A search for neutrino oscillations will begin at Fermilab in the early part of the next decade. The Fermilab NuMI Project will produce a wide band neutrino beam using

120 GeV protons from the Main Injector which will enable physicists to do both short and long baseline experiments and hence directly address two of the three "smoking guns" in the neutrino mass mystery. For both the short and long-baseline experiments, the Fermilab advantage is that the neutrino beam will have a significant flux over $\tau$ threshold, and can therefore directly observe the process $\nu_\mu \rightarrow \nu_\tau$ via the subsequent charged-current interaction of the $\nu_\tau$. Since actually seeing a $\tau$ requires very high resolution emulsion detectors such as the ones used in E872, the experience gained to date as well as that which would be gained by extended running of E872 should provide a valuable input to the design and construction of the NuMI detectors.

We are also motivated to request further running for E872 for the basic reason of understanding the interactions of the $\tau$ neutrino, as well as exploring several additional physics topics. From data collected in the second run we will be able to measure the charged-current cross section and *y* distribution of the $\nu_\tau$ and will verify that the $\nu_\tau$ is a "standard" type neutrino. These measurements are only possible with the improved statistics and better quality data that can be obtained from a second run. We believe that in a 20 week run such as the one proposed for 1999 we will be able to triple our first run statistics. A brief description of two additional searches which we can carry out with the second-run data are described in Appendix A.

# 2. Production and Detection of Tau Neutrinos

## *2.1 Production of Tau Neutrinos*

Experimental observation of $\nu_\tau$ charged-current interactions requires high proton intensities at high energy and extremely good detector resolution. An 800 GeV primary proton beam from the Fermilab Tevatron in conjunction with a high-resolution active target meets the requirements for this experiment. In E872 we produce tau neutrinos in a beam dump and directly measure $\nu_\tau$ charged-current interactions by observing $\tau$ production and subsequent decay in an emulsion target. This is the same technique which has been used to search for $\nu_\mu \rightarrow \nu_\tau$ oscillations in the CERN CHORUS[1] experiment and is also proposed for the Fermilab Main Injector experiment, COSMOS[2]. Since E872 will see the signal the oscillation experiments hope to observe, we view E872 as an important first step in addressing the exciting question of neutrino mass and mixing.

Tau neutrinos are produced predominantly from the leptonic decay of the $D_S$ meson in the decay sequence $D_S \rightarrow \tau + \nu_\tau$, $\tau \rightarrow \nu_\tau + X$. In this experiment $D_S$ mesons are produced by 800 GeV protons interacting in a tungsten beam dump. Both the $D_S$ and the daughter $\tau$ decay in the dump, each decay producing one $\nu_\tau$. The number of $\nu_\tau$ per incident proton produced in the beam dump through this process is estimated to be $1.68\times10^{-4}$ [i] The number of $\nu_\tau$ charged-current interactions that occur per centimeter of target material is determined by the $\nu_\tau$ energy and interaction cross section. Because of the energy dependence of the $\nu_\tau$ cross section, the neutrinos from each of the decays ($D_S \rightarrow \tau + \nu_\tau$ and $\tau \rightarrow \nu_\tau$ ) have very different interaction probabilities. Their energy spectra are determined by the $x_f$ dependence of the $D_S$ production cross section. We have used an effective interaction cross section of $0.42\times10^{-37}$ $cm^2$ to estimate the interaction yield in E872. Within the solid angle acceptance of the E872 experiment ($\leq$ 7.1 mr ) we obtain $5.0\times10^{-18}$ $\nu_\tau$ charged-current interactions per centimeter of emulsion ($\rho$=3.72g/$cm^3$) per proton. Taking into account $\tau$ sources other than $D_S$, such as B meson decays, $D^\pm$ decays, Drell-Yan and secondary production from charm, increases the yield by 14% to $5.8\times10^{-18}$ $\nu_\tau$ charged-current interactions per centimeter of emulsion per proton.

In the *original* E872 proposal (January 1994) we planned to use 15 cm of

[i] see Appendix B for details on E872 rate estimates

emulsion and set as a goal to accumulate $2 \times 10^{18}$ integrated protons. Before fiducial volume and efficiency cuts this would have yielded approximately 220 interactions. We estimated that cuts would reduce the sample by about 15%, giving a total of ~ 180 observed interactions. In the subsequent sections of this document we will describe in detail the actual design, accomplishments, and expected yield of the first run.

### 2.2 Detection of Tau Neutrinos

The $\nu_\tau$ interaction candidates are recognized in emulsion by topology only: one of the charged tracks from an interaction decays within a distance of 5mm. Since 86% of the $\tau$ decays have only one charged track ( a "kink" decay), and the mean lifetime is short ($<\gamma c\tau_\tau> \sim 2.5$ mm), very high spatial resolution on tracks near the vertex is essential. Such capabilities are possible only with nuclear emulsion. Today these capabilities are greatly enhanced by automatic digital scanning technology, developed at Nagoya University. One can describe an emulsion sheet as a detector with a resolution of a few μm ($10^{-6}$ m) in either transverse direction, and 4μm along a track.

The use of event topology as the primary means of identification is valid because other physical processes that match the criteria are rare, even compared to $\nu_\tau$ interactions. There are two processes that *can* create events with signatures identical to those of $\nu_\tau$ CC interactions

- $\nu_{e,\mu}$ charged-current production of charm (*i.e.* $D^\pm$ ) that subsequently decays to only one charged particle *and* the $e^\pm$ or $\mu^\pm$ from the primary vertex is not identified
- hadron scattering in the emulsion *not* accompanied by visible nuclear fragments ("white star kinks")

The charm background is estimated from a product of factors

$$\text{fraction } \textit{charm} \text{ background } = f(\nu N \to c) \cdot f_\pm \cdot f_{1prong} \cdot (1 - \varepsilon_\ell)$$

where the factors are, respectively, the fraction of interactions producing charmed hadrons[3] (8%), the fraction of charged charm hadrons[4] (40%) , the fraction of decays into

only one charged daughter[5] (40%), and the inefficiency of the lepton identification (~10%). The product is $1.3\times10^{-3}$.

The second background is estimated from measurements of the mean free path between white star kinks of hadrons in emulsion. The m.f.p. is very sensitive to the transverse momentum cut-off of the emulsion measurements, but the experimentally determined value, at the limit of angular resolution, is 50m [6]. There are an average of 4.5 tracks per interaction that are followed for 5mm each, so that the probability of a white star kink per interaction is $5\times10^{-4}$.

The increased size of the event sample from the second run will allow other sensitive tests from distributions of measured quantities that will further confirm that the selected candidate events are $\nu_\tau$ interactions. Three examples are: (1) lifetime of the $\tau$ lepton, (2) branching ratios and (3) distribution of interactions in transverse coordinates $(x,y)$. The excellent spatial resolution of emulsion allows a precise impact parameter ($b$) measurement ($\delta b \sim 2$ μm) of the tau decay tracks with respect to the primary interaction. The mean $b$ value is a good estimator of the lifetime $c\tau$, Monte Carlo calculations indicate that a sample of 100 $\tau$ decays would yield a relative lifetime uncertainty of 18% which would unambiguously separate these decays ($c\tau$ of 87μm) with from $D^{\pm}$ decays that have a $c\tau$ of 350μm.

The experiment will also measure branching fractions in (at least) three categories: $\tau \rightarrow \mu(\nu\nu)$ , $e(\nu\nu)$, $3h(\nu)$. The event selection and emulsion analysis are not very sensitive to how the $\tau$ decays, so the candidate events should sample the known branching fractions directly. Finally, the $\nu_\tau$ beam which interacts has a significantly different transverse distribution at the emulsion target due, mostly, to the higher energy needed to create the massive $\tau$ lepton. The $\nu_\tau$'s should show a concentration toward the beam center, compared with $\nu_e$, and $\nu_\mu$ interactions.

# 3. Beam Requirements and Design

When E872 was first proposed, it was realized that the success of the experiment would crucially depend on two factors : 1) on the number of primary protons which could be delivered to the beam dump target and 2) on adequate attenuation of the backgrounds produced in the prompt neutrino beam. While the first factor was primarily one of program planning, the second was determined by the beam design and the background tolerance of the emulsion targets.

The beamline and shield design were optimized to reduce backgrounds to a minimum, subject to the constraint of keeping the emulsion as close as possible to the dump to maximize the $\nu_\tau$ flux through the target. Other constraints on the design were the size of the experimental hall and the capability of the existing sweeping magnet in PW8, which appeared to be the ideal place to construct the experiment.

As will be discussed in much more detail in Section 4.1, the most severe background for the nuclear emulsion used in E872 is penetrating tracks, parallel to the neutrino beam direction. These background tracks, almost entirely muons, must be kept $<5\times10^5$ cm$^{-2}$ in all emulsion sheets. A second background is due to Compton scattered electrons from ~MeV photons or direct soft electrons. This background is particularly serious for thick layer ("bulk") emulsion types. Based on experience from other experiments ( primarily CHORUS at CERN ) the electron background must be kept $<7\times10^5$ cm$^{-2}$ per 300μm emulsion layer. These limits on the allowable background from the beam were the primary concern in the design.

## *3.1 Primary Proton Beam*

Prior to the 1990-91 Fixed Target Run the PW beamline was used to produce and transport a high intensity 300 GeV secondary pion beam, or tertiary anti-proton beam to the experimental hall, PW8. This was accomplished by targeting a high intensity primary proton beam on a target located just upstream of the momentum selecting magnet PW6W2. For the 1990-91 run the PW beamline was upgraded to transport 800 GeV primary protons through its entire length, from switchyard into the PW8 enclosure. By the use of pin-hole collimators located in the PW2 and PW5 enclosures the intensity was limited to $< 10^9$ protons/spill at the experimental target in PW8. For E872 it was

necessary to be able to transport up to $10^{13}$ per spill all the way to PW8. To allow this, some reconfiguration of the beam line was required. The major tasks included removal of the pin-hole collimators and removal of limiting apertures from the former pion transport design in PW6. Continuous vacuum was installed along the entire length of the beamline. Minor modifications to the quadrupole tunes were made to insure that the beam spot remained as small as possible as it passed through limiting apertures in the transport system.

### *3.2 Prompt Neutrino Beam*

For E872 we upgraded the existing Proton West area (PW8) to become the home of a prompt neutrino beam, that would contain a significant flux of tau neutrinos. A prompt neutrino beam is one in which the primary proton beam is dumped into a relatively short, high-density target, such that all the protons interact in the dump. The pions and kaons, which ordinarily are the valued particles in neutrino beam design, interact before they have a chance to decay. The important particles in the beam dump interaction are the charmed particles, which decay leptonically before they can be absorbed to produce e, $\nu_e$, $\mu$, $\nu_\mu$, $\tau$, and $\nu_\tau$. The electrons are absorbed by the dump; the muons penetrate the dump (and presented a serious technical challenge in the design of such a beam); the $\tau$'s also decay before interacting in the dump and produce an additional $\tau$ neutrino. The three flavors of neutrinos constitute the prompt neutrino beam. For the beam designed for E872 we calculated that the beam should contain approximately 5% $\nu_\tau$ by number. The predicted spectrum of interacted prompt neutrinos is shown in Figure 1.

Since many other particles besides charm are also produced in the interaction, these and the products of their interactions must be absorbed in the dump. However, about 1% of the interactions in the dump produce a muon which may be able to penetrate tens of meters of steel; these must be swept clear of the sensitive experimental apparatus, particularly the emulsion target. This is accomplished by placing a combination of high field sweeping magnets and passive shielding just downstream of the dump.

The key elements of the beam are a water cooled tungsten/copper dump, a 7 meter long sweeping magnet (SELMA), with no aperture, operated at 3 Tesla, a specially designed 5 meter long toroid operated at 2 Tesla, followed by 18 meters of passive steel shielding. Construction of the PWest Prompt Neutrino Beam was approved as an FY95

Accelerator Improvement Project. Some design work began shortly after January 1995. Fabrication, construction, and installation of the elements began in early 1996 and was completed in October 1996.

A brief summary of the major tasks which were accomplished with this project were :

- a water cooled tungsten dump was constructed and installed
- the primary sweeping magnet was moved upstream by 17 meters from its original location in the PW8 hall
- the coils in the primary sweeping magnet were removed and completely reinsulated and repotted
- new pole pieces were installed in the primary sweeping magnet
- steel and concrete shielding were installed around the beam dump and upstream end of the sweeping magnet to meet prompt shielding and groundwater protection requirements
- a new secondary sweeping magnet was constructed and installed
- 18 meters of passive steel shielding were placed downstream of the second sweeping magnet

### 3.2.1 Beam Dump

The beam dump assembly consists of a 1m long tungsten block, 10cm × 10cm transverse to the beam, that is jacketed by 10cm of copper. The copper pieces are cooled by a closed-circuit radioactive water system (RAW) to remove the 25KW of heating produced by the proton beam. The tungsten block was made so that one side was solid metal, while the other half was machined to give an effective density of 0.5 with respect to the nuclear interaction length. It can be moved so that it presents either the full-density side to the beam, or the half-density side. The interaction length for tungsten is 10cm while the average decay length for $\pi$'s (primary and secondary production) is about $5\times10^4$ cm, so the fraction of $\pi$'s that decay is about $10^{-3}$. Nevertheless, the number of $\pi$ decays exceeds the number of all other leptonic short-lived decays (<< 10cm) by a factor of 10. To understand accurately the number and effect of these sources of $\nu_\mu$ and muons, we planned to take some fraction of the data, ~20%, with the dump in half-density

position. The half-density side is realized by removing 2.5cm of metal every 5cm along the beam direction. See Figure 2 for a schematic drawing of the tungsten and a picture of the final assembly.

### 3.2.2 Active Shielding

The most technically challenging aspect of creating a prompt neutrino beam is dealing with the intense flux of muons produced in association with the desired neutrinos as well as from a number of other sources. To determine a proper design for this beam it was necessary to correctly model each of the sources of this muon flux. The philosophy used to attenuate this flux was to use a combination of magnetic sweeping and passive shielding. The emulsion is placed in a "shadow" of muons 36m from the dump. The reduction of the muon flux in this "shadow" can be very large, $>10^5$, compared with regions just two meters away. The optimization of maximizing neutrino interactions includes size and distance of the emulsion from the source with the contraints from the distribution of the background flux from the shielding system.

Two magnets are used to provide the necessary muon sweeping. The primary element of the muon sweeping system was constructed using the existing magnet PW8AN1, also known as "SELMA." A second magnet, which we refer to as MuSweep2, was specifically designed and constructed for E872. The SELMA magnet was operated at 2450 amps to produce a central field of 3.0T. MuSweep2 was especially designed to sweep re-entrant muons out of the beam. The magnet was operated at 800 A to provide 2.1T. This magnet is very similar in design and function to the MuSweep magnet which was constructed for the KTeV experiment.

### 3.2.3 Passive Shielding

Following the active sweeping, 18 meters of passive steel shielding was required to attenuate the mid to low energy muon flux which finds its way back into the beam region. The configuration of this shielding along with the active sweeping elements is shown in Figure 3. This is a total of more than 500 metric tons of steel. A large fraction of this shielding came from the decommissioned E705/E771 downstream muon system.

The two plumes of high-energy muons created by the sweeping system pass

within 2m of each side of the beamline at the emulsion location. Interactions of these muons in shielding steel would generate an intolerable background. Thus, the passive shielding was built with notches so that the muon plumes would pass through air rather than material so near the emulsion.

The predicted muon flux remaining at the location of the emulsion target is shown in Figure 4 .

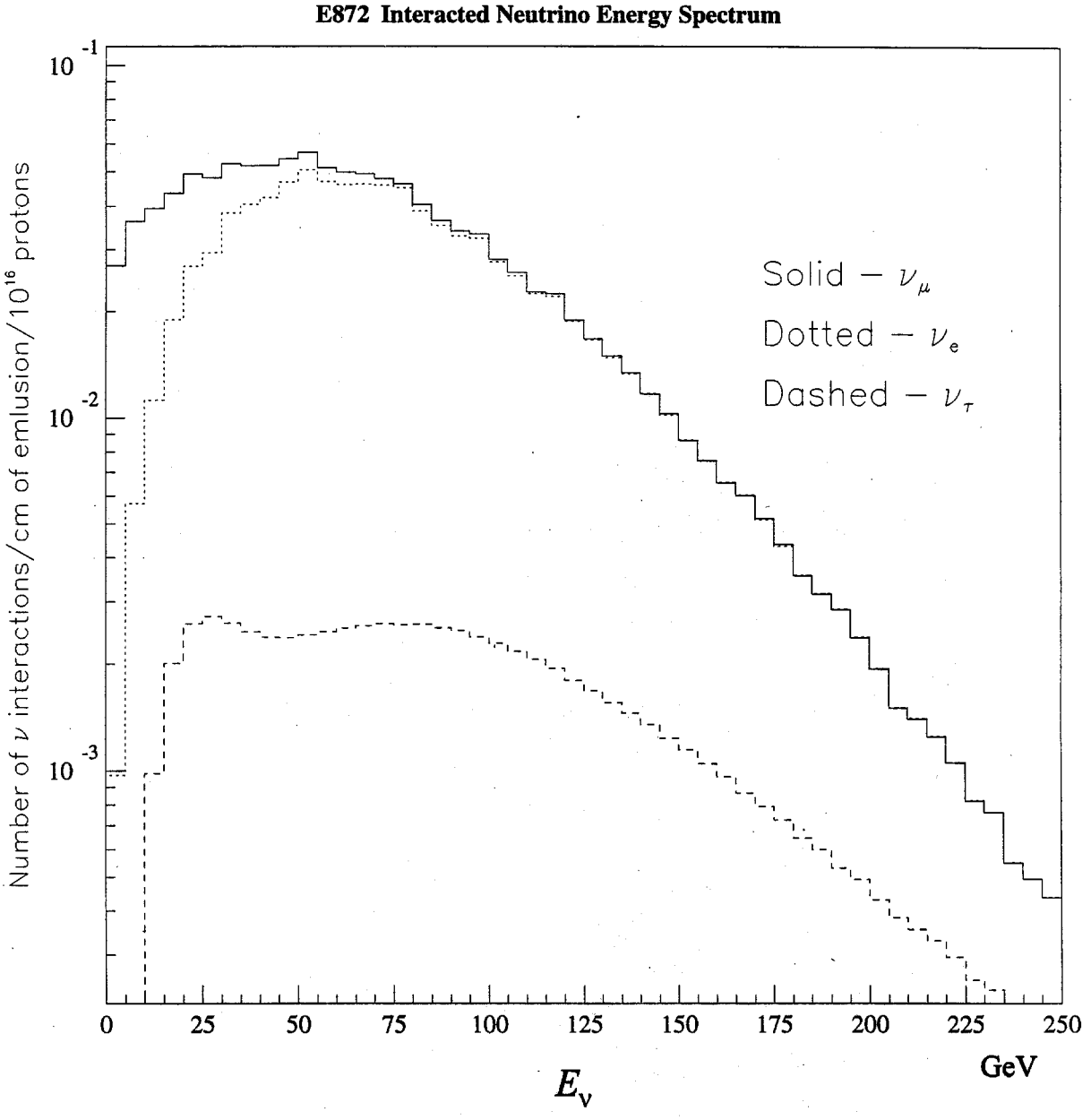


**Figure 1: The predicted spectrum of interacted prompt neutrinos.** About 5% of the interacted flux is calculated to be tau neutrinos.

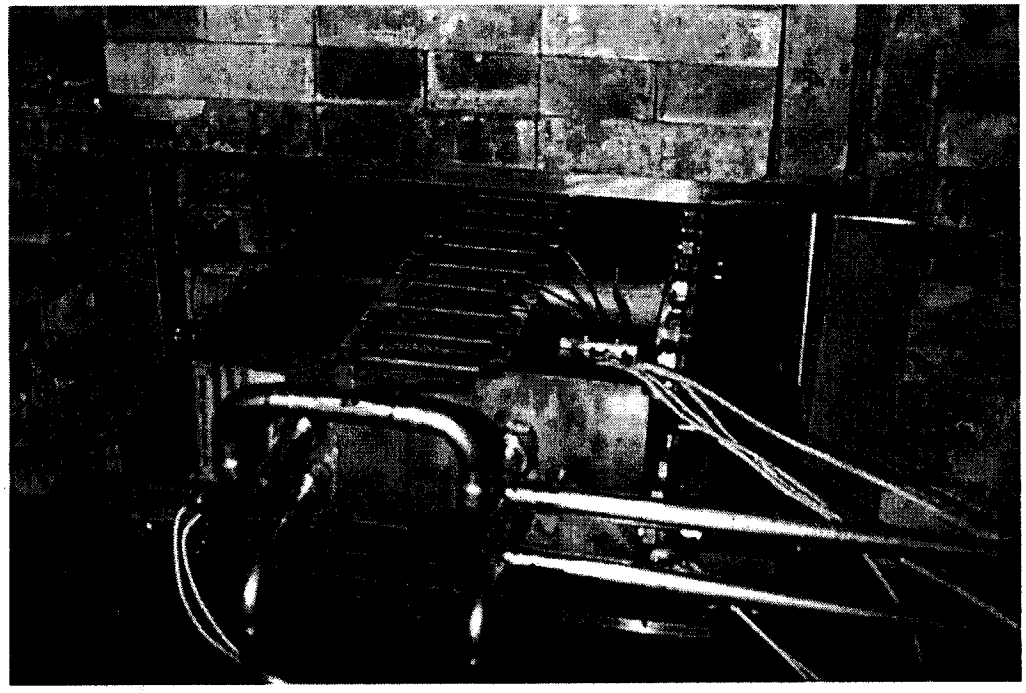

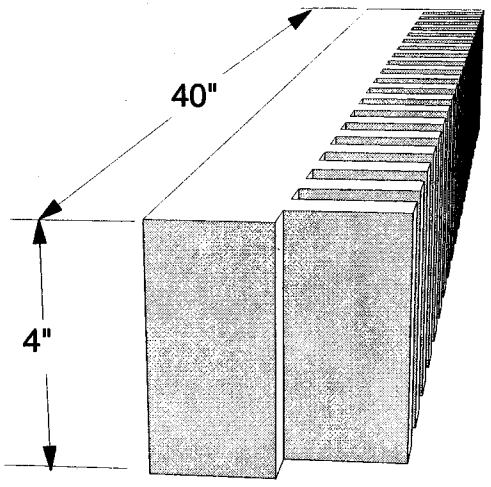


**Figure 2: The prompt neutrino beam dump.** A photo of the installed assembly is shown as well as a schematic of the tungsten block with the half-density side on the right.

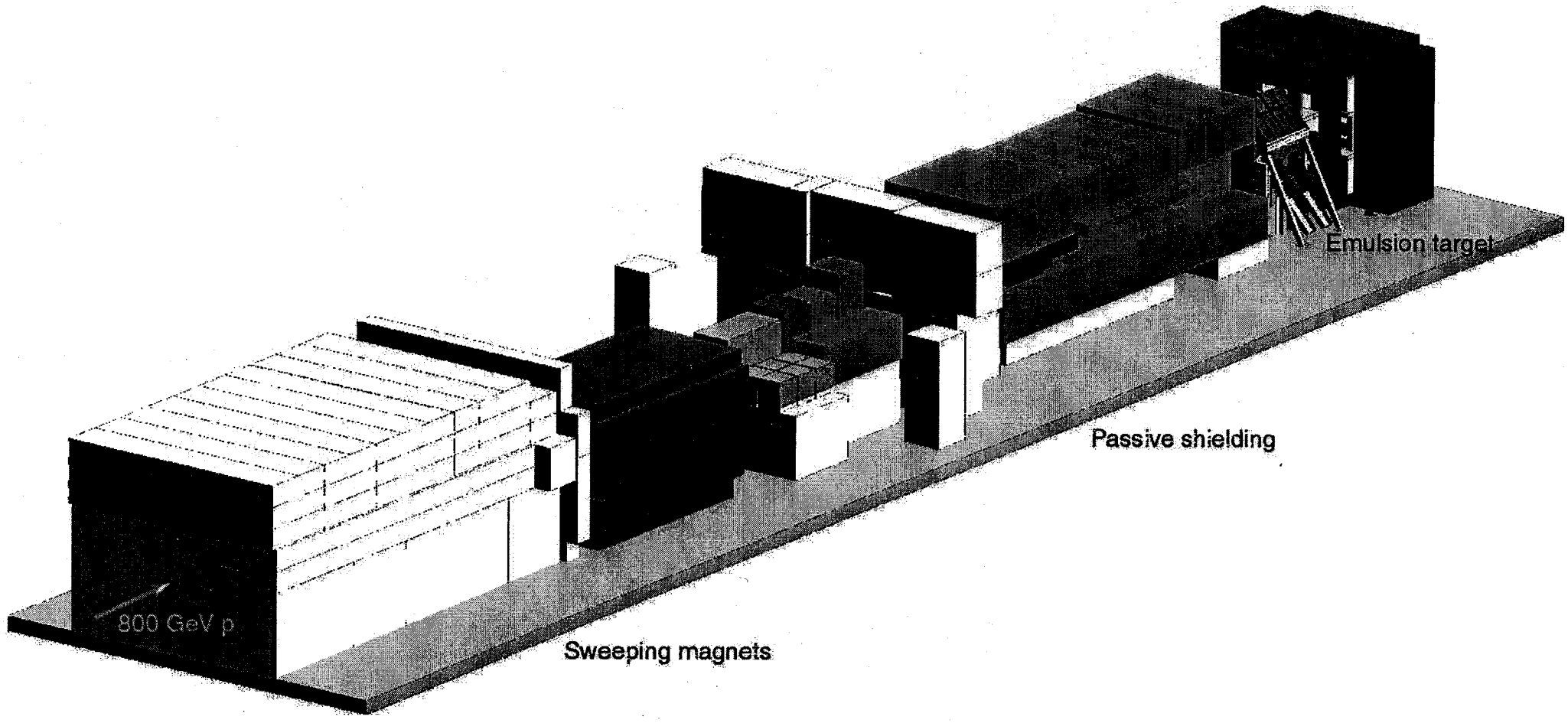


**Figure 3: The prompt neutrino beam active and passive shielding.** The proton dump is located at the arrow. The shield surrounding the dump and much of the spectrometer are not shown. The first magnet (SELMA) is encased in concrete.

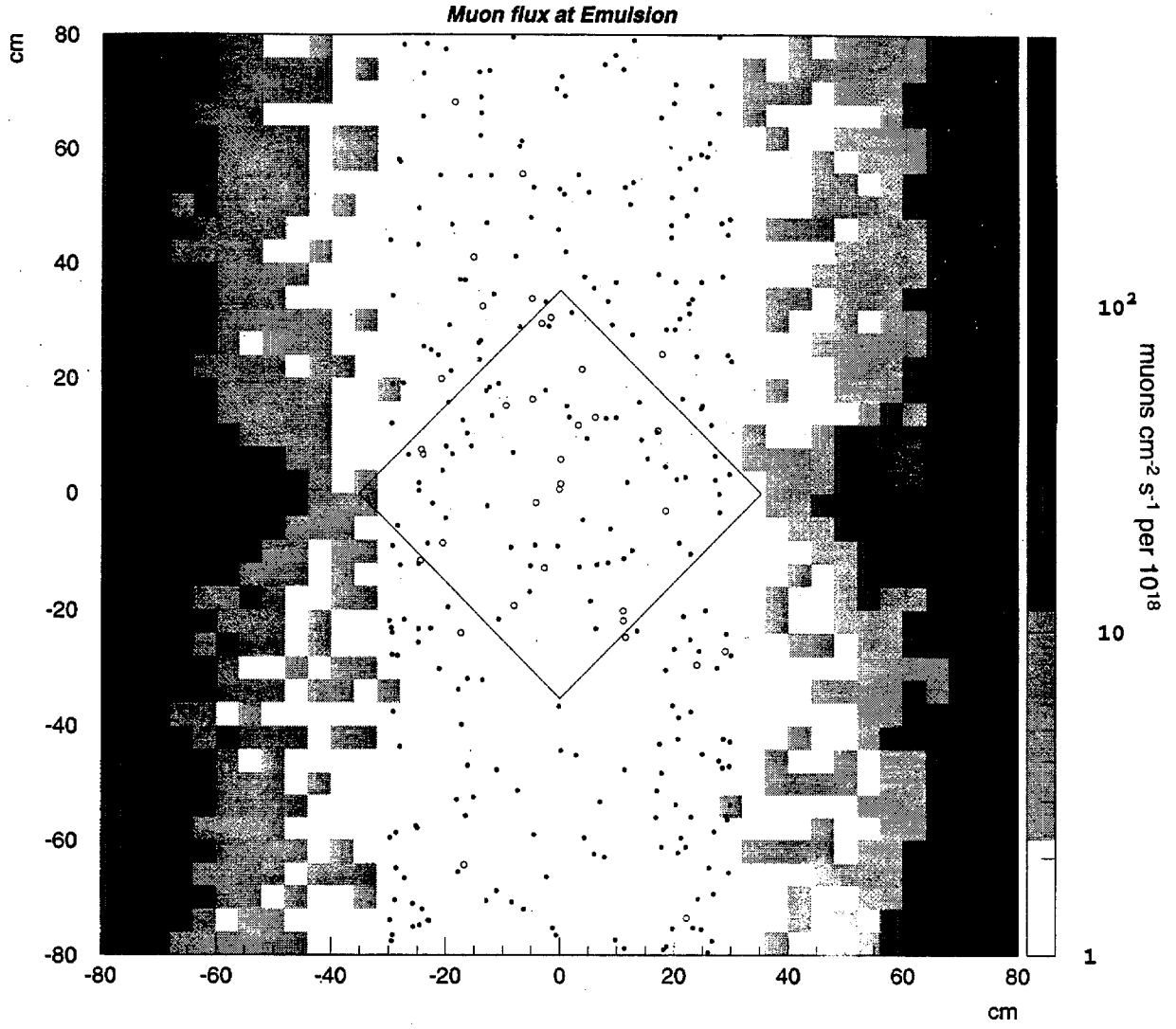


**Figure 4: The predicted muon flux at the emulsion target location.** The region of |x|>30cm is indicated with levels of shading (note the log scale) while in the low density region, |x|<30cm, each event is shown. The dots are direct muon from the dump and the circles represent direct-pair muons. The boumdary of the emulsion target is shown by the rotated square.

# 4. Detector Requirements and Design

The concept of a hybrid emulsion spectrometer (HES) was pioneered in previous Fermilab experiments E531 and E653.

The requirements which motivated the design of the E872 HES were modest. The $\tau$ lepton has a $c\tau$ of 0.087 cm. Since typical decay lengths for $\tau$'s produced by the beam dump $\nu_\tau$'s are a couple millimeters, they will be easily visible in an emulsion target. Several Monte Carlo distributions characteristic of the tau and its decay are shown in Figure 5. The major task of the spectrometer will be in reconstructing the decay products of the $\tau$ and other tracks from the primary interaction in order to locate the interaction vertex in the emulsion. The location of the primary interaction in the emulsion requires at minimum, a single non-interacting reconstructed spectrometer track from the primary linked to the emulsion.

In this experiment all neutrino interaction candidates will be scanned, requiring us to study in detail ~10,000 events of which less than 100 will be $\nu_\tau$.

The major components of the E872 HES are :

- a set of emulsion target modules
- high resolution tracking downstream of each module provided by planes of scintillating fibers
- coarser resolution drift chamber tracking downstream of the target region
- a large aperture dipole magnet to provide a 225 MeV/c $p_T$ kick for momentum analysis (ROSIE)
- an electromagnetic calorimeter to aid in the identification of electrons
- a muon ID system using range to screen out hadrons

## *4.1 Emulsion and Scintillating Fiber System*

Emulsion is used as the neutrino interaction target in E872 because of the very high resolution necessary to resolve $\tau$ decays. On the other hand, a neutrino target needs to be as massive as possible to collect enough events. The target design had to optimize the number of interactions while retaining the ability to find and measure the events in the emulsion with high efficiency. The design described here is an attempt at this optimization

with the added constraint of the high cost of the nuclear emulsion: 100kg of target costs \$300K.

### 4.1.1 Emulsion Target Design

The emulsion target consists of four separate *modules* aligned and mounted on a precision stand. Each module is a stack of 50 to 80 individual *sheets*, 50cm × 50cm, oriented perpendicular to the ν beam direction and compressed tightly together under vacuum to form a solid unit 7cm in thickness. The emulsion sheets are two coatings of nuclear emulsion on each side of a plastic sheet needed for mechanical rigidity.

Modules can be made of almost any total thickness, but there is a practical limit imposed by multiple scattering and electromagnetic showering in the emulsion. The entire volume of the emulsion cannot be comprehensively scanned; the total number of fields-of-view digitized would be $>10^7$, containing almost $10^9$ tracks. Instead, predictions from time-sensitive detectors, drift chambers and scintillating fiber planes, are used to greatly reduce the area that must be scanned, by about a factor of $10^3$. In order to use predictions from detectors downstream of the emulsion, the practical maximum emulsion thickness is ~6 cm. This was determined mostly from experience in other experiments that have used thick targets, such as E531 (5cm), E653 (3cm) and CHORUS (3cm). The finding efficiency decreases as a function of $z$ (alont the beam direction) regardless of the vertex finding strategy. In CHORUS the efficiency drops about 15% in 3cm, so that in E872 we expect the vertex finding efficiency to be about 30% lower in the most upstream sheet compared to the most downstream sheet. It is important to note that the ratio of events *located* in the emulsion to the number predicted is nearly independent of $z$, reflecting the fact that the efficiency for following a given track through the emulsion, from sheet to sheet, is very high ($\geq$98%).

In order to reduce the total volume of emulsion that must be scanned, predicted track positions where the track exits the module must be sufficiently precise: errors in the transverse coordinates ( $\sigma_{x,y}$ ) should be held to less than 150μm. This is difficult to achieve using standard detectors alone, but a high resolution device (*i.e.* scintillating fiber planes) in conjunction with special emulsion sheets, spaced apart from the module, will achieve the desired accuracy. These special emulsion sheets are useful only if the their track density is much lower than the density in the module sheets, so that there the

number of predicted tracks in the field-of-view is of order one. In the special emulsion sheets, called "changeable sheets", we hold the number of predicted tracks per field-of-view to about one by changeing these sheets frequently, once per week. The location of tracks at the module follows a "bootstrap" procedure, where moderate resolution devices (*i.e.* drift chambers) point to tracks in higher resolution detectors ( scintillating fiber planes ) that, in turn, are able to point to tracks in the changeable sheet with the necessary precision, then finally from the changeable sheet to the downstream module sheet. The changeable sheets are calibrated with respect to the transverse coordinates ($x$, $y$) by a grid of 16 collimated x-ray sources ($^{55}$Fe) set into the plate that registers the sheet along $z$.

The actual design of this system is shown in Figure 6. Note that there are changeable sheets on *both* sides of each module and there is a set of scintillating fiber planes behind each module. We believe that this configuration is adequate to locate events even in the most upstream module, which is the most challenging.

### 4.1.2 Emulsion : Overview of Analysis

Emulsion analysis proceeds by following tracks, predicted by the electronic spectrometer, from downstream to upstream until the primary vertex is found or the track ends. This requires going from sheet to sheet since the module is made of sheets stacked perpendicular to the beam. Thus, each sheet must be calibrated in $x$ and $y$ with penetrating (muon) tracks at angles. The accuracy needed is high, about 10μm for alignment.

Track finding and following is accomplished with automated precision tables with imaging and pattern recognition systems that recognize, fit, and record tracks on standard mass storage media. A CCD camera and frame-grabber digitize a 200μm × 200μm area for 16 different depths in each emulsion layer. Tracks are seen by this system as a set of dots such that when the 16 frames are compared, a set of dots add coherently depending on position and angle. A custom programmed track selector (firmware ) finds the tracks using a fast transform and histogramming method on the frames. This information is then reformatted with a PC and all tracks in the field-of-view are recorded. In practice, tracks are followed logically using the stored information since each sheet remains on the scanning station until *all* predictions for that sheet are searched. If other tracks are found, an attempt is made to fit a vertex. Finally, if a vertex is reconstructed, tracks originating

from the vertex can be followed downstream for as long a distance as desired. Note that this will almost always require remounting previously scanned sheets on a station since the diverging tracks will not be within the field-of-view of the original, tagged track.

Candidates for $\tau$ tracks are discovered by measuring a significant apparent deflection of the track within a few millimeters for most (86%) of the $\tau$ decays. In E872 the predicted average decay length is 2.5mm, and the mean decay angle is 50 mrad. This signature will be easy to spot using standard emulsion analysis. After the first 100μm of track, the decay angles ("kinks") as small as 2mrad can be resolved. It is expected that all tracks will be followed for 5mm from a recognized primary vertex.

This analysis description is a reasonable approximation of the analysis of *bulk* type emulsion (see below), but additional steps are required for ECC type modules, and that discussion is deferred to the section on ECC type emulsion.

### 4.1.3 Emulsion : Limiting Factors

The dominant limiting factor of emulsion is its continuous sensitivity. In this medium tracks from background sources accumulate, and these, if too numersous, cause severe scanning problems and compromise event finding efficiency. These background sources include unwanted through-going tracks (*i.e.* muons) and $\gamma$ and x-rays which cause Compton-scattered electron tracks. Muons are components of cosmic rays, but in E872, cosmic rays are negligible compared to the muon flux originating at the dump. Similarly, $\gamma$ photons are always present as decay products from isotopes in concrete and other structures, but in this experiment this measured source is only 1% of the total soft photon flux. Neutrons, also, can cause background in two ways. If they are high energy, above 1 MeV, they can scatter off protons in the emulsion, generating short, highly ionizing tracks. Very low energy neutrons are captured in nuclei of surrounding material, exciting them and generating photons in the MeV range that scatter in the emulsion.

The two main background sources, penetrating particles and $\gamma$'s, have very different effects on emulsion data. Muon tracks cause loss of efficiency simply by the combinatorics of associating tracks from one sheet to the next. In E653, the track density sometimes exceeded $3\times10^5$ cm$^{-2}$ without a significant loss in efficiency, although the scanning time was long. In E872, an upper limit of $5\times10^5$ cm$^{-2}$ was set for all modules exposed in the first run.

In contrast, the $\gamma$ generated background does not cause general tracking confusion in the usual sense. The scattered electron tracks are short (typically < 100μm long ) and scatter wildly, their visible tracks are usually bent or curly and "heavy" from ionization. As one scans *through* the emulsion layers these tracks cause a darkening of the view and a loss of contrast, making digitization of images problematic. The experience at CHORUS has shown that a density of $7x10^5$ $cm^{-2}$ per 300mm layer is not yet a severe problem and this value was adopted in E872 as the upper limit for the exposure of each module. Some test sheets were exposed at higher densities, and it may be that some relaxation of this limit is possible in future exposures.

### 4.1.4 Emulsion : Bulk Type

The E872 experiment, as originally proposed, used only this type of module, which was used successfully in E-531, E653, and in CHORUS. It is the "classic" type of emulsion detector, with 95% of the module mass being nuclear emulsion. Each sheet is made by coating both sides of a 90μm plastic base with 320μm of emulsion (this is the thickness after drying). These sheets, called *bulk* emulsion, are stacked together (with a thin paper sheet as a separator) to form a module, with 84 needed for a 7cm thick mechanical structure of which 6cm is emulsion. Each bulk module requires 15 liters of emulsion gel. Since they are thick, this type is fully sensitive to the effects of soft $\gamma$s in the analysis of the developed sheets.

The analysis of a bulk module is conceptually straightforward. Tagged tracks are scanned through the emulsion volume as described above. It is important to recall that for scanning events in E872, only one non-interacting track needs to linked to the emulsion for location of the primary vertex.

### 4.1.5 Emulsion: ECC Type

Large scale implementation of bulk type emulsion has some important, practical, disadvantages. Its manufacture is highly specialized as it has no commercial uses and requires great care to insure that the thick coating is very uniform in thickness. Emulsion gel suitable for high energy physics is also quite expensive so that the experiments such as CHORUS (mass of 2t ) are probably at the limit of what can be done with bulk targets.

An alternative that is being explored in E872 is to replace most of the mass of the target with inert material in the form of thin plates, and build a module with alternating inert plates and emulsion sheets made with a thin coating. This detector philosophy is similar to the "cloud chambers" used several decades ago and hence the designation: Emulsion Cloud Chamber or ECC.

The ECC design used in E872 is illustrated in Figure 7. The inert matter is stainless steel plates 1mm thick and the emulsion sheets have 100μm coatings on each side of a 200μm plastic base. In essence, the ECC type module is not a volume tracking detector like the bulk type. It is more like pixel detector planes sampling every 1mm along the beam direction. Only 5% of the module mass is emulsion. Further, because the layers are thin, the emulsion analysis is more "radiation hard" with respect to soft $\gamma$ effects. The penetrating track limit is the same as with the bulk type.

Because the volume tracking has to be abandoned, the analysis is also more like 2-D tracking systems, albeit with very high precision. There is no longer as much useful angular information per layer. In fact most of the information comes from measuring a point in each layer right at the plastic boundary ( $\sigma_{x',y'} \sim 5\times10^{-3}$ radians ). The track is extrapolated to the next emulsion sheet, picked up with position and angular measurements, and so on. Since one has to extrapolate tracks through the inert target material, the probability of linking incorrectly in the next sheet is larger than the bulk type. Following incorrect links would tend to increase the analysis time, which is not too serious. A more serious potential problem is the incorrect identification of $\tau$ decay tracks which deserves more discussion.

There are two methods to locate $\tau$ decay candidates. First, if the decay occurs *after* the emulsion sheet immediately following the steel plate, then once the vertex is fit in ($x$ $y$ $z$ ) the daughter track segment can be found by using the constraint that it must intersect the projected $\tau$ track. This situation is illustrated in the top interaction in Figure 7. If the decay occurs *before* the next emulsion sheet (inside the steel) then one of the tracks found near the vertex will not fit the vertex hypothesis as it will have a large impact parameter. This is illustrated in the bottom interaction in Figure 7.

In an experiment without background, either method is valid and efficient. In E872, however, the background track densities are up to $3\times10^5$ cm$^{-2}$ so that each field-of-view will have 100 background tracks, in addition to the interesting one. In the first

method, the 2-D angular constraints reduce the random background to a 4% chance of false association (for a uniform spatial and angular distribution of background tracks). For the impact parameter method, one loses the constraint in one dimension and the corresponding random link probability is almost 90%. The analysis of the ECC type is being studied and will evolve rapidly in the next 4 months.

### 4.1.6 Scintillating Fiber Tracking System

The scintillating fiber system is used to select event candidates for scanning the emulsion modules and to point tracks to the changeable sheet so that they can be connected to tracks in the modules. The system has four units, one unit is installed downstream of each module position. There are two types of units; type 1 is used following modules 1 and 3 and type 2 is installed following modules 2 and 4. This is illustrated in Figure 6. Each plane consists of either two or four layers of 500 μm fibers, readout by image intensifiers (IITs) provided by Hamamatsu. Magnetic shielding of the IITs is done with large soft iron canisters. The mean readout time is 24 ms and dominates the DAQ deadtime and event size.

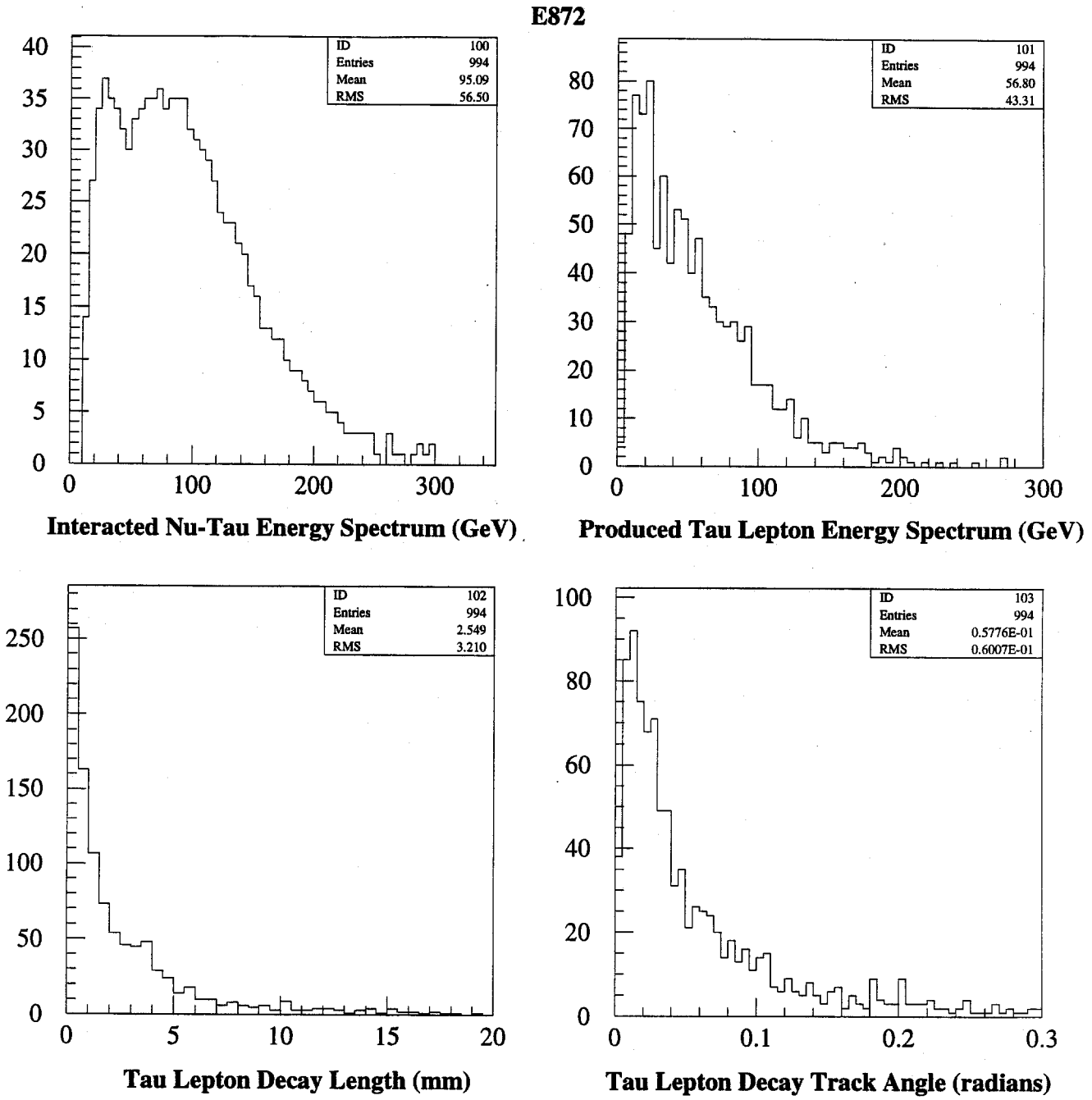


**Figure 5: Characteristics of the E-872 tau neutrino interactions.**

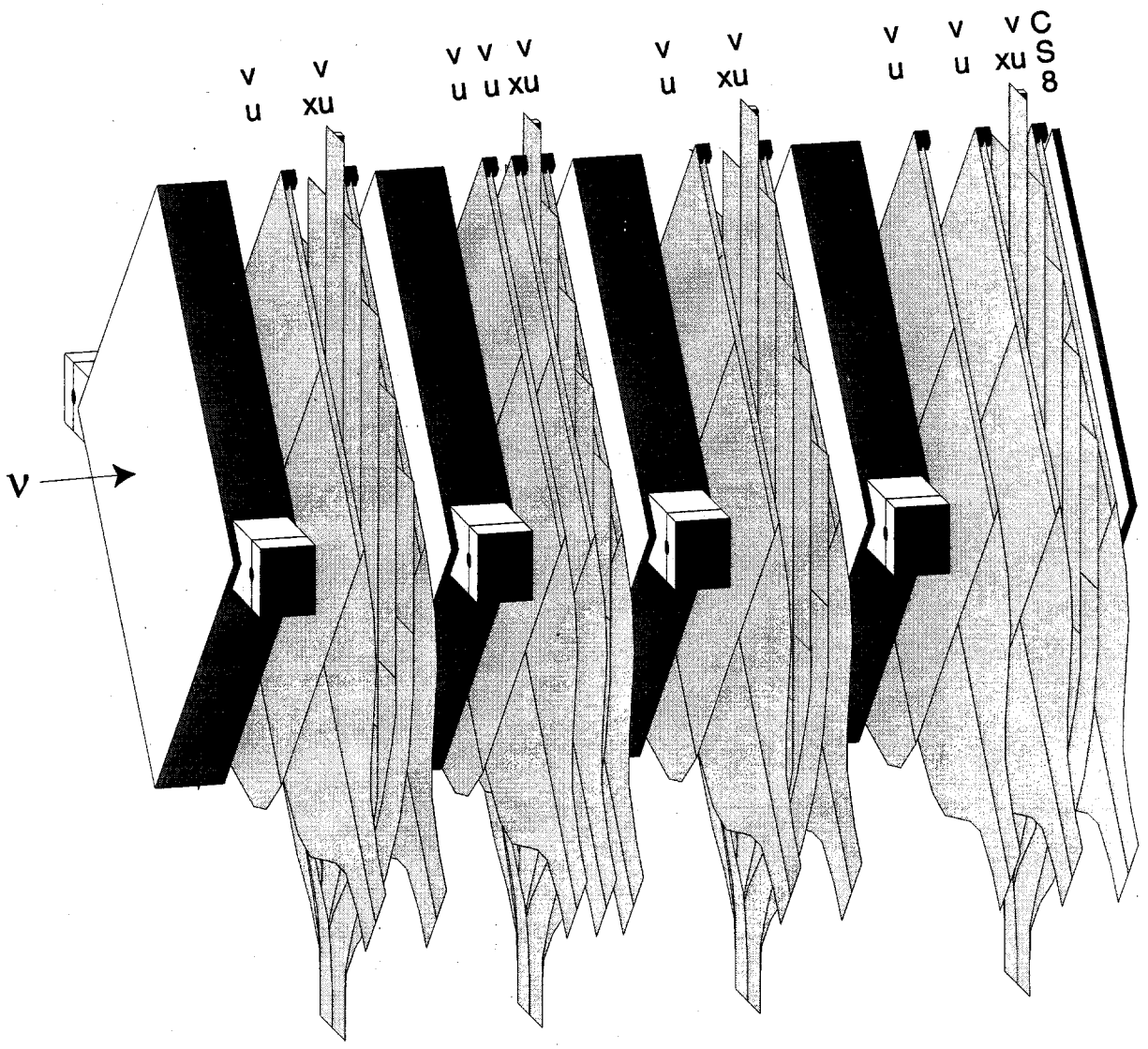


**Figure 6: The target / fiber tracker system.** The scintillating fiber planes are arranged in three views. The six readout image intensifiers and CCDs are not shown for clarity. Each of the four emulsion modules shown has a "changeable sheet" mounted between it and the fibers.

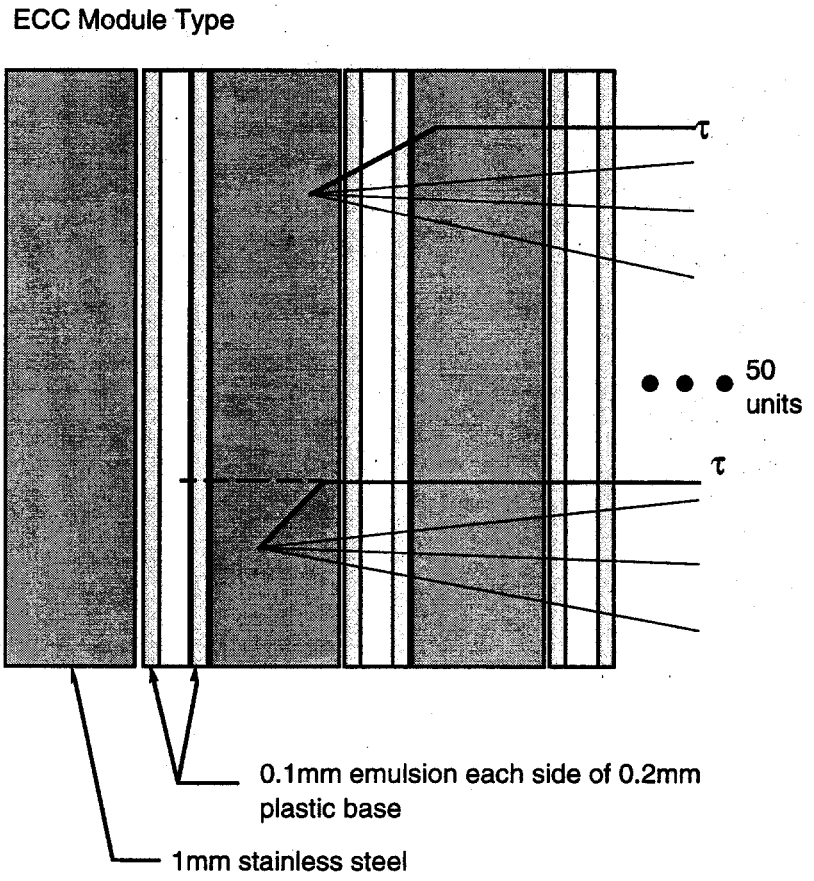


**Figure 7: The configuration of an ECC type emulsion module**

## *4.2 Conventional Spectrometer*

### 4.2.1 Trigger Counter System

To trigger on neutrino interactions occurring in our emulsion targets we require that the interaction signature be *nothing in* **AND** *one or more charged tracks out* as detected by a system of scintillation trigger counters.

*Nothing in* is accomplished by using a veto wall just upstream of the emulsion/fiber target assembly. It consists of a double scintillator wall constructed with 10 4"x12"x76" counters with PMT's on both ends. The first wall contains 5 side-by-side counters followed by a second wall of 5 counters. These 20 PMTs are **OR**'d to achieve a rejection rate of $10^3$ or better. The total singles rate in the veto wall must be kept under 100Khz in order to keep the self-vetoing below a few per cent.

*One or more charged tracks out* is accomplished by using programmable logic units which have as input signals from three planes of segmented counter hodoscopes, T1, T2 and T3. T1 and T2 are located just downstream of the 2nd and 4th emulsion module respectively, while T3 is located in the upstream aperture of the analysis magnet. The T1 and T3 planes consist of eight counters each while T2 contains 9 counters.

The T1 and T2 planes are constructed out of scintillating fibers. Each plane covers an area of $\sim 70$ cm$^2$ and is segmented into (8) and (9) 10 cm wide bundles respectively. Each bundle is read out by a Hamamatsu R5600 phototube.

T3 is located downstream of the target/fiber system. It is composed of plastic scintillator paddles each 10 cm x 80 cm. The counters are 5 mm thick and are attached to 49 cm long light guides and phototubes on each end. The phototubes are Philips 2262B 12 stage tubes.

Imposing a counter adjacency requirement between paddles in *T1* **AND** *T2* **OR** *T2* **AND** *T3* forces a maximum track angle condition on tracks produced in $\nu$ interactions. In turn this vetos large angle muons produced in the dump that miss the upstream veto wall but still enter the target region.

Because the fiber tracker has a readout time of $\approx 30$ milliseconds, in order to keep the deadtime of the experiment down to an acceptable level (<10%) the trigger rate needs to be maintained at ~5 Hz. (Note that the "true" neutrino interaction rate is measured to be only a few millihertz.) Meeting this requirement in not trivial since there is a relatively

high flux of muons from the dump which is directed either directly toward the spectrometer (~ 500 Hz) or traversing part of the spectrometer at large angles (~ 700 Hz). The vertical penetrating cosmic ray flux in the experimental hall has been measured to be ~ 60 $m^{-2}s^{-1}$. The rate for counters oriented at $\theta = 90^0$, such as spectrometer trigger counters would be was measured to be $38m^{-2}s^{-1}$. The system of veto and trigger counters described above has been designed to accommodate these rates.

### 4.2.2 Drift Chamber Tracking

The main function of the downstream tracking spectrometer is to assign a momentum and charge to tracks observed in the emulsion and fibers, particularly decay products of the tau. A momentum resolution of at least 3% is required to clearly observe the $p_T$ cutoff of a 2-body tau lepton decay, with the statistics expected from E872. This value can be achieved with an analysis magnet $p_T$ kick of 225 MeV and angular track resolutions of 300 microradians for 15 GeV tracks. The mean energy of the daughter tracks from tau lepton decays in the emulsion target is 15 GeV.

The first set of drift chambers are installed within the aperture of the upstream mirror plate of the analysis magnet. These chambers were previously used in E665 as one of the Vertex Drift Chambers, hence its name, VDC. This chamber has an active area of 100 cm x 70 cm and is composed of three jet cell chambers, each of which has 16 cells with 6 wires per cell along the beam direction, for a total channel count of 96 wires per chamber, or 288 for the system. In the first chamber ($x$) the wires are vertical (oriented along the $y$ direction). The second chamber ($u$) is oriented at an angle of $+5^0$ to $x$ and the third chamber ($v$) is oriented at $-5^0$. The distance between wires is 7 cm. Because of the large cell size and the relatively high multiplicity of the neutrino interactions the LeCroy 3377 multi-hit TDC's are used for the readout of this chamber.

To improve the overall tracking in E872 additional jet chamber samples, inside the magnet volume, were added during the Summer 1997. The first jet chamber built by KSU was installed July 8, 1997 and was in place for approximately 2/3 of the data run. This chamber (KSY) had 17 cells (6.6 cm) which measured position in the $y$ direction with 4 samples taken along the beam direction. It should be noted that tracking in the $y$ direction had been particularly weak prior to the installation of this device. KSY had a total of 68

channels readout through LeCroy 3377 TDCs. The second chamber (KSX) had a total of 22 cells and measured position in the x direction with four $x$ samples taken along the beam direction. These 88 channels were also readout through LeCroy 3377 TDCs. KSX was installed July 31, 1997 was in place for only ~1/3 of the data run

Following the analysis magnet were three stations of drift chambers. These were previously used in E537/705/771 (DC1) and E557/683 (DC2 and DC3). Each chamber has four planes, $x,x',y,$ and $u$ and covers an active area of 330 cm x 160 cm. In each of the chambers the $u$ and $v$ planes are oriented at an angle of 17° with respect to the $x$ plane. The $x'$ planes are off set from the $x$ planes by one-half cell size. The wire spacings are 1.905 cm. All three chambers are read out into LeCroy 4291B (10-bit) CAMAC TDC's. A fourth chamber, identical to DC1 is maintained as a spare. The chambers operate with a gas mixture of 50% Argon - 50% Ethane, bubbled through ethanol at 0° C. A position resolution of ~ 300 microns is desirable.

A plan view of the spectrometer, Figure 8, shows the layout of the drift chamber system.

### 4.2.3 EM Calorimeter

The primary purpose of the Electromagnetic Calorimeter (EMCAL) is to aid in the identification of electromagnetic energy coming from $\nu_e$ interactions or from electrons from $\tau$ decay. The energy measured in the calorimeter will also contribute to the measurement of the total energy in the neutrino interaction.

The EMCAL is a 400 element Lead Glass and Scintillating Glass wall. A beam view of this 375 cm x 195 cm array is shown in Figure 9. The central region is made of SCG1-C scintillating glass and contains 100 7.5 x 7.5 x 89 $cm^3$ and 74 15 x 15 x 89 $cm^3$ blocks. These blocks are 20.9 radiation lengths and 2.0 nuclear absorption lengths deep in the beam direction. The outer region is made of SF5 lead glass and contains 224 15 x 15 x 41.5 $cm^3$ blocks, 16.8 radiation lengths and 1.0 nuclear absorption lengths in depth. The 15 x 15 $cm^2$ and 7.5 x 7.5 $cm^2$ blocks are instrumented with EMI 9791KB and RCA 6342A photomultiplier tubes respectively. A system of two LeCroy 1440 power supplies supply individually adjustable high voltages to the photomultiplier tubes, controlled by a PC. The PMT anode signals are connected via RG8U cable to a passive splitter, a fraction of the signal is used as an input to a calorimeter trigger system, and

most of the signal (70%) is delayed by 400 ns and is driven to the inputs of 15-bit ADCs using the LeCroy 2280 ADC system. The RG8U serves to minimize losses, dispersion, and noise due to long cable runs (about 200 ns). The integrating gate has been chosen to be 260 ns for the lead glass blocks and 350 ns for the scintillating glass blocks, due to the longer decay time of the latter. An LED system is used to continuously monitor the performance of the EMCAL and help track and correct for gain variations of the PMTs. The LED light is distributed to the surface of the block by 0.3 mm diameter fibers. Pedestal and LED measurements are taken between spills.

### 4.2.4 Muon Identification

The primary purpose of muon identification in this experiment is to identify muons coming from the charged-current interaction of muon neutrinos in the emulsion target. In such interactions the muon track will point back to the primary interaction vertex and hence can be rejected as a candidate for a $\nu_\tau$ interaction. The muon identifier is a three-layer sandwich of steel walls and planes of particle detectors. The upstream steel wall is 3.7 m high by 6.25 wide and is 0.42 m thick. The two remaining walls are each 3.25 m high by 5.48 m wide and 0.91 m thick. Downstream of each wall is a plane of detectors to measure the vertical and horizontal positions of charged particles emerging from the steel. Proportional tubes cover 80% of the cross section; the remainder is covered by scintillator hodoscopes. The detectors were constructed at Tufts University and shipped to Fermilab in the summer and fall of 1996.

The principal structural element of the proportional tubes is a four-cell aluminum extrusion. Each cell is a square 4 cm on a side. A total of 248 four-cell modules were constructed with lengths ranging from 1.3 to 6.25 m. The current signals from the sense wires are processed by a four-channel amplifier/discriminator card mounted on each module. The discriminator outputs are translated on the card to differential ECL levels for transmission over 100 m of twisted pair cable to coincidence registers. The proportional tubes are operated with a 95-5 $ArCO_2$ gas mixture.

Measurements in a cosmic ray test stand at Tufts showed that the efficiency of the proportional tubes is 97%. The slight inefficiency can be attributed to the insensitive area between the cells formed by the 2 mm thick interior walls.

Scintillator hodoscopes fill apertures in the proportional tube planes left in the

regions on both sides of the beam line where there is an intense flux of muons from the dump. The 1-μsec resolving time of the proportional tubes is too long to handle this intense flux. The width of the scintillator elements is 4 cm to match the proportional tube cell width. The range of element lengths is 1.0 m to 2.3 m. There are a total of 448 elements distributed over the six hodoscopes.

Hamamatsu R1666 tubes epoxied to the scintillator are used to view 256 of the elements. The remaining 192 elements are viewed by a set of 12 Hamamatsu 16-ch multianode photomultiplier tubes. Waveshifting fibers of 4 mm square cross section are placed in grooves milled along the lengths of these 192 elements. The fibers are gathered in 4 by 4 bundles and coupled to the multichannel tube by optical grease.

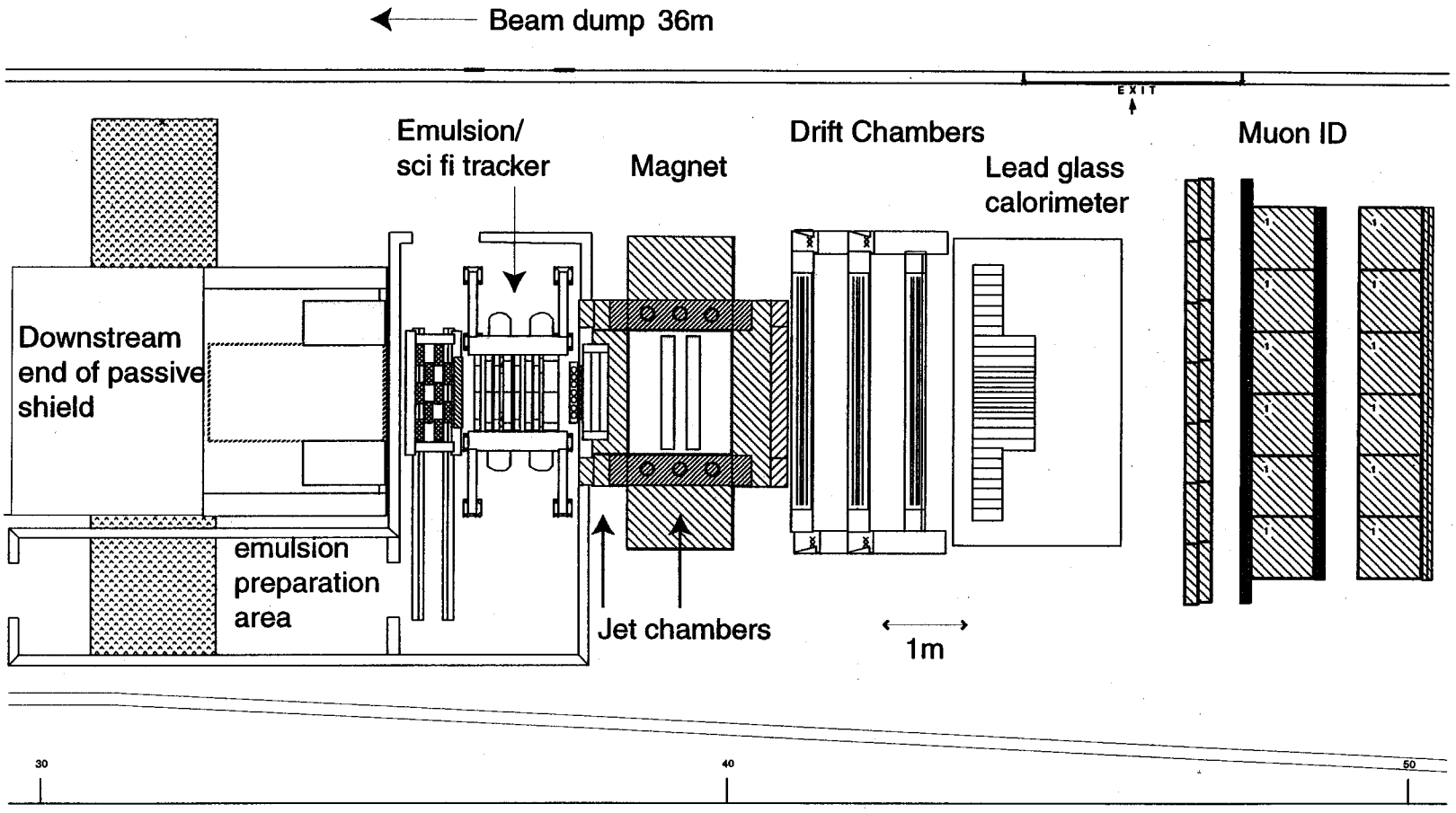


**Figure 8: Plan view of the spectrometer.** The high flux of muon from the dump are swept ~1m to each side of the emulsion.

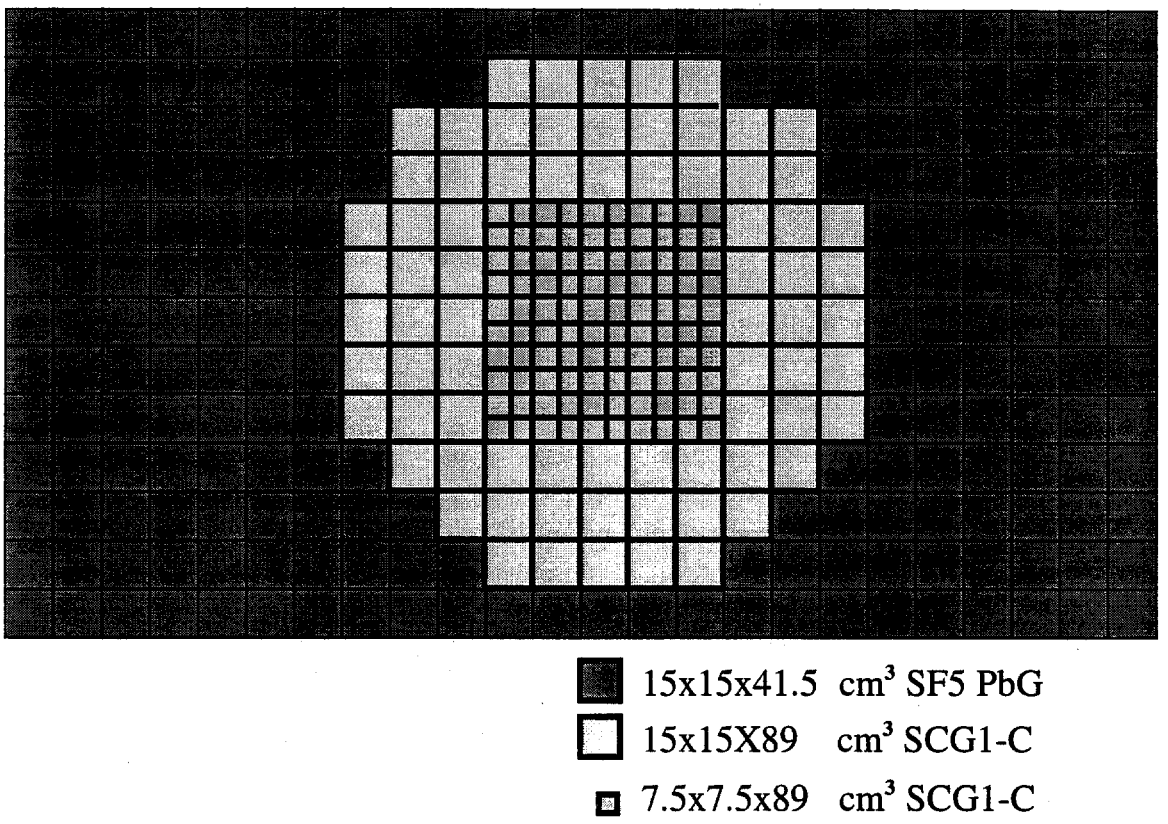


**Figure 9: The EM Calorimeter (beam's eye view).** The array is built of both scintillator-doped glass (near center) and un=doped lead glass. This configuration was retained from a previous experiment (E-771).

# 5. First Run Performance and Accomplishments

When the fixed-target run began in late June 1996, E872 was in its construction and assembly phase. The beamline and major shielding components were in place by mid-October and the first protons hit our PW7 dump on 28 October 1996. This marked the beginning of a two month evaluation phase of the shielding and beamline which had to be completed before the emulsion targets were installed. Beginning in early January modifications to the beam shielding were begun and were completed by the end of February. A second period of evaluation took place in March. Data taking began in April and continued until early September. In the later part of the run we operated at very high intensity and demonstrated the robustness of our beam and spectrometer performance. Table 1 is a summary of the important parameters of the experiment during the final 6 weeks of running. "Available beam" is the fraction of time that useable protons were not being transported to the dump. "T1" is the first of three trigger hodoscopes described in Section 4.2.1.

| Parameter | Value |
|---|---|
| Beam Intensity | $8\times10^{12}$ spill$^{-1}$ |
| Available beam @ PW7 | 94% |
| Electronic live-time | 87% |
| Relative pot on tape | 96% |
| $\mu$ flux in emulsion vol. | $2\times10^{4}$ spill$^{-1}$ |
| $\mu$ flux 1.5m from x = 0 | 6 kHz cm$^{-2}$ |
| T1 single rate | 8kHz |
| exp. triggers | 80 spill$^{-1}$ |
| $\nu$ interaction rate (all types) | 0.038 spill$^{-1}$ |

**Table 1: Important parameters during high intensity running**

## *5.1 Beam Performance*

### 5.1.1 Primary Beam

Special demands were set on the transport of the 800 GeV protons in PW beamline to prevent interactions with beamline elements and monitoring equipment. The goal in design was to keep the total beam loss to $<10^{-4}$. There are two important concerns:

1. Minimize continuous losses, especially in the final 300m, so that the integrated flux of muons from $\pi$ decays do not exceed the allowable limit for penetrating tracks
2. Prevent catastrophic beam loss in last 300m which would not be adequately attenuated by the muon shielding downstream of the dump

It was immediately clear after turning the beam on, that there were sources of muons in the beamline causing rates 20 times too high at the location of the emulsion target. The main source was quickly confirmed to be a break in the beam vacuum for instrumentation 350m upstream of the target. It amounted to 50cm of air and 150μm of titanium. This material was removed in late November and with some additional improvements in the beam vacuum, the upstream rates became invisible under normal conditions.

Throughout the run the concerns about the primary beam were controlled by providing good continuous vacuum ($<10^{-2}$ torr), large apertures and careful beamline tuning. Normal running conditions with high intensity beam ($>1\times10^{12}$ protons per spill) required that all, but one, of the wire chambers used for beam position monitoring be removed by remotely retracting them from the beam trajectory. The only exception was the final chamber, 1m from the dump. The insertion of just *one* upstream chamber, about $5\times10^{-3}$ of an interaction length, would increase the charged particle rates at the emulsion by a factor of 32 and was instantly detected by the experiment via an equipment protection interlock circuit.

### 5.1.2 Prompt Neutrino Beam

#### *5.1.2.1 Muon backgrounds*

After correction of the primary beam vacuum problem another significant source of muons was discovered originating in the beam dump itself. These muons were bent out of the beam direction by the first magnet (SELMA) and into the magnetic return steel of the second magnet (MuSweep) and then toward the target. The Monte Carlo shield calculations had anticipated only 10% of the total flux due to an error in the simulation which modeled an early version of the MuSweep design instead of the as-built magnet. This problem was corrected by placing an additional 5m of steel just downstream of the return leg of the MuSweep magnet and by December the muon rates through the emulsion target were acceptable.

For the remainder of the run the muon shielding, active and passive, performed as expected for the high momentum muon flux. Under normal operating conditions, the muon flux through the emulsion volume was $<2.5\times10^{-9}$ muons per incident proton. The muon flux distribution along the horizontal plane is shown in Figure 10. The figure shows the muon flux at the emulsion location measured per $cm^{-2}$ at a proton intensity of $8\times10^{12}$ per spill. It is shown at beam height ($y$=0) and 27cm above and below. Also shown are estimates of the muon flux using MARS, calculated by N. Mokhov. The low energy (<10 GeV) muons in the emulsion volume were measured to be higher than originally predicted due to the asymmetry in the shield design. The flux of these low energy muons increased when the half-density dump target was inserted by 40%. Not surprisingly, most of this increase was due to low energy muons from the east side.

#### *5.1.2.2 Neutron and Electron/gamma Backgrounds*

Shortly into our evaluation phase, it was also discovered that there were high background rates from non-penetrating particles. This background was first found by observing anomolously high "singles" counts in the spectrometer trigger counters. These high rates had not been well predicted and were too high for the emulsion targets to be able to withstand an exposure which would be adequate to meet the goals of the experiment.

Upon studying this background, these rates could be separated into two

components: a source that showed build-up after beam was turned on and decay after shut-off, and a prompt source proportional to beam intensity. The sources were investigated with NaI counters to see low energy $\gamma$s and LiI counters (with moderating spheres) to measure the neutron flux.

Neutrons create a background in the emulsion mainly by ~MeV $\gamma$'s produced after capture in surrounding material or in the emulsion itself. The most effective way to eliminate neutrons at the spectrometer is to absorb them near the dump using heavy shielding followed by concrete. In our initial configuration the outer layer of concrete was greater than 1.35m thick around the dump and at least 90cm around the dump magnet, SELMA. To reduce the neutron background the concrete shield thickness was increased around the dump. As counted with the LiI crystals (bare and with 2", 3", 5" poly moderators) , the total neutron flux decreased with additional concrete shielding by a factor of 9±1. The single counting rates at the emulsion target however only decreased by a factor of 3 after shielding, revealing another kind of background seen by the counters and emulsion.

The electron background present in the emulsion is believed to be due to muon radiation through material near the emulsion. The two main sources are: (1) very high energy muons that are not swept far enough to the side of the material in the emulsion and scintillation fiber support stand or the shielding just upstream and (2) muons striking the analysis magnet steel. To protect against these local sources, a lead cover was built around the light-tight box holding the emulsion. It is 20mm thick on the front and sides. At the downstream end, a 6mm lead cover was installed. The top pieces (250kg) can be removed with a hoist so that the changeable sheet replacements could be done once per week. The lead cover attenuated the electron background by a factor of 5. As a point of information, a 20mm sealed shield can attenuate by factor of 12.

In summary, after 10 weeks of investigation and diagnosis by the experimenters and Laboratory staff the following background reduction measures (some of which have been mentioned above) were taken:

- Provide an additional 1m of concrete shielding around the dump area and the SELMA magnet
- Install sand bags with 20% polyethylene beads in the dump cave preventing neutrons and other hadrons from emerging upstream from the dump
- Install a concrete wall downstream of MuSweep to provide additional neutron and $\gamma$ protection from sources in the dump
- Build a lead box around the emulsion target stand to provide local protection against $\gamma$s from muon bremstrahlung in the steel shield (See Figure 11)
- Provide a powerful ventilation scheme to exhaust activated air from near the dump away from the experiment

The sum of all these measures decreased the single counting rates by 25 at the position of the first target module, and by 15 at the position of the last target module. These rates were confirmed with emulsion test pieces, exposed, developed and scanned for background tracks. This was considered a sufficient reduction for the installation of the emulsion and the beginning of the data phase where an exposure of $5\times10^{17}$ protons on target would enable a sufficient yield of tau neutrino interactions while at the same time keeping the total backgrounds in the emulsion at an acceptable level.

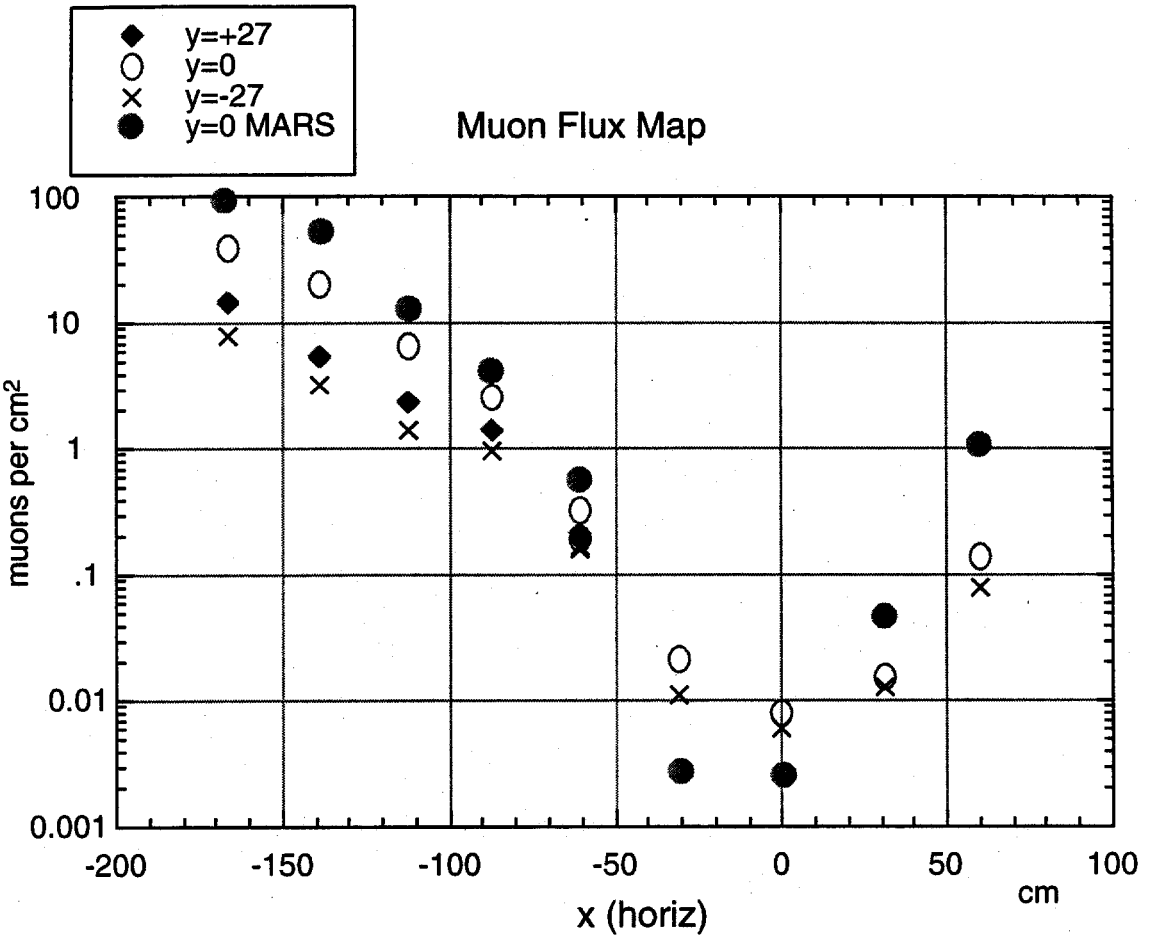


**Figure 10: The measured muon flux at the emulsion location**

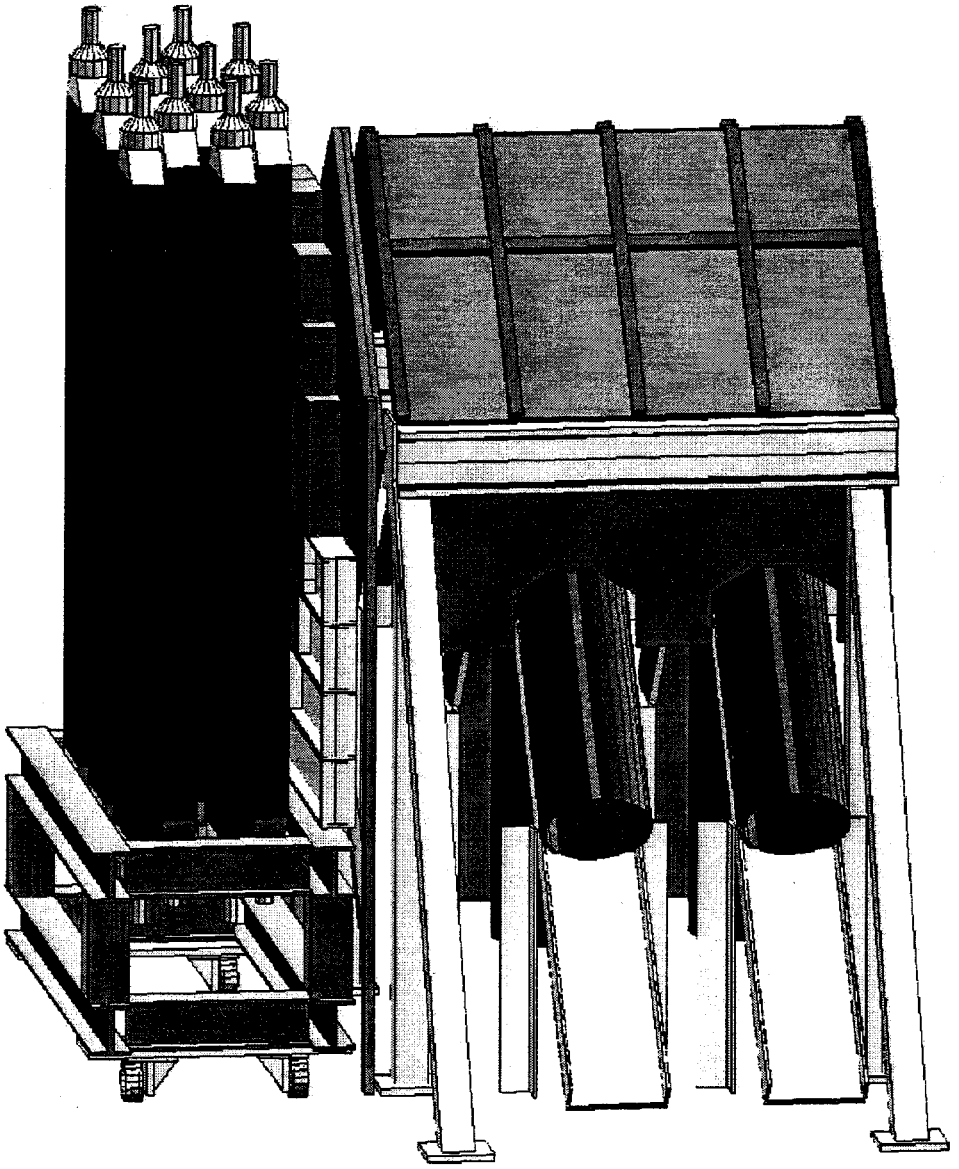

**Figure 11: The emulsion target showing the protective lead shield.** The neutrino beam comes from the left. The large vertical counters comprise the veto wall.

## *5.2 Detector Performance*

Commissioning, calibration and monitoring of the spectrometer was accomplished using a muon beam produced by having the primary proton beam "dump" in the PW5 beam dump. For $10^{11}$ protons on the dump, 500 muons would pass through the spectrometer. Using a simple coincidence trigger between two scintillator hodoscopes in the emulsion target region we were able to cleanly trigger on these muons. The detector performance plots discussed in the sections which follow are representative of the calibrations which were done throughout the run.

### 5.2.1 Trigger System

The two primary concerns of the trigger system was to trigger with high efficiency on neutrino interactions but at the same time keep the trigger rate low enough (< 5 Hz) so as to keep the deadtime below 15%.

It was determined that at full beam intensity ($8\times10^{12}$/spill) it was impossible to keep the trigger rate below 5 Hz if we allowed triggers that were consistent with ***ONE*** charged track exiting the target region based ***ONLY*** on the hits in the segmented trigger counters. We therefore limited our triggers initially to those which had hits in the segmented trigger counters consistent with more than one track emanating from an neutrino interaction. Our trigger rate for this condition at full beam intensity was measured to be 3 Hz. It was determined from Monte Carlo studies that the multi-track trigger requirement still allowed us a high trigger efficiency: $\nu_\tau$ charged-current interactions; 97%.

However the collaboration still wished to trigger on neutrino interactions that produced only one charged track, primarily to allow us the ability to record elastic interactions. Therefore for triggers that had hits in the segmented triggers counters consistent with one track, the additional requirement of at least a single hit in the EM calorimeter consistent with a minimum ionizing particle was imposed. This trigger was implemented mid way through the run and increased out trigger rate from 3 Hz to 4 Hz.

Our total deadtime was therefore 13%, with 11% deadtime from our 4 Hz trigger

rate and 28 ms fiber tracker readout time, and 2% from the self-vetoing rate in our veto wall.

### 5.2.2 Scintillating Fiber Tracker

The performance of the fiber system is summarized below. The system experienced no downtime during the run. Efficiency and resolution are measured with muon triggers and results are preliminary. U and V are rotated ±45 degrees with respect to the X measurement. The X plane efficiency is not shown in the Table and is estimated from examining muon tracks with the event display to be comparable to the other views. The resolution can be seen in Figure 12.

| Name | Location | Samples | Efficiency | Resolution |
|---|---|---|---|---|
| Station 1 | downstream of target 1 | 1X, 4U, 4V | ??94?(U)<br>??95?(V) | 200μm |
| Station 2 | downstream of target 2 | 1X, 6U, 6V | 0.94(U)<br>0.95(V) | 200μm |
| Station 3 | downstream of target 3 | 1X, 4U, 4V | 0.94(U)<br>0.95(V) | 200μm |
| Station 4 | downstream of target 4 | 1X, 6U, 6V | 0.94(U)<br>0.95(V) | 200μm |

**Table 2. Summary of Scintillating Fibers.**

### 5.2.3 Drift Chambers

A summary of the drift chamber tracking performance is given in Table 3. Efficiencies are measured with muon triggers, and are lower for high multiplicity events. Resolutions are preliminary and are based on analysis of residuals for muon tracks from the PW5 calibration data. A summary of the residuals for DC1-3 are shown in Figure 13. X is the magnet bend plane, Y the non-bend plane. The table illustrates a major deficiency in the tracking: because of the small-angle stereo there is insufficient sampling in the y view. This deficiency was partially remedied by the addition of the KSY

chamber.

An additional challenge for tracking results from absorbers placed before and after the VDC chambers, consisting of one radiation length of lead upstream of the VDC, and 2 inches of polystyrene downstream. This material lowers the flux of showering tracks produced by muon bremsstrahlung in the magnet flux return which would otherwise curl back in the magnetic field and enter the emulsion target. The drawback is additional difficulty in connecting VDC track segments to other measuring stations due to scattering in these absorbers.

The overall efficiency of reconstruction of muon triggers is ~90%. Work is in progress on chamber alignment and on algorithms.

| | Location | Type | Samples | Orientation | Efficiency | Resolution |
|---|---|---|---|---|---|---|
| VDC1 | ROSIE Entrance | Jet | 6 | X | 0.95 | 200μm |
| VDC2 | ROSIE Entrance | Jet | 6 | X-3.5° | 0.95 | 200μm |
| VDC3 | ROSIE Entrance | Jet | 6 | X+3.5° | 0.95 | 200μm |
| KSY | Inside ROSIE | Jet | 4 | Y | 0.99 | 225μm |
| KSX | Inside ROSIE | Jet | 4 | X | 0.98 | 225μm |
| DC1-3 | After ROSIE | Single | 12 | 4X,4U,4V | 0.90 | 350μm |

**Table 3: Summary of E872 Drift Chambers**

### 5.2.4 EM Calorimeter

Calibration of the lead glass blocks was also done using the PW5 muon beam. An example of a block's response to muons can be seen in Figure 14. Response curves such as this were made for each block and used to balance the phototube gains.

The stability of pedestals was found to be better than 1%. The stability of the LED system is at the level of 2%. A small sample (about 10) of the blocks with representatives from all three types were exposed to electrons, pions, and muons in a test beam at BNL. From this the e/μ response was measured in order to be used for the calibration of the calorimeter. The individual block energy resolution was found to be about 6.5% for SF5 LG, 7.5% for the large SCG1_C blocks, and 12.5% for the small SCG1-C blocks, at an energy of 1 GeV. Due to the lack of a calibration beam during the

run, we expect that the overall energy resolution to be not as good, but not worse than 20% at 1 GeV.

### 5.2.5 Muon ID

The performance of the tubes was evaluated using tracks found in the upstream drift chambers. Extrapolation of these tracks into the muon identifier allowed plots of the difference between the extrapolations and the observed positions in the proportional tubes to be formed. We have achieved the resolution expected for a detector with a least count of 4 cm. Analysis showed that the efficiencies of the proportional tube planes are in the range 93 - 97% which is consistent with our knowledge of our ability to maintain the dead electronic channel count at an acceptably small number.

Evaluation of the performance of the scintillator hodoscopes is underway. Preliminary results show that the hodoscopes do measure the general profile of the muon flux expected from the dump. However it is clear that there is an unacceptably high level of cross talk between the channels. The problem is especially acute for the multianode tubes where there is a strong component of optical cross talk in addition to the electronic cross talk observed generally throughout the system.

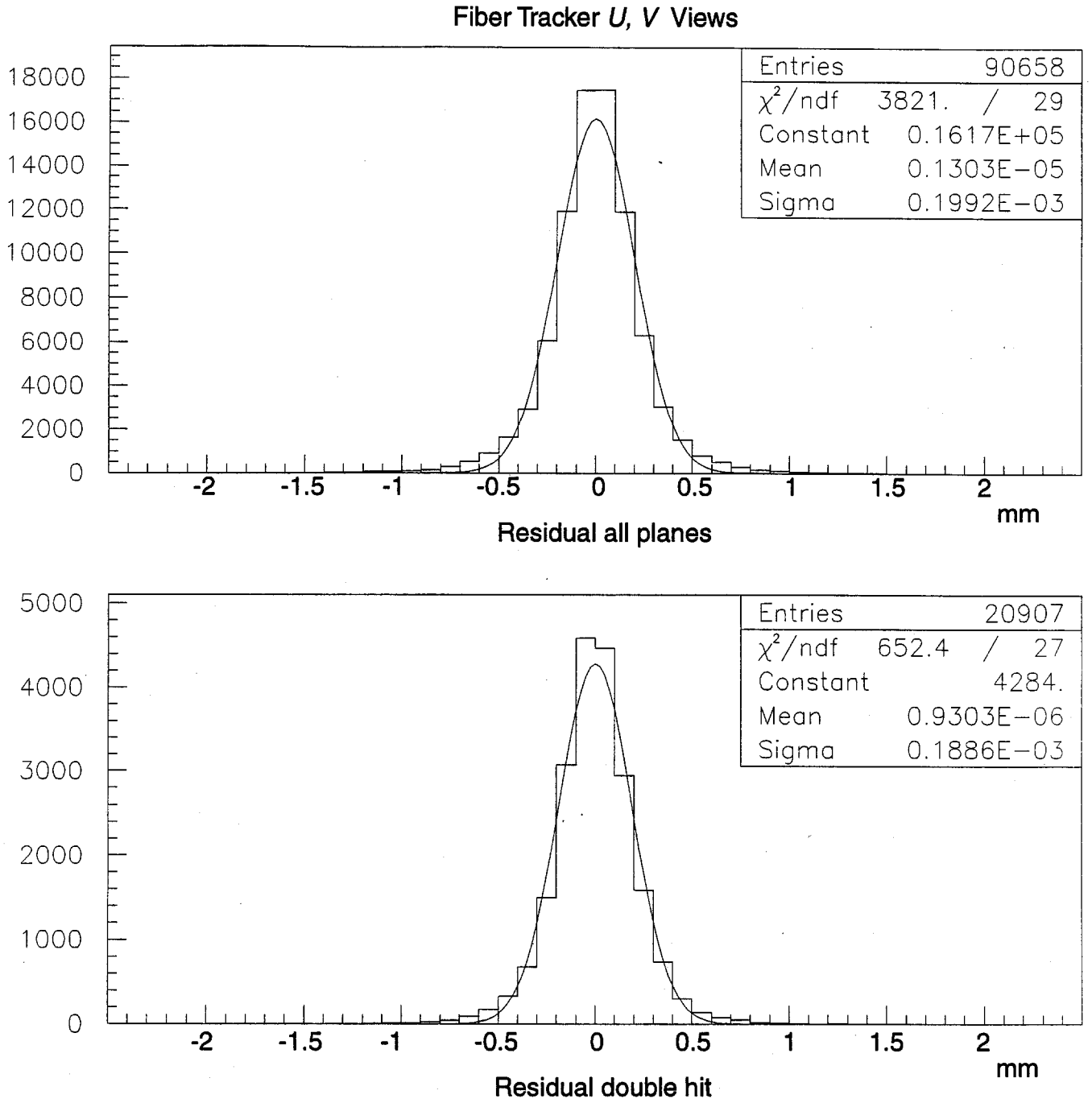


**Figure 12: Residuals for the scintillating fiber tracker.** The *u,v* planes are made of two layers of fibers 0.5mm in diameter. The top plot shows the residuals for all hits, and the bottom plot shows residuals when two fibers are hit per layer. This calibration indicates that the resolution is better than 200μm per plane.

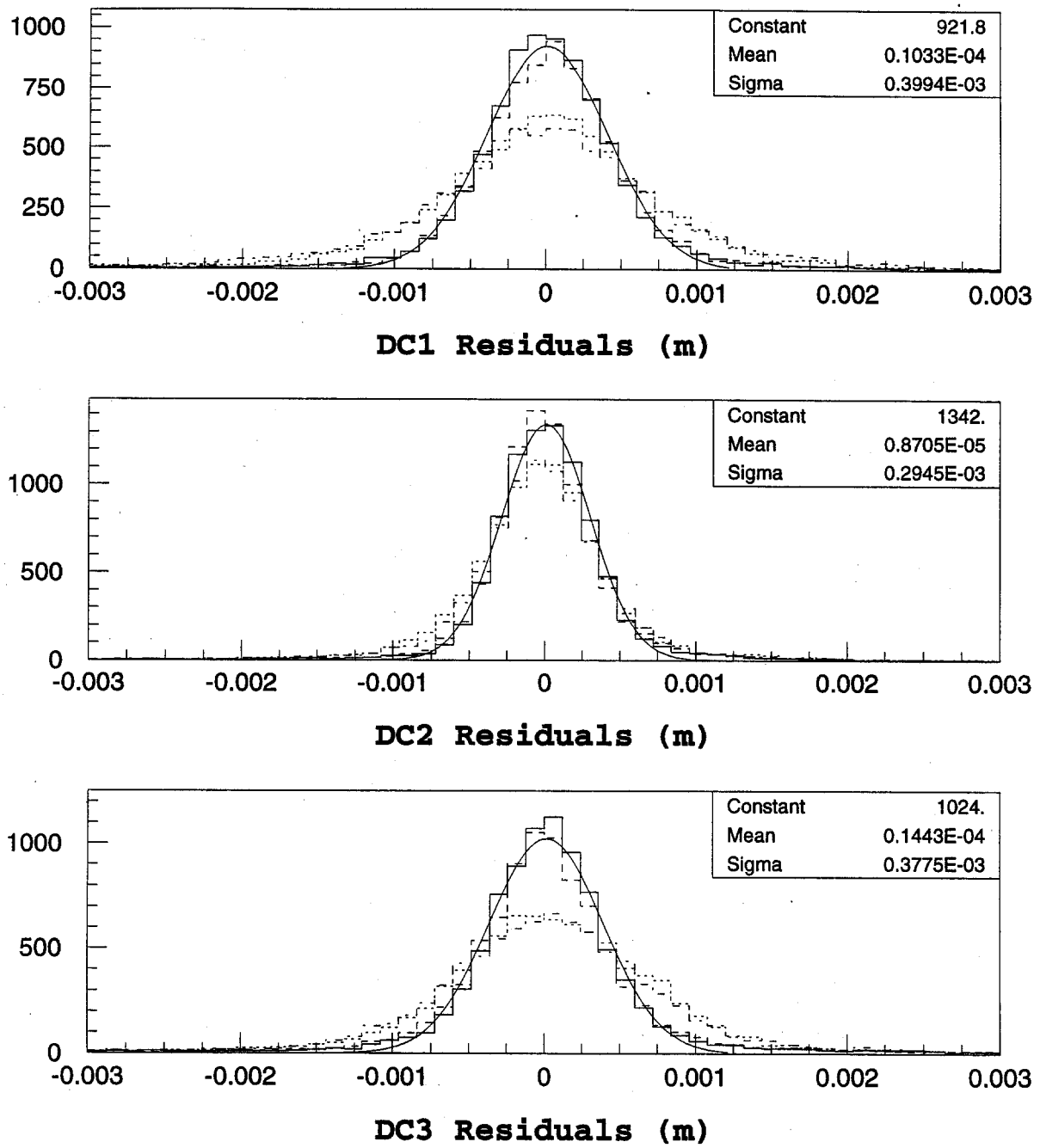


**Figure 13: DC performance.** These are drift chamber residual plots using muons from calibration data. There are four planes in each of the three chambers with distributions superposed. The actual intrinsic resolution of each chamber is lower than the fitted rms value.

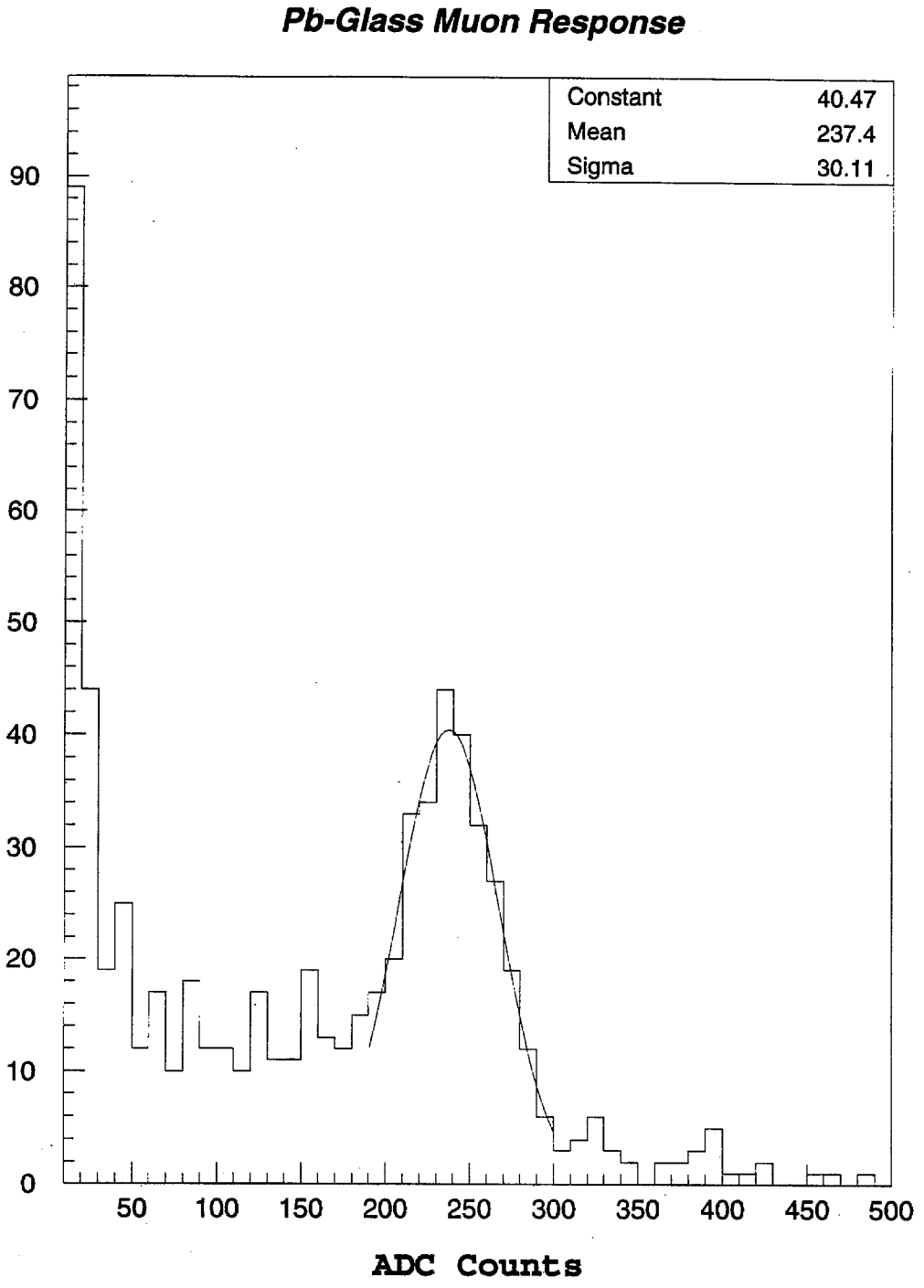


**Figure 14: Muon response for a typical lead glass block.** A muon calibration of all 400 calorimeter blocks was done periodically. This provides gain balancing for the system but not energy response.

### 5.3 Emulsion Exposure

Two ECC emulsion modules were installed on 13 April 1997, and a full complement of four modules were in place by 13 June. Because of the residual backgrounds, it was decided to be conservative in the total amount of beam time allowed for each module, and keep the level about a factor of 2 lower than the limits stated above. This implied that each module would have to be changed out once during an exposure of $5\times10^{17}$ protons on target. The beam intensity on the dump was progressively increased from $1\times10^{12}$ per spill in April to $8\times10^{12}$ for the last six weeks of the run. Table 4 lists the final results of the data exposure for the seven modules used in the run. There are four stations in the target stand (See Figure 6), and three modules were removed and replaced during the run.

Although the goal of nearly $5\times10^{17}$ pot was delivered to the beam dump, not all emulsion targets were ready to be installed for the full amount of beam. Also note that the interaction yields in Table 4 are based only on the total protons on target for each module and do not take into account other experimental inefficiencies. Roughly, a net yield estimate should use a "weighted" POT of $\sim4.0\times10^{17}$ and include the live-time corrections (0.89) and event finding efficiency (~0.7). The beam-weighted installed target for the first run was 260 kg. Measured $\nu$ interaction yields are given in the next subsection.

| Module | Station | Type | mass (kg) | $\Sigma$ pot ($10^{17}$) | est. $\nu$ int. | est. $\nu_\tau$ int. |
|---|---|---|---|---|---|---|
| 1 | 1 | ECC | 98.4 | 2.57 | 395 | 18 |
| 2 | 3 | ECC | 98.4 | 1.17 | 180 | 8 |
| 3 | 4 | ECC / Bulk | 70.9 | 1.89 | 210 | 10 |
| 4 | 2 | ECC / Bulk | 67.9 | 3.35 | 356 | 16 |
| 5 | 3 | ECC / Bulk | 66.6 | 3.35 | 349 | 16 |
| 6 | 1 | ECC / Bulk | 69.4 | 1.87 | 203 | 9 |
| 7 | 4 | Bulk | 54.8 | 1.87 | 161 | 7 |
| $\Sigma$ | | | | 4.55 | 1854 | 84 |

**Table 4: Summary of the seven emulsion modules exposed in the 1997 run**

### 5.4 Data Analysis

The analysis for extracting ν interaction candidates from module 2 (ECC type in position 3), with predictions from reconstructed spectrometer tracks, is in progress (1 Sep.). This module was extracted and processed in June and will be the first to be analyzed with an automatic scanning station at Nagoya University. The results below are preliminary and based on electronic detector information only. The total number of interactions in the emulsion from all three flavors is expected to be approximately 2000, as estimated in Table 4. The total number of triggers recorded on 8mm tape is $10^7$ so that the ratio of interesting events to triggers is low, about 1 in 4000. Extraction of the interaction candidates might seem a difficult task, but the great majority of the events on tape originate from muon interactions in the shield steel and spectrometer magnet and are characterized by a few hits in the scintillating fiber planes that are not seen as tracks. They are usually soft electrons or γ's scattering in targets and the first pass software reconstruction can reject these easily. This first stage typically provides a reduction of 200. The first pass keys on the fact that interesting events will have:

- ≥ 1 tracks in the drift chambers pointing within 50cm of the fiber tracker, OR...
- a vertex in an emulsion volume made from the *u*-view of the fiber tracker, OR...
- ≥ 30 GeV deposited in the lead glass calorimeter

If an event passes, then all planes of the fiber tracker are decoded and used to reconstruct a vertex in space (the most time consuming part of analysis). The effect of the above requirements on ν interactions have been checked with Monte Carlo simulation: >95% of $\nu_\tau$ and $\nu_\mu$ CC events were kept, and >97% $\nu_e$ and >85% of NC events were kept. The interactions are usually easy to recognize with event displays of hits and tracks, mostly because the energies of the ν's are high, with a typical $E_\nu$ of more than 50 GeV. Thus the multiplicity of the primary vertex is usually 4 charged tracks and several electrons from $\pi^0 \rightarrow \gamma\gamma$ conversion. Because of the ease of recognizing a large class of physics events by eye, and because of the great reduction of the triggers after the reconstruction filtering, scanning with display software is efficient and relatively fast.

| | Σ pot | $\nu_e$ CC int | $\nu_\mu$ CC int | $\nu_\tau$ CC int | NC int | Total |
|---|---|---|---|---|---|---|
| Calculated | | 17 | 18 | 1.6 | 13 | 50 |
| Calc × effic. | | 15 | 16 | 1.4 | 12 | 44 |
| Measured | $4.5\times10^{16}$ | * | 16 | * | * | 51 |

**Table 5: Yields from the present method of data analysis**

The main goal in this analysis scheme, illustrated in Figure 15, is to have a set of events for the first emulsion analysis with a high probability of success per event. (The gray boxes are steps with physicists scanning with display graphics.) When the scanning in the relatively high background environment is better understood, the criteria will be relaxed and much larger set of events could be scanned, at least a factor of 5 times more candidates. Module 2 was exposed to a modest $1.2\times10^{17}$ protons on target. The muon and electron backgrounds have been measured in the individual sheets of this module and have densities of = $2.3\times10^5$ cm$^{-2}$ [muons] and = $3\times10^5$ cm$^{-2}$ [*e*].

Table 5 gives some results of this analysis. The yields are for about 40% of data of Module 2, compared to expected interactions. Note that there is considerable ambiguity in distinguishing between electron neutrino tau neutrino and neutral-current interactions electronically.

Figure 16 through Figure 18 show three events from this sample which are "golden" in terms of event appearance and measured total energy. They are believed to be a $\nu_\mu$ CC interaction, a $\nu_e$ CC interaction and a NC interaction, respectively. Note that Module #2 is located in the 3$^{rd}$ position with empty slots both upstream and downstream of it (slots 2 and 4 empty) so tracking is especially clean. After software selection, but before human scanning, the interaction vertex distribution in *z*, Figure 19, is dominated by secondary showers of $\gamma$s from muon interactions. Figure 20 and Figure 21 show the spatial distribution of the interaction vertices for the neutrino candidates. The estimated yields have an uncertainty of 20% even for the $\nu_{\mu,e}$ CC interactions since the total charm cross section and its differential longitudinal distribution are not so well measured in *pN* interactions. We are very encouraged by these first, electronic only, results and are hopeful to have interactions measured in emulsion before the end of October.

| Module | %Bulk (mass) | # $\nu_\tau$ expected in Module (from Table 4) | # $\nu_\tau$ expected in Bulk |
|---|---|---|---|
| 3 | 55 | 10 | 6 |
| 4 | 40 | 16 | 6 |
| 5 | 36 | 16 | 6 |
| 6 | 25 | 9 | 2 |
| 7 | 100 | 7 | 7 |
| Σ | | | **27** |

**Table 6: Expected Yield from Bulk Modules**

(before live time and spectrometer efficiency applied)

All ν interaction events recognized from the reconstruction of the information from the electronic spectrometer will be searched for in the emulsion. Monte Carlo generated ν events that are analyzed using the reconstruction software are selected with at least a 95% probability. The actual fraction of events found in emulsion to events predicted by the spectrometer varies with experiment. In E872, no intended cuts are made to reduce the scanning, load so we expect this fraction to be high. The CHORUS experiment reports that their located to predicted ratio is 77%. In addition, as mentioned in Section 4.1.1, there is an inefficiency in locating events in a thick emulsion target, that increases with depth. In CHORUS there is a 20% decrease in the number of events in the most upstream side of the module compared with the most downstream (nearest the spectrometer) side. As a conservative estimate of the event finding efficiency in E872 one can multiply these two factors to give $(0.77)\times(0.85) = 0.65$.

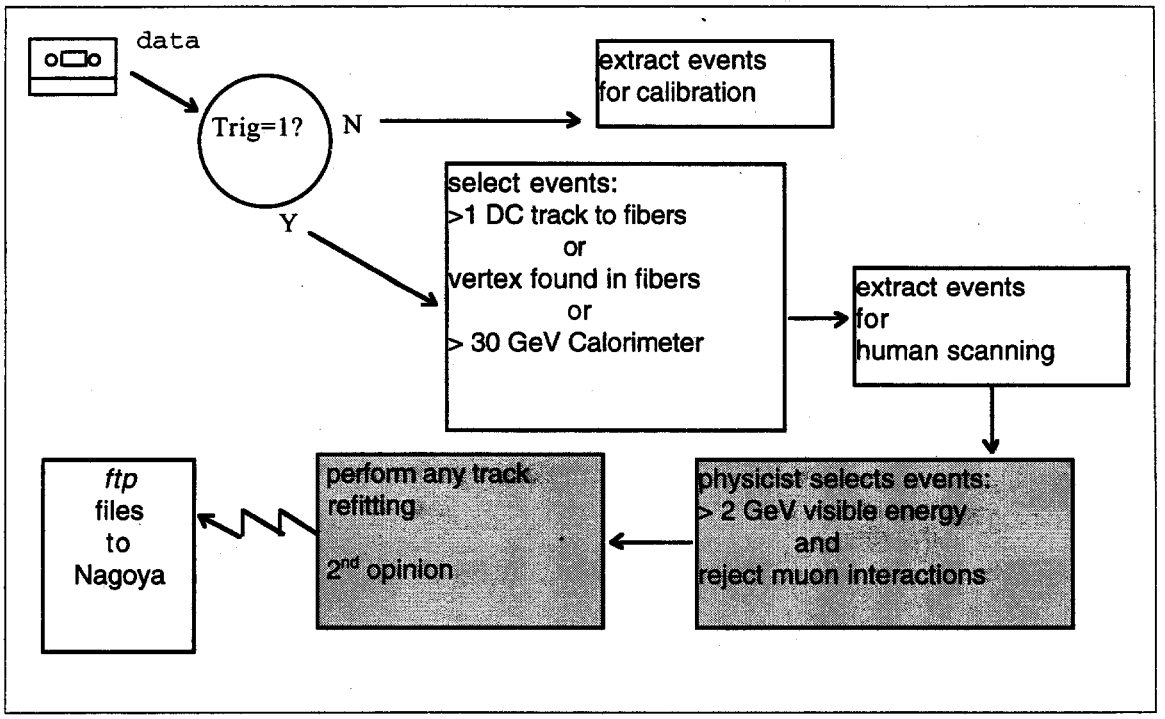


**Figure 15: Schematic diagram of present analysis of Module 2.**

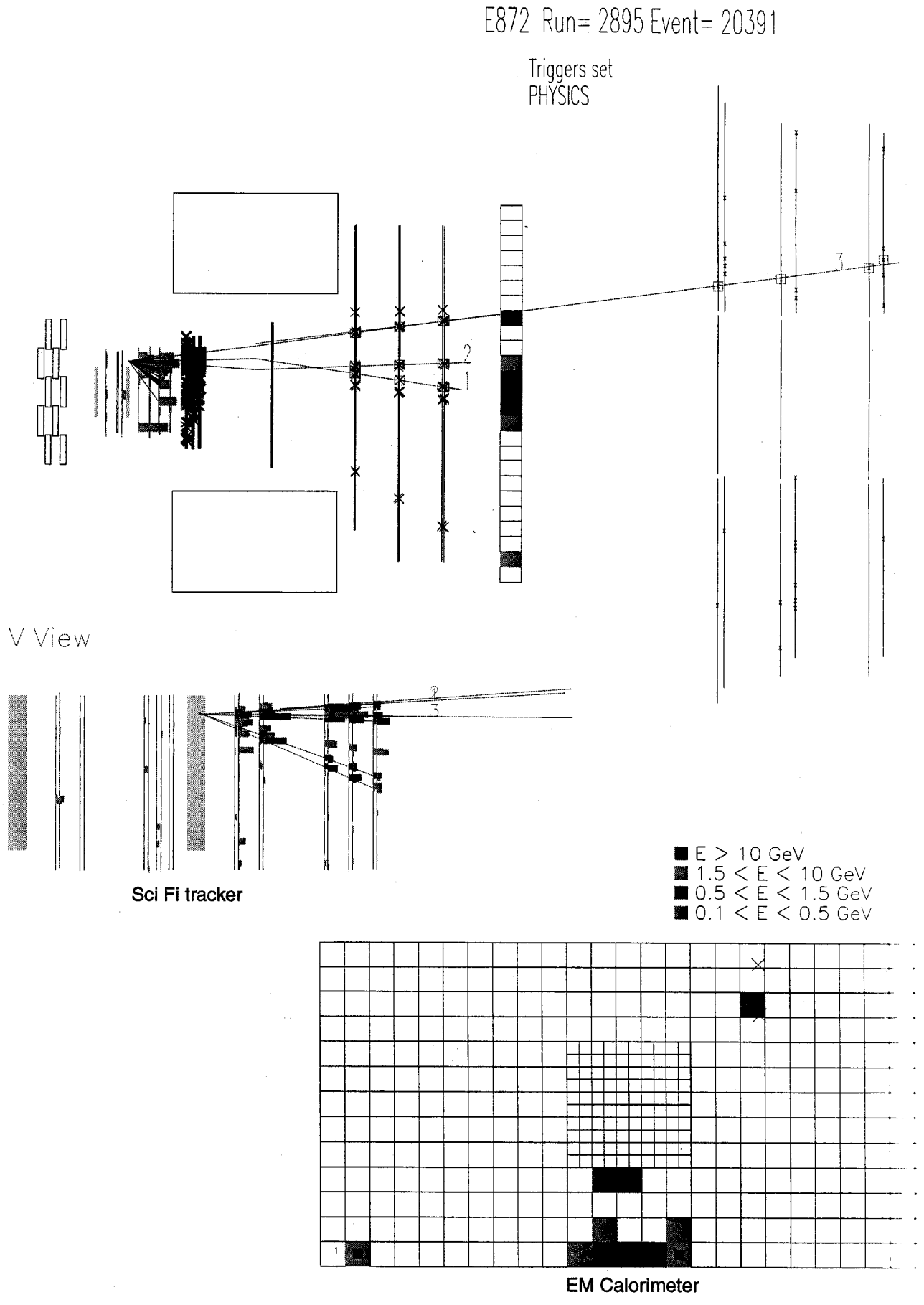


**Figure 16: A muon neutrino CC interaction candidate in Module 2.**

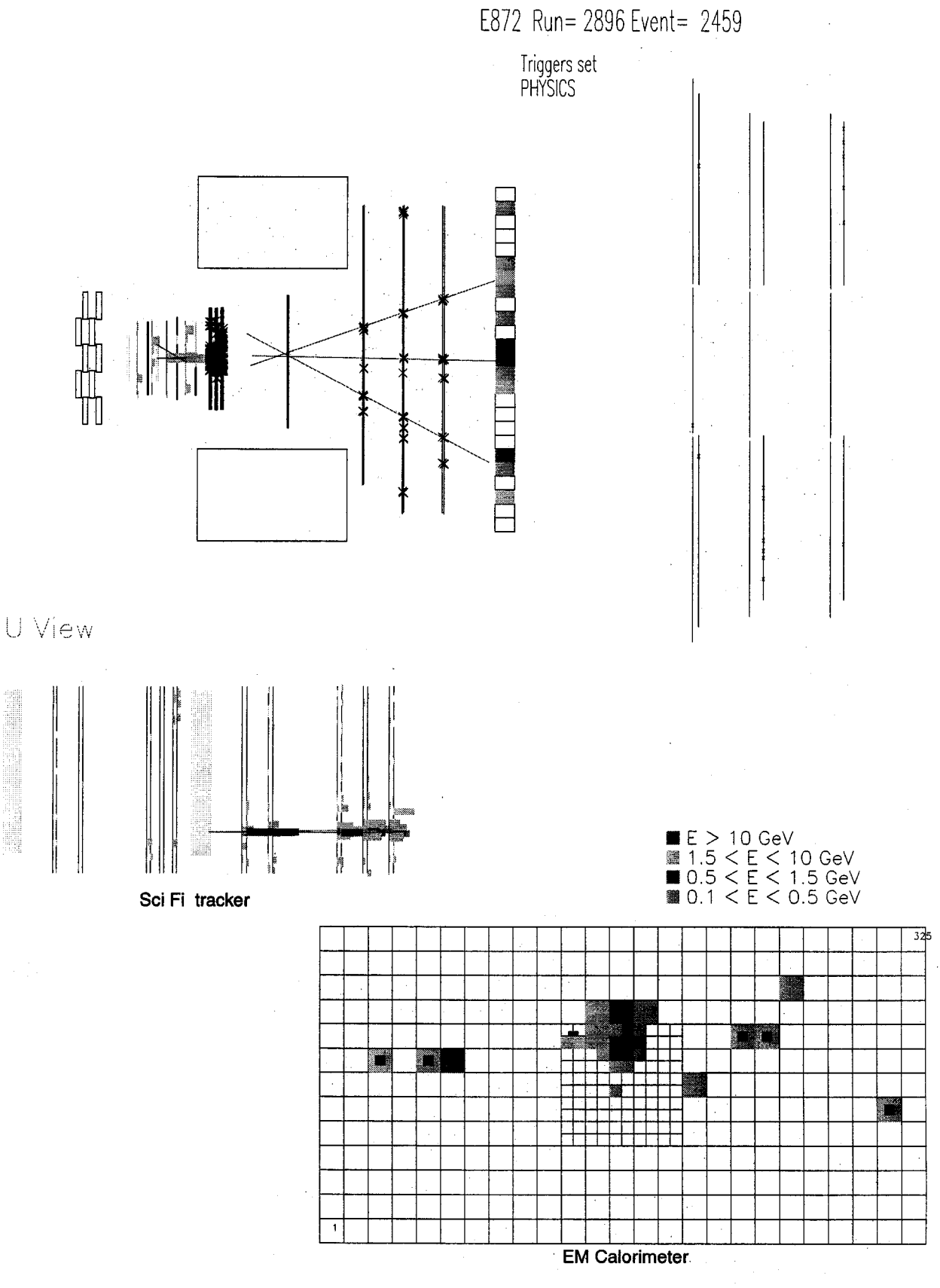


**Figure 17: An electron neutrino CC interaction candidate in Module 2.**

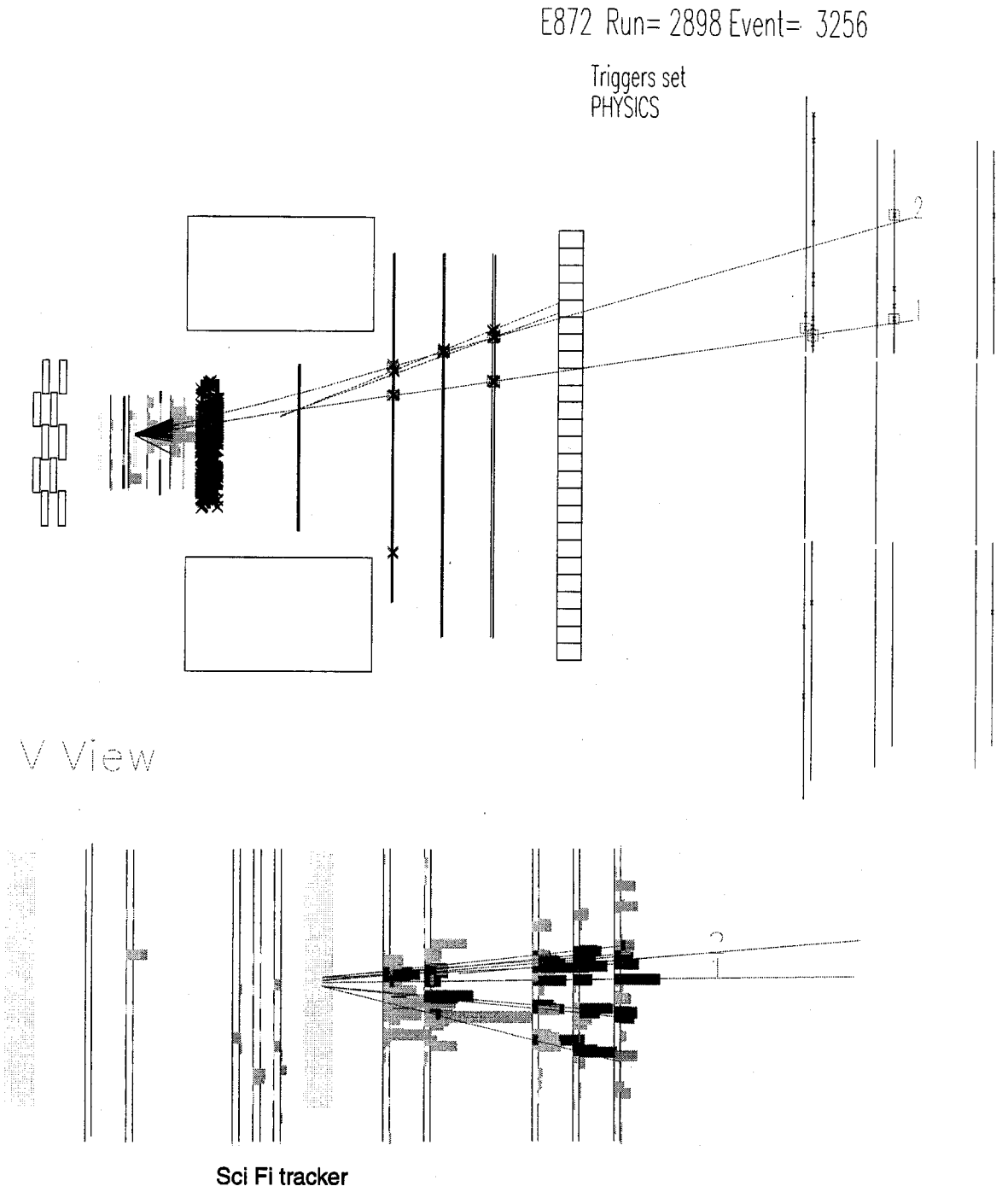


**Figure 18: A NC neutrino interaction candidate in Module 2.**

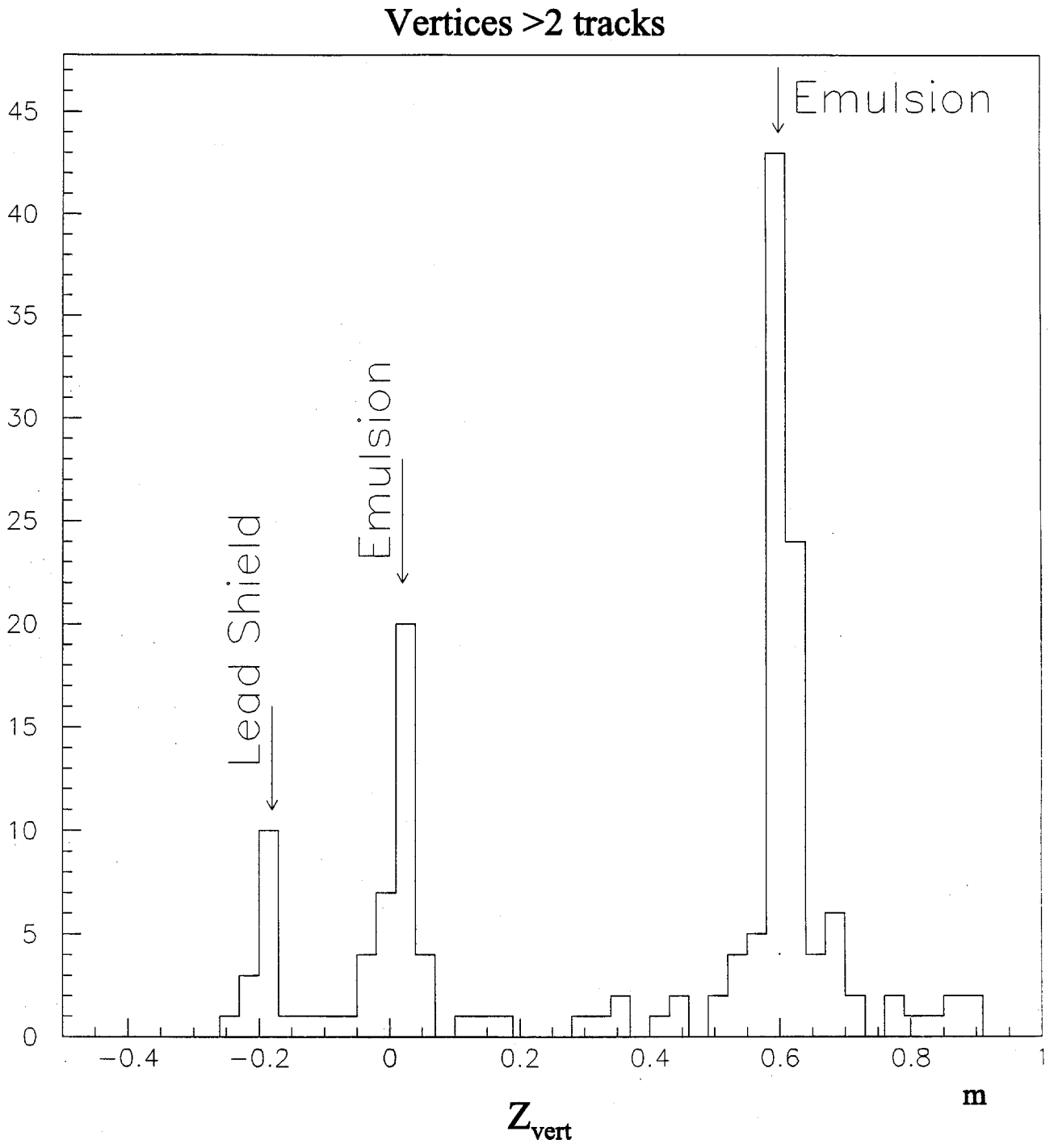


**Figure 19: Z distribution of interactions in emulsion targets.** This data was taken after passing the first stage of the offline analysis, *before* the scan by the physicists. Most of these events are *not* neutrino interactions and this distribution reflects the fact that more non-neutrino interactions occur at the downstream end.

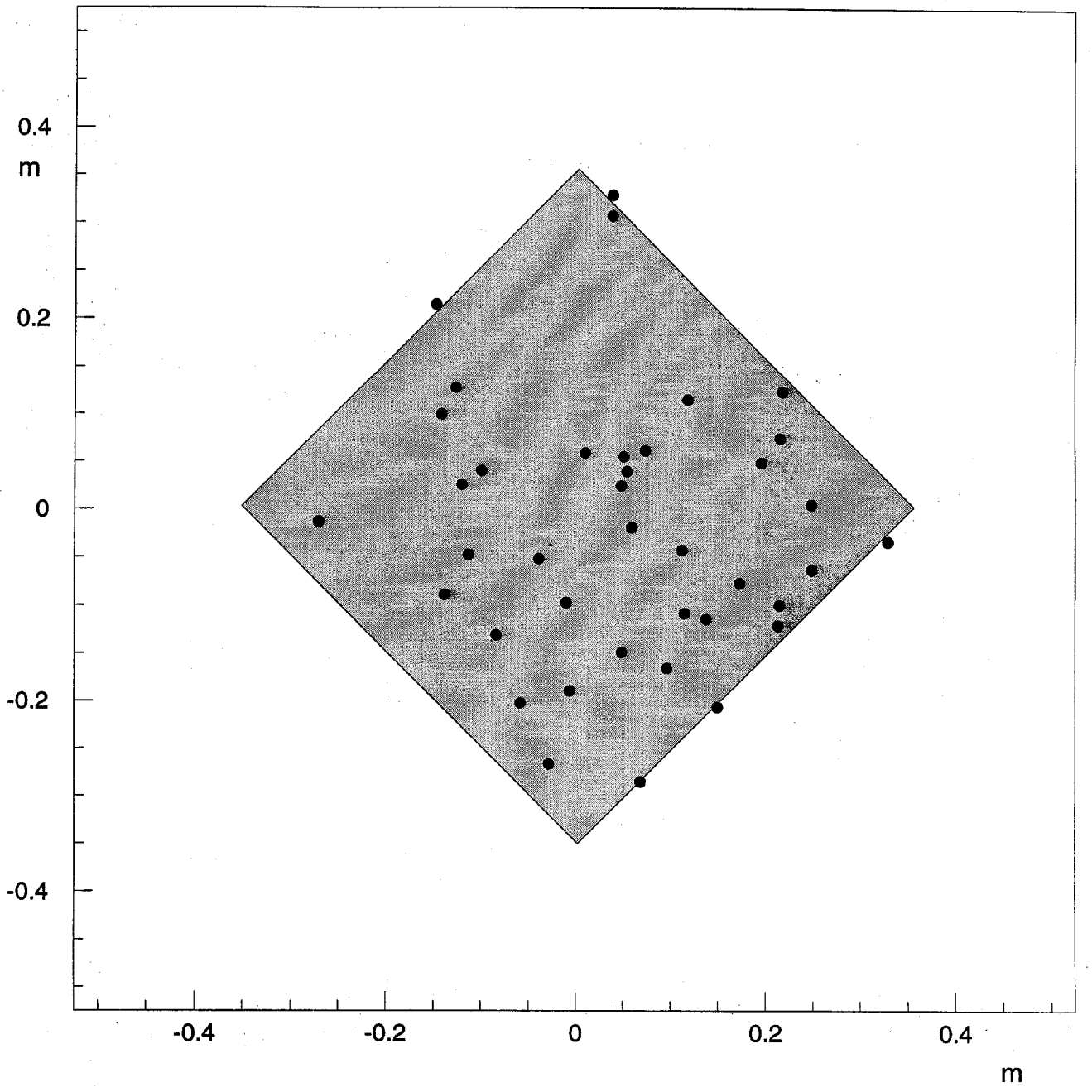


**Figure 20: X-Y distribution of neutrino interaction candidate vertices in Module 2.** The gray area represents the emulsion area.

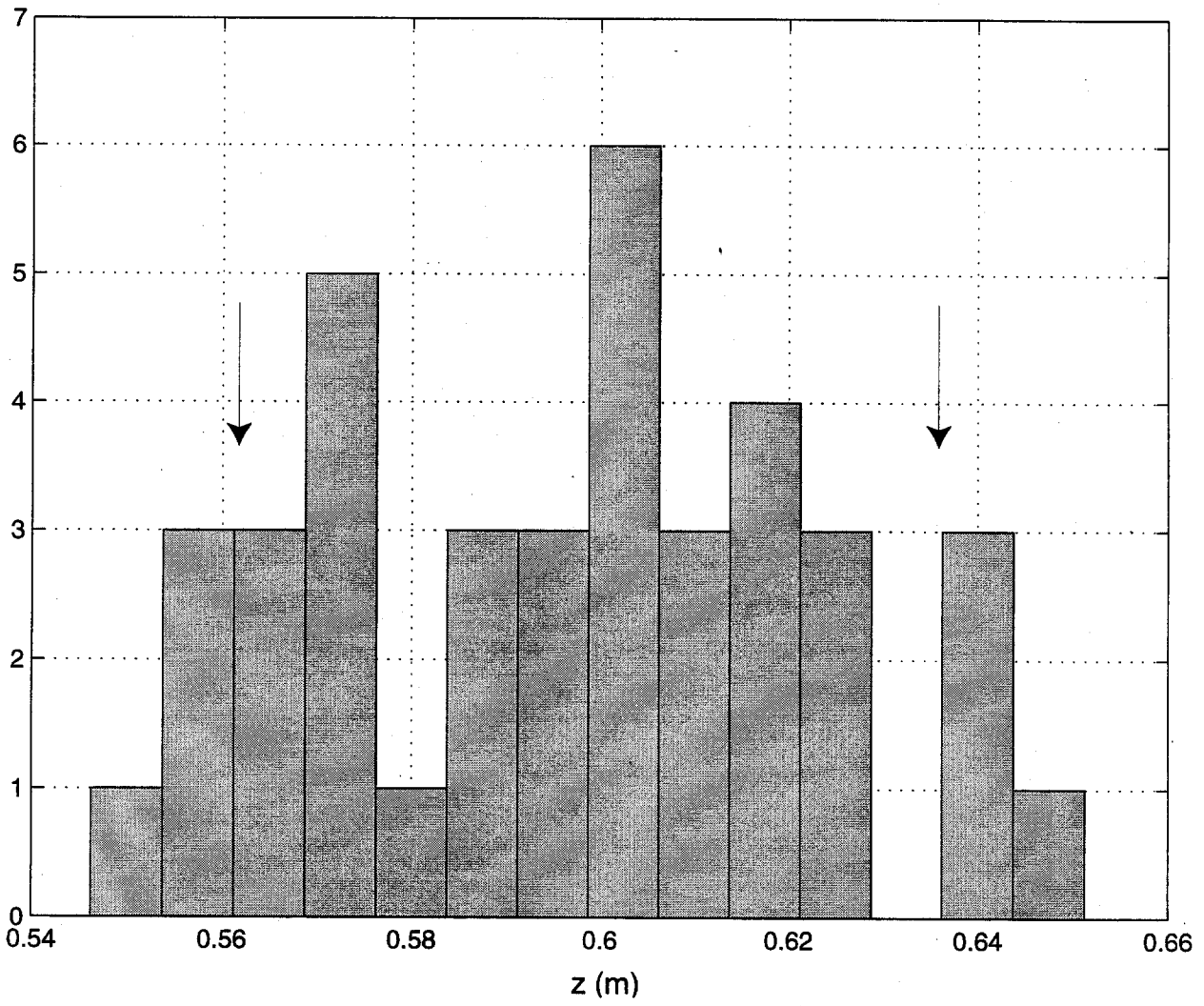


**Figure 21: Z distribution of neutrino interaction candidates.** These are the same events that are shown in Figure 20. The arrows show the beginning and end of the emulsion module.

# 6. Second Run Proposal

## *6.1 Motivation*

The original goal of the E872 proposal was to identify ~200 tau neutrino interactions. We proposed to achieve this goal by using 60 liters of pure bulk emulsion modules and exposing them to $2x10^{18}$ integrated protons on target. When the experiment was approved in June 1994 it was with the understanding that a minimum of $1 \times 10^{18}$ protons should be delivered to the experiment . Though this implied an immediate factor of two reduction in the data set, it was a realistic number that matched the proton economics of the laboratory and the shield design that appeared feasible and cost effective to build.

Between June 1994 and October 1996 the Laboratory and the E872 collaboration worked to design, construct and install the P-West Prompt Neutrino Beam and the E872 spectrometer. We believe that both our beamline and spectrometer were built in an efficient and cost effective manner. Most of our Prompt Neutrino beam was made out of existing or recycled material as were many pieces of the spectrometer. As with many new beamlines and experiments the commissioning period was challenging and took somewhat longer than originally anticipated.

By the time our data taking phase began in mid-April it was obvious that reaching $1x10^{18}$ protons on target by the end of August was an unrealistic goal. Based on proton economics, the residual beam backgrounds which remained in our experiment and the total amount of emulsion which we had available (45 liters), we modified our goal to have $5x10^{17}$ protons delivered to our beam dump target. As described in Section 5.4, that goal was nearly met and our first run should yield the first sample of tau neutrino interactions, albeit well below the original 200 we had hoped to get.

Nevertheless, we are pleased with the performance of both our beamline and detectors and and we believe that a second running period for E872 would enable us to fully exploit the investment which has been made in building this experiment. If the 1999 fixed target run will be as proposed we will be able do double the number of protons delivered to the experiment. We have summarized how this is possible in Table 7.

| | First Run | Second Run |
|---|---|---|
| Spill length | 20 sec | 40 sec |
| Avg. Protons/spill | $5x10^{12}$ | $1x10^{13}$ |
| Max. Protons/spill | $8x10^{12}$ | $1x10^{13}$ |
| Protons/second (avg.) | $2.5x10^{11}$ | $2.5x10^{11}$ |
| Duty Cycle | 20 on/40 off | 40 on/40 off |
| Spills per hour | 60 | 45 |
| Hours/week "live" | ~100 | 126 |
| # of weeks start-up | 20 | 4 |
| # of weeks data | 18 | 16 |
| Σ Protons on target | $4.55x10^{17}$ | $9.5x10^{17}$ |
| Spectrometer Live time | 88% | 93% |
| Σ Protons on tape | $4.0x10^{17}$ | $8.8x10^{17}$ |

**Table 7: Comparison of first run protons delivered with a proposed second run.**

In Table 8 we summarize how the increased number of delivered protons will translate into the proposed yield from a second run.

| | First Run (Actual) | Second Run (Proposed) |
|---|---|---|
| Σ Protons on tape | $4.0x10^{17}$ | $8.8x10^{17}$ |
| Target Mass | 260 kg | 300 kg |
| Est. Tau Yield on tape | 75 | 190 |

**Table 8: Comparison of first and second run tau neutrino yields**

## *6.2 Improvements*

In the sections which follow we discuss a number of topics which we will be investigating over the next several months. In planning for a second run we are working with the constraint that we make only those changes which are absolutely necessary to achieve the primary goals of the experiment. At the present time we believe all improvements will be modest and cost effective. We anticipate that as we analyze our first run data we will gain insight into how to prioritize our efforts at improvement.

### 6.2.1 Target Configuration

During the first run we took data using two types of emulsion targets with a total of $4.55 \times 10^{17}$ protons on target (POT). Approximately 45% of the POT was used with the "standard" bulk emulsion target in which most of the target mass is emulsion. The remainder was used on a new type of sampling emulsion detector, which if successful, presents a new opportunity to do large mass, high resolution experiments using emulsion. These sampling modules, called "ECC type", are explained in detail in Section 4.1.5.

We will make a decision regarding the emulsion module type after the analysis of the Run 1 data from the ECC type target is understood . Assuming that the data from our ECC modules yield results consistent with our expectations, we will be prepared to fully utilize a sampling emulsion target.

### 6.2.2 Emulsion Processing

The use of nuclear emulsions requires some special purpose facilities at the experiment and at the universities. For E872 the facilities are located at Japanese universities and at Fermilab. The pouring of all full-sized emulsion sheets is done at Kobe University. The sheets are shipped to Fermilab and stored prior to use in a lead-shielded enclosure. The individual sheets are assembled into modules at Fermilab just prior to installation. The modules are built in aluminum fixtures that allow them to be mounted on the precision stand in the beamline. After exposure, the modules must be disassembled, the sheets removed, and marked with a grid pattern of 50μm dots that can be measured at scanning time. These dots, called a "grid print", give an accurate measure of the amount of shrinkage and distortion of the emulsion after it has been developed. This grid printing must take place in a carefully controlled environment which is dark, temperature held to

±1°C and humidity kept to ±10% of the relative humidity at which is was packed. This was done for the first run in a small extension to the target house surrounding the emulsion area in the beamline.

Development of all bulk type sheets are done in Japan at Nagoya University. All "thin" emulsion sheets, ECC type, are processed at Fermilab in darkroom / drying rooms at the New Muon Lab (NMS). It is anticipated that the total amount of processing needed for Run 2 would be about a factor of two more sheets than in the first run. There is adequate capacity now for this and the handling of the chemical wastes from the processing is established, including recycling of the silver-laden liquid waste.

It is proposed that modifications be made to one of the counting rooms at our experiment (HIL) so that modules can built and then "grid printed" without having to interrupt the beam for significant periods, up to 24 hours. This would be a more efficient procedure, under better controlled conditions. This same room could also be the home for the proposed automatic scanning station that would be used for several groups using emulsions at Fermilab.

### 6.2.3 Emulsion Scanning

The use of automated scanning stations, pioneered at Nagoya University, has brought emulsion analysis into the digital era. The data recorded in the emulsion is extracted and summarized on standard mass storage media with speeds and efficiency that exceed human scanners by three orders of magnitude. These stations also allow the scanning technology to be far more easily exported to institutions that have little direct experience with emulsion analysis. The University of Michigan and Fermilab have proposed to purchase, assemble and commission a Nagoya-type scanning station within the next year. It would be a tool for learning, and a tool for analysis of data from several sources, including E872. Although the total number of events to scan is not that large for E872, ~$3\times10^4$, some part of the analysis could be done, such as changeable sheet scanning. Most importantly, it would be part of a program to establish an analysis path for much larger use of emulsions proposed for NuMI experiments.

### 6.2.4 Drift Chamber Tracking

Inadequacies in the tracking system were partially remedied during the first run by the addition of the KSU drift chambers with 4 samples each. A remaining weakness is the fact that there is only one $x$ measurement per station in the scintillating fiber system and we are investigating means to add additional $x$ measurements just downstream of the last target.

Tracking resolution and efficiency in the $y$ (non bend) view is limited by the small-angle stereo of the VDC chambers. A possible solution is to add one or both of the two 2.5m x 2.5m jet chambers now in the E815 calibration beam (SNOW and WHITE). These chambers would be mounted just downstream of ROSIE's magnetic shield plate. To make room we would need to move the existing DC1 and DC2 chambers downstream about 3/4 m, thus compacting the existing chambers.

During the next few months we must confirm with careful measurements that these two large chambers can be brought into the E872 pit and rigged into place without major disruption of the spectrometer. This rigging could be simulated with light 120"x 124" wooden mockups of the chambers.

Total new costs to implement this upgrade depend on the availability of the LRS 3377 TDCs. Assuming that the DC Readout is done with existing electronics, the project cost is less than $20K including probable labor and shop costs. Kansas State University will provide the drift chambers and on-board discriminator/amplifiers. We expect the mounting and gas hookups of the chambers and the TDC readout will be provided by Fermilab.

### 6.2.5 Muon ID System

We plan to upgrade the waveshifting fiber scheme by replacing the 4 mm square single-clad fibers with bundles of seven (or fewer) 1-mm diameter multiclad fibers. We expect the optical cross talk at the face of the 16-ch tubes will be thereby greatly diminished. We also plan to improve the isolation and shielding of the twisted pairs that carry the signals from the anodes to the discriminator inputs in an effort to reduce the electronic cross talk.

### 6.2.6 DAQ System

The E872 DAQ system uses a relatively simple implementation of the Fermilab DART architecture of hardware and software. The throughput bottleneck in this system is completely understood to be the link between the VME processor and the workstation which receives the data and writes it to tape. In the 1997 run this data link was standard ethernet with TCP/IP. The link was very reliable, but the speed was typically 500 to 600 KB per second, and often fluctuated to below 400 KB/s. At a proton intensity of $8x10^{12}$ per spill, the total amount of data needed to be transferred in the 40 seconds during interspill averaged 15MB, requiring 30 seconds for transfer but requires 50 seconds at 300 KB/s. These long transfers would interfere with data coming in during the next spill, because the CAMAC data stream is synchronized to the events and not buffered like the scintillating fiber data. This leads to a large effective dead-time and sensitivity to many other factors on a heavily loaded workstation.

The proposed 40 second spill is advantageous for E872 since we can keep the instantaneous rates and live-time constant, while improving the duty time by a factor of 1.5. However the longer spill time in the second run with the same interspill time of 40 seconds implies that twice as much data will need to be transferred in the same amount of time. Based on discussions with Computing Division/DART experts we propose to eliminate the ethernet connection and replace it with a BIT3 VME to workstation interface which has a much higher bandwidth.

### 6.2.7 Offline Computing

E872 will require the use of some fraction of the FNAL computing farm to reduce our data tapes to a small number of events to be scanned by the emulsion groups. At present it takes ~15hr/node/tape on the FNAL Unix cluster. The total number of tapes to be processed is 400.

We anticipate approximately 800 data tapes written during the proposed Run 2 and request the use of 10 nodes on the cluster to finish our event selection within a three month period.

### 6.2.8 Shielding

The shielding used for the 1997 run is adequate for a second run provided that there are financial resources available to make enough emulsion modules for exposure to twice the amount of protons in the dump ($10^{18}$ vs $5x10^{17}$). Using the same module design and proportions of ECC-type and bulk emulsion, this would require 70 liters of emulsion gel which we presently estimate would cost \$700 K (~60M¥). We will investigate whether a more cost-effective solution might be to reduce the backgrounds by a factor of two (hence requiring half the total emulsion volume) with modest improvements to the shielding. The challenge in background reduction is that both the soft electron and muon backgrounds would need to reduced by about the same factor in order to lower the amount of required emulsion.

We know that there is a localized source of muons which penetrate the east side of the emulsion with three times the flux as the west side. As shown in the shielding schematic above, the shield symmetry is broken by the MuSweep magnet causing muons to be deflected or scattered by the steel east of beamline. This source is at large angles with respect to the beamline, ~0.2 rad, and 80% of the flux is less than 2 GeV/c. Thus we could attenuate these muons with less than 2m of steel strategically placed upstream of the emulsion target area. More study with Monte Carlo is needed to find a place to put steel that would not introduce yet another source. We expect to have a proposed solution by December 1997.

Attenuation of the $\gamma$ and $e$ flux at the emulsion location is not as straightforward. Neutrons contribute only a small fraction of this component, and instead we believe we would need to improve the local shielding around the emulsion. The present configuration of this important shielding is shown in Figure 11. Most of the $\gamma$ sources are in the $x$-$z$ plane, which is the plane of high energy muons that are swept to each side of the target by the magnets in the upstream shield. These muons strike the analysis magnet and the edge of the last part of the passive shielding just upstream of the target. While it is certainly true that more lead surrounding the target would reduce this background, it is critical to note that:

- the attenuation length for 2 MeV γ's in lead is not small, 0.6cm
- one cannot introduce more material on either side of the target
- one must avoid adding material downstream of the emulsion

We are not considering a total redesign of the emulsion target stand in order to implement more shielding as this would require a new stand and fiber tracking system. Instead we will continue to investigate the known sources and propose a solution by February 1998. Our goal would be to achieve at least a factor of four (on paper) in attenuation over the present rates and to fit into the present design of the target area.

### 6.2.9 Beam Dump Repair

The beam dump copper is cooled by continuously flowing 30gpm of water through holes drilled along its length. The cooling system is a closed-circuit with a heat exchanger between it and the "outside world", thus keeping the potentially activated water ($^3$H) isolated. Late in the run, during the third week in July, the system developed a leak close to the dump itself, inside a nearly inaccessible shielded cave. The leak was less than 2 gallons per day when discovered, but increased linearly over time to 13 gallons per day at run's end. The water from the leak that did not evaporate was contained and monitored for tritium.

Repair of the dump needs to be accomplished before the second run, of course, but since the exact nature of the leak (fitting leak, pipe crack ... ) is unknown we cannot give accurate estimates of how and when the repairs will take place. It is likely that the diagnostics will not take place until the radioactivity in the dump cave is reduced to acceptable levels (ALARA). A committee at the Lab has been appointed responsible for the evaluation and recommendations for recommissioning of this dump.

## *6.3 Cost Estimates for a Second Run*

In the following tables have summarized the costs which we have estimated will be required for the preparation and operation of a 20 week run.

| | | Cost | FNAL | non-FNAL | source |
|---|---|---|---|---|---|
| 1 | Emulsion Targets | | | | |
| 1.1 | Emulsion Gel & Module Construction | | | | |
| | Gel | $350,000 | | 40M¥ | US-Japan |
| | Temp/Humid.Room | $10,000 | $10,000 | | |
| 1.2 | Scanning | $50,000 | $50,000 | | |
| 1 | Sub-total | $410,000 | $60,000 | 40M¥ | |
| | | | | | |
| 2 | Spectrometer Improvements | | | | |
| 2.1 | Upstream Tracking | | | | |
| 2.2 | Downstream Drift Chambers | | | | |
| | Mechanical Support Stand | $4,000 | $4,000 | | |
| | Rigging Fixtures | $1,000 | $1,000 | | |
| | Rigging into Place | $5,000 | $5,000 | | |
| | Gas System Modification | $1,000 | $1,000 | | |
| | Cables | $1,000 | $1,000 | | |
| | 10 - 3377 TDC's | ($30,000) | | | PREP |
| 2.3 | Muon ID | | | | |
| | Fiber Improvements | $5,000 | | $5,000 | Tufts (DOE) |
| | Noise Reduction | $1,000 | | $1,000 | Tufts (DOE) |
| 2.4 | DAQ | $20,000 | $20,000 | | |
| 2 | Sub-total | $38,000 | $32,000 | | |
| | | | | | |
| 3 | Beamline Improvements | | | | |
| 3.1 | Shielding | | | | |
| | Materials | $20,000 | $20,000 | | |
| | Rigging | $40,000 | $40,000 | | |
| 3.2 | BPM's for Monitoring | $50,000 | $50,000 | | |
| 3.3 | Beam Dump Repair | $5,000 | $5,000 | | |
| 3 | Sub-total | $115,000 | $115,000 | | |
| | | | | | |
| | Total Cost Estimate for 2nd Run | $563,000 | $207,000 | | |

**Table 9: M&S cost estimates in preparation for a second run**

| | |
|---|---|
| Gas | |
| Drift Chambers | $26,000 |
| Muon ID | $2,000 |
| | |
| Supplies | |
| Cables | $1,000 |
| Tools | $1,000 |
| Tapes | $5,000 |
| Emulsion Processing Chemicals | $10,000 |
| | |
| Visitors | |
| Guest Sci. Salary & Housing | $50,000 |
| Summer guest | $12,000 |
| | |
| Totals | $107,000 |

**Table 10: Operational costs for a second run**

# 7. Appendix A - Other Physics Topics

## *7.1 Determination of the Nu Tau Magnetic Moment*

A non-vanishing neutrino magnetic moment has implications in both solar neutrino physics and astrophysics. In addition a large magnetic moment for the tau neutrino affects Big-Bang nucleosynthesis calculations [1].

The current limit for the $\nu_\tau$ magnetic moment of $\mu_{\nu(\tau)} < 5.4 \times 10^{-7}\ \mu_B$ was obtained in the BEBC beam dump experiment [2]. Their analysis is based on the same neutrino-electron scattering mechanism that is proposed here.

A diagonal neutrino magnetic moment $\mu_\nu$ can be measured through interactions with atomic electrons. The neutrino exchanges a photon with an electron and changes helicity. The total cross section for this process is given by:

$$\sigma^\mu = \mu_\nu^2 \alpha^2 \left(\ln(E_\nu/E_t) + (E_t/E_\nu) - 1\right)$$

where $E_t$ is the lower energy threshold for electron detection and $E_\nu$ is the energy of the incoming neutrino.

In this experiment, the process can not be distinguished from neutral current neutrino-electron scattering. The cross sections therefore have to be added:

$$\sigma^{total} = \sigma^\mu + \sigma^{NC}$$

Here, $\sigma^{NC} = 10^{-42}\text{cm}^2\ E_\nu/1\text{GeV}$, independent of $E_t$ for small $E_t$.

Since $\sigma^\mu$ increases as $E_t$ decreases, a low energy detection threshold for the recoil electron is advantageous. To detect single electrons, we will trigger on electromagnetic showers and use the fiber-tracker to find events that have only one electron emanating from the vertex. With the current trigger configuration we expect to be able to set a lower threshold of 1 GeV for electrons and hence set a limit of $10^{-8}$ Bohr magnetons for Run 2.

[1] D. Grasso and E. W. Kolb, Phys Rev. **B 54**, 1374 (1996)
[2] A. M. Cooper-Sarkar et al., Phys. Lett. **280 B**, 153 (1992)

### *7.2 Search for the Decays of Neutral Heavy Leptons and New Particles.*

Several models predict the existence of weak isosinglet neutral heavy leptons[1,2,3]. The experimental results of searches for the decays of these particles are described in references[4,5,6]. Compared with these previous experiments, the E872 detector is much closer to the beam-dump target. In the E872 configuration, the distance between the beam-dump tungsten target and the detector is only 36m while in the case of other experiments, for example CHARM[1] and WA66[2], it was 480m and 820m, respectively. Currently, the NuTeV collaboration[7] is also searching for the decays of neutral heavy leptons but the distance to their dump is 1300m. Another decided advantage of E872 is that in our experiment *all* of the protons interact in the dump whereas in the other neutrino-production experiments, only a fraction of the protons interact in the target. The remaining protons in these experiments interact downstream in a secondary dump where the products from the interaction have minimal acceptance to their detectors. In summary, the flux of neutral heavy leptons which are produced in the E872 beam-dump target is much higher than those generated in other experiments, and the short distance between dump and detector maximizes detector acceptance.

We can also search for the decays of other new particles. These particles must be neutral because of the trigger algorithm (described below), and have a low interaction cross section because they must penetrate the shielding. In addition these particles must have a relatively long lifetime ($>10^{-9}$sec) in order to reach the detector in sufficient number. For the decay space, we will use the region from the upstream face of the ROSIE analysis magnet to the drift chamber array downstream of ROSIE, for a total volume of ~$7m^3$.

For this search, we will construct a new trigger type. A new trigger counter (1m x 2m) will be placed downstream of the downstream drift chamber array. The veto system will be the same that was used for the "$\nu_\tau + N \rightarrow \tau + X$" events but include the trigger counter T3. Since we don't need the scintillating fiber information, we can tolerate a much

higher trigger rate without accruing an appreciable DA deadtime.

The candidate events should contain two tracks that form a vertex, with no other hits in the chambers. In the case of the decay of neutral heavy leptons, one of the two tracks must be a lepton (EMCal and Muon ID information) for event selection. If the vertex is upstream of the KSU chambers we can also measure the momenta of the two tracks and include kinematical constraints such as $p_T$ balance along the flight direction. With $1x10^{18}$ protons, minimal background and an efficiency of 100%, our sensitivity should be more than 100 times better than previous experiments.


[1] L.Wolfenstein Nucl. Phys. **B218**, 205(1983)
[2] C.N.Leung and Jonathan L.Rosner Phys. Rev. **D28**, 2205(1983)
[3] Loretta M.Johnson, Douglas W.McKay and Tim Bolton hep-ph-9703333(1997)
[4] J.Dorenbosch et al. (The CHARM Collaboration) Phys. Lett. **166B**, 473(1986)
[5] A.M.Cooper-Sarkar et al. (WA66 Collaboration) Phys. Lett. **160B**, 207(1985)
[6] M.E.Duffy et al. Phys. Rev. **D38**, 2032(1988)
[7] T.Bolton et al. "Precision Measurements of Neutrino Neutral Current Interactions Using a Sign Selected Beam",Fermilab-Proposal-P-815(1990)

## Appendix B: Interaction Rate Calculation for Tau Neutrinos Produced in the E872 Beam Dump

To detect $\nu_\tau$ interactions E872 plans on using 800 GeV protons impinging on a tungsten target and placing 24 cm of emulsion approximately 35 meters downstream of the tungsten dump covering $\pm 7.1$ mr in both transverse directions (60 liters). The number of tau neutrinos that interact in the emulsion target is a function of both the number of tau neutrinos produced in the dump and the energy spectrum of these neutrinos. Recall the interaction probability of neutrinos is directly proportional to the energy of the neutrino and in the case of the charged current(CC) interaction of the $\nu_\tau$, kinematic effects play a role because of the production of a massive tau lepton.

To determine the number of $\nu_\tau$s exiting the dump the $D_s$ production cross section for 800 GeV protons and the leptonic branching ratio for $D_s \rightarrow \tau\nu_\tau$ must be obtained:

$$N(\nu_\tau)/proton = 2 \times [\sigma_{D_s}/\sigma_{tot}]Br(D_s \rightarrow \tau\nu_\tau)(A^{1.0}/A^{0.7}) \qquad (1)$$

Where $\sigma_{D_s}$ is the $D_s$ cross section, $\sigma_{tot}$ the total pp cross section, Br($D_s \rightarrow \tau\nu_\tau$) is the leptonic branching ratio, A the atomic mass of tungsten, and the factor of 2 since two tau neutrinos are generated with each $D_s$ decay.

There has been no direct measurement of the $D_s$ Cross section at 800 GeV p interactions. However the ratio of the inclusive cross sections for $\sigma_{D_S}/\sigma_{D^+}$ is consistent over a wide range of energies and beam types as shown in table 1. In addition the inclusive charged charm meson cross section has been measured in 800 GeV p interactions (table 2). Therefore

$$\sigma_{D_s}^{800\ p\ interactions} = \left\langle \frac{\sigma_{D_s}}{\sigma_{D^\pm}} \right\rangle \cdot \sigma_{D^\pm}^{800\ p\ interactions} \qquad (2)$$

where $\left\langle \frac{\sigma_{D_s}}{\sigma_{D^\pm}} \right\rangle$ is the mean of values listed in table 1.

Measurements of the fully leptonic decay modes of the $D_s$ have been recently made and are listed in table 3.

Using equation 1 and the mean values obtained from experiments for $\sigma_{D_s}$ $=(\sigma_{D_S}/\sigma_{D^+} \times \sigma_{D^+})$, and the branching ratio for $D_s \rightarrow \tau\nu_\tau$ one obtains an expected tau neutrino flux of:

$$\Phi_{\nu_\tau} = 1.68 \times 10^{-4}\nu_\tau/proton \qquad (3)$$

| Experiment | Beam type | Beam Energy (GeV) | $\sigma_{D_S}/\sigma_{D^+}$ |
|---|---|---|---|
| E691[1] | $\gamma$ | 100-275 | 0.48±0.11 |
| NA32[2] | $\pi$ | 250 | 0.43±0.15 |
| E653[3] | $\pi$ | 600 | 0.56±0.18 |
| CLEO[4] | $e^+e^-$ | 10(CM) | 0.81±0.29 |
| E769[5] | $\pi$ | 250 | 0.62±0.15 |
| Mean Value | | | 0.53±0.07 |

Table 1: Inclusive $\sigma_{D_S}/\sigma_{D^+}$ ratios for different energies and interaction types.

| Experiment | $\sigma_{D^\pm}$ ($\mu$barns/nucleon) |
|---|---|
| E653[12] | $38^{+3+13}_{-3-13}$ |
| E743[13] | $26^{+7}_{-7}$ |
| Mean | $29^{+6}_{-6}$ |

Table 2: Inclusive $D^\pm$ cross section in 800 GeV $pp$ interactions.

| Experiment | Detection Mode | BR($D_s \to \tau\nu_\tau$)% |
|---|---|---|
| E653[6] | $D_s \to \mu\nu_\mu$ | $2.9^{+1.4}_{-1.4}$ |
| E653[7] | $D_s \to \tau\nu_\tau$ | $5.5^{+3.6}_{-3.6}$ |
| WA75[9] | $D_s \to \mu\nu_\mu$ | $4.4^{+2.8}_{-2.1}$ |
| CLEO[10] | $D_s \to \mu\nu_\mu / D_s \to \phi\pi$ | $9.3^{+4.6}_{-3.6}$ |
| BES[11] | $D_s \to \mu\nu_\mu$ | $14.6^{+12.6+2.9}_{-5.8-1.9}$ |
| L3[8] | $D_s \to \tau\nu_\tau$ | $7.4^{+3.7}_{-3.7}$ |
| Mean | | $4.6^{+1.0}_{-1.0}$ |

Table 3: Leptonic Branching Ratio for $D_s \to \tau\nu_\tau$. For $D_s \to \mu\nu_\mu$ detection mode $\mu - \tau$ universality is assumed and hence the branching ratio is scaled by 9.74 ($= \frac{D_s \to \tau\nu_\tau}{D_s \to \mu\nu_\mu}$).

Other sources of tau neutrinos in the tungsten dump are B decays, Charged D decays and secondary hadronic interactions in the dump. It is estimated from the beauty(charged D) production cross section and semi-leptonic(leptonic) decays of B mesons(charged D mesons) that the contribution from B's($D^{\pm}$) is approximately 1.5%(4.5%).

The FRITIOFF Monte Carlo was used to calculate the $\nu_\tau$ contribution from secondary pion/kaon interactions and determined to increase the yield of produced $\nu_\tau$'s by 40%. However these $\nu_\tau$'s have a relatively soft energy spectrum and wider angular distribution and hence only increase the interacted yield by 7.5%.

As mentioned above to determine the neutrino interaction probability the energy spectum of the produced neutrinos must be obtained. The $D_s$ are assumed to be produced according to the following differential cross section:

$$\frac{d^2\sigma}{dX_F dp_T^2} = e^{(-bp_T^2)}(1. - |x_F|)^n \tag{4}$$

Since there has been no direct measurement of the $D_s$ cross section in 800 GeV $pp$ interactions it is assumed that the differential cross section shape (eq. 2) for $D_s$ production is equal to the charged and neutral charm meson production. The experimental measurements of the $b$ and $n$ terms in the the differential form (equation 4) for 800 GeV protons are shown in table 4.

The decay of the $D_s$ into $\tau\nu_\tau$ and subsequent decay of the tau lepton are generated isotropically. The branching ratios and modes used in the decay of the tau lepton are listed in table 5. The resultant non-interacted $\nu_\tau$ spectrum can then be determined.

From this spectrum an average tau neutrino interaction probability ($< \sigma_{\nu_\tau}^{CC} >$) per produced tau neutrino can be calculated from:

$$\sigma_{\nu_\tau}^{CC} = (\alpha \times 10^{-38} cm^2/GeV) E_\nu K_F \tag{5}$$

Where $\alpha$ is 0.67(neutrino) or 0.34(anti-neutrino)[1], $E_\nu$ is the neutrino energy, and $K_F$ is the kinematic factor required for the production of the tau lepton in CC interactions[2].

[1]It is assumed that tau neutrinos and anti-neutrinos are produced in equal numbers hence is taken into account when calculating $< \sigma_{\nu_\tau}^{CC} >$.

[2]Note $K_F$ is a function of $E_\nu$

| Experiment | b | n |
|---|---|---|
| E653[12] | $0.84^{+0.10}_{-0.08}$ | $6.9^{+1.9}_{-1.8}$ |
| E743[13] | $0.8^{+0.2}_{-0.2}$ | $8.6^{+2.0}_{-2.0}$ |
| Mean | | $7.7^{+1.4}_{-1.4}$ |

Table 4: Fit values to the differential form $\frac{d^2\sigma}{dX_F dp_T^2} = e^{(-bp_T^2)}(1. - |x_F|)^n$ for the production of charmed mesons in 800 pp interactions.

| Decay Mode | Branching Ratio |
|---|---|
| $\tau \rightarrow \mu\overline{\nu_\mu}\nu_\tau$ | 22% |
| $\tau \rightarrow e\overline{\nu_e}\nu_\tau$ | 21% |
| $\tau \rightarrow \pi\nu_\tau$ | 14% |
| $\tau \rightarrow \rho\nu_\tau$ | 29% |
| $\tau \rightarrow \pi\rho\nu_\tau$ | 14% |

Table 5: The branching ratios used in Monte Carlo for the decay of the tau lepton.

From equation 5 and the generated $\nu_\tau$ spectrum the average tau neutrino interaction probability ($< \sigma^{CC}_{\nu_\tau} >$) per produced tau neutrino is determined to be:

$$< \sigma^{CC}_{\nu_\tau} >= 0.42 \times 10^{-37} cm^2 \quad (6)$$

The target acceptance is not included in above value. The ratio of anti-tau neutrinos to tau neutrinos is assumed to be 1 and the kinematic factor $K_F$ is assumed to be equal for both types of neutrinos.

The number of tau neutrino CC interactions per proton per centimeter of emulsion at the target can be written as:

$$N(\tau_{CC})/proton/cm = N(\nu_\tau)/proton \times < \sigma^{CC}_{\nu_\tau} > \times N_{Av} \times \rho \times \beta \quad (7)$$

Where $N_{Av}$ is Avogadros number, $\rho$ is the density of the emulsion, and $\beta$ is the weighted angular acceptance of the target.

Using equation 7 with the above value for $< \sigma^{CC}_{\nu_\tau} >$, $\Phi_{\nu_\tau}$ given in equation 3, and the weighted angular acceptance of the emulsion target one can determine the number of tau neutrino charged current interactions per proton on dump per centimeter of emulsion target. The emulsion target size is 50cm $\times$ 50cm $\times$ 24 cm and located 35 meters downstream from the dump, therefore the angular acceptance of the target is $\pm 7mr$. A target angular acceptance of $\pm 7mr$, $\beta$ is equal to 32%. Therefore N($\tau_{CC}$)/proton/cm is determined to be 5.8 $\times$ $10^{-18}$. This value includes the 14% increase from other sources of $\nu_\tau$'s as descibed in section 2.4. Hence for 2 $\times$ $10^{18}$ protons on dump and 24 cm of emulsion approximately 270 tau neutrino interactions are expected in the E872 emulsion target.

The error on the yield is best represented by running a series of Monte Carlo "experiments". An "experiment" is preformed in which the errors on all the measured input variables are taken into account by randomly choosing a value from the propability distribution function appropriate for that variable. These values are then used to calculate an expected $\nu_\tau$ charged current yield in the emulsion target. This "experiment" is repeated $10^5$ times for 2 $\times$ $10^{18}$ protons on dump. At 90% CL we expect in excess of 160 $\nu_\tau$ charged current interactions observed.

# References

[1] **E691** Physics Review Letters, **62**, 513 (1989)

[2] **NA32** Z Phys. C, **49**, 555 (1991)

[3] **E653** Phys. Lett. B, **309**, 483 (1993)

[4] **CLEO** Physics Review D, **37**, 1719 (1988)

[5] **E769** FERMILAB-Pub-96/083

[6] **E653** To appear in Phys. Lett. B, hep-ex/9606017

[7] **E653** Preliminary, Private Communication

[8] **L3** CERN-PPE/96-198

[9] **WA75** Prog. Theor. Phys., **89**, 131 (1993). Corrected with new PDG(1996) branching ratio values.

[10] **CLEO** Phys. Rev. D, **49**, 5690 (1994)

[11] **BES** Phys. Rev. Lett., **74**, 4599 (1995)

[12] **E653** Phys. Lett. B, **263**, 573 (1991)

[13] **E743** Phys. Lett. B, **183**, 110 (1987)

## 9. References


[1] CHORUS collaboration, N.Armenise *et.al.* CERN-SPSC/90-42 (1990)
[2] COSMOS collaboration, Fermilab E-803 Proposal (Oct 1990); update (Oct 1993)
[3]Ushida *et.al.* Phys.Lett. **B206**, 375 (1988)
Foudas *et.al.* Phys. Rev. Lett. **64**, 1207 (1990)
consistent with simulation with the LEPTO package of the LUND Monte Carlo
[4] Particle Data Group (1996)
[5] *ibid*
[6] S.Hasegawa *et.al.* Prog. Theor. Phys. Suppl. **47**, 126 (1971)